VIETNAM JOURNAL OF HYDRO - METEOROLOGY

ISSN 2525 - 2208

VIETNAM METEOROLOGICAL AND HYDROLOGICAL ADMINISTRATION

No 07
04-2021

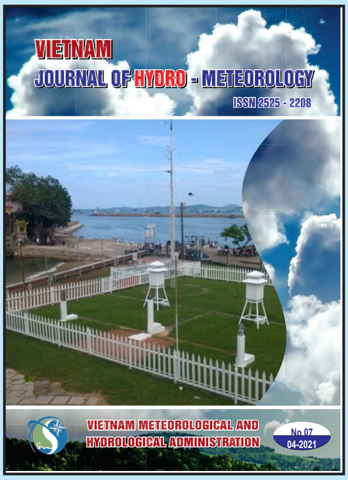

Publishing licence
No: 166/GP-BTTTT - Ministry of Information
and Communication dated 17/04/2018

Editorial office
No 8 Phao Dai Lang, Dong Da, Ha Noi
Tel: 024.39364963
Email: tapchikttv@gmail.com

Engraving and printing
Vietnam Agriculture Investment Company Limited
Tel: 0243.5624399

VIETNAM JOURNAL OF HYDROMETEOROLOGY
Volume 07 - 4/2021

TABLE OF CONTENT

VIETNAM JOURNAL OF
HYDROMETEOROLOGY

Research Article

Research solutions biological activated sludge for seafood wastewater treatment

Vinh Son Lam[1*], Vu Phong Nguyen[1], Phu Huynh[1]

[1] Hochiminh University of Technology (HUTECH), Vietnam. Add: 475 A Dien Bien Phu Street, 25 Ward, Binh Thanh District, Hochiminh City, Vietnam; lv.son@hutech.edu.vn; nv.phong@hutech.edu.vn; h.phu@hutech.edu.vn
* Correspondence: lv.son@hutech.edu.vn; Tel: +84–903399800

Received: 22 December 2020; Accepted: 05 February 2021; Published: 25 April 2021

Abstract: This article presents aquatic wastewater treatment with the addition of probiotics. Due to the high salinity (5–10‰), the microorganisms are inactive because plasmolysis occurs in the presence of table salt, the contraction of the protoplasm away from the cell wall of the bacteria due to dehydration under the action of osmotic pressure, leading to gaps between the cells and the cell membranes. The use of probiotics containing *Saccharomyces* yeast in combination with some bacteria strains to treat aquatic wastewater with high salinity has drawn much interest, but there are no specific studies. By employing experimental method, using two synthetic preparations Microbe–Lift IND and EM–WAT1 contribute to improving the treatment efficiency of activated sludge at different salinity to give the appropriate dosage for application. into practice. Research results show that the optimal load is 4.5kg COD/m^3/day, with a retention time of 8 hours, the optimal salinity after the test is about 5 ‰ to 10 ‰, using 0,25mL Microbe–Lift IND and EM–WAT1 for a liters of wastewater.

Keywords: Halophilic microorganisms; High salinity; Salty favored microorganisms; Seafood wastewater.

1. Introduction

According to the Vietnam Association of Seafood Exporters and Producers (VASEP), Vietnam is among the top 5 countries in the world for aquaculture and seafood export, the brackish water shrimp farming area in Vietnam is more than 685,000 hectares, with an output of more than 660,000 tons and there are more than 500 seafood processing factories nationwide [1]. Many factories and processing factories were established and put into operation, environmental isuses and wastewater quality after treatment. Many seafood processing factories located on the coast often use seawater for many stages such as thawing, washing raw materials due to the lack of fresh water used…Besides, the usual pollution indicators type of wastewater, there is also an index of high salinity from 10 to 30 g/l NaCl) [2]. In such an environment, microorganisms will lose activity because the plasmolysis process takes place because of the presence of NaCl, which means the phenomenon of protoplasm is far away from the cell wall of the bacteria due to the lack of water [3–4].

There are many species of microorganisms that desperately need salinity for growth and development known as halophilic microorganisms, which often have low intracellular salt concentrations in order to maintain the osmotic balance between cytoplasm with the external medium, by accumulating high concentrations of organic osmoling agents [5].

Many studies of saline wastewater treatment have applied biological methods with the participation of oxygen and combination with halophilic microorganisms [6–7]. There has been a study to eliminate the chemical oxidation demand (COD) in saline wastewater by using a rotating biological disc system (RBC–Rotating Biological Contactor) with microbial sludge biomass supplemented with Halobacterium Halobium [8–11].

Nowadays, the use of probiotics in general and liquid probiotics in particular containing the yeast Saccharomyces strain, combining a number of bacteria strains to treat high–salt aquaculture wastewater are being interested in but no specific research. Currently on the market there are many different types of probiotics, but there are two types of probiotic products such as Microbe–Lift IND and EM–WAT1. Researching a biological solution of activated sludge suitable for treating aquatic wastewater with a high salt concentration, along with the addition of the yeast Saccharomyces strain combining some bacteria strains to enhance the treatment capacity is essential. This study contributes to the evaluation of the treatment efficiency of activated sludge when supplemented with 2 inoculants, Microbe–Lift IND and EM–WAT1 at different salinity levels and to give appropriate dosage for practical application.

2. Methods of research

2.1. Experimental method

a) Building aerobic bio–treatment model combining active sludge consisting of 7 tanks. With the operating parameters of the model include: tank volume of 36 liters, water storage time of 8 hours, wastewater flow of 1.25 ml/s, organic load of 4.5 kg/m^3.day. Seafood wastewater treatment with different concentrations from IND and EM–WAT1 bio–preparations. Sampling and analyzing COD, BOD$_5$, MLSS, S, pH targets to determine and evaluate the processing performance of the model.

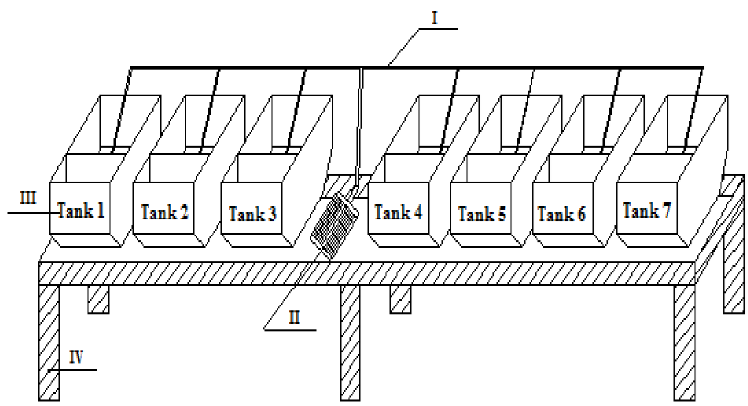

Figure 1. Model of experimental tank.

b) Model operation: Experiments 1, 2: During the test run, select the salinity and load limits: the total sample number is 126 samples with 5 indicators so there should be a total of 630 samples analyzed (126 samples x 5 indicators = 630 samples analyzed). The stage for determining the appropriate salinity: the stage determines the appropriate salinity: the total sample volume is 162 (54 + 108) samples, so there are a total of 324 samples analyzed (54 samples x 4 indicators + 108 x 1 indicators = 324 samples analyzed). Experiment 3: The optimal dosage determination phase of the supplement: with 294 samples analyzed (84 samples x 2 indicators + 42 x 3 indicators = 294 samples analyzed).

2.2. Sampling, preservation and analysis methods

Conduct measurement survey, sampling analysis of aquatic wastewater dynamic parameters for assessment of wastewater treatment capacity when supplementing preparations. Sampling, preservation and analysis methods.

– National standards TCVN 6663–1:2011 (ISO 5667–1:2006) with Water Quality–Sampling–Part 1: Sampling Program Guide and Sampling Techniques.

– National standards TCVN 6663–3:2008 (ISO 5667–3:2003) with Water Quality–Sampling. Guidelines for preservation and storage of water samples.

– National standards TCVN 5999:1995 (ISO 5667–10:1992) with Water Quality–Sampling. Instructions for wastewater sampling.

2.3. Comparison method

Assessment of the effectiveness of seafood wastewater treatment when supplementing preparations based on QCVN 11–MT: 2015/BTNMT; Level B National technical regulation on the effluent of aquatic products processing industry.

Table 1. Table on the analysis of seafood wastewater targets.

Parameter	Analysis method	Unit	Maximum allowable value (B)
Sample	TCVN 6663–3:2008 Water quality – Sampling, preservation	–	–
COD	TCVN 6491:1999 Water quality – Determination of chemical oxygen demand (COD)	mg/l	150
BOD_5	TCVN 6001–1:2008 Water quality – Determine biochemical oxygen demand after n days (BODn)	mg/l	50
Cl–	TCVN 6194 : 1996 Water quality – Determination of chloride salinity	mg/l	
pH	TCVN 6492:2011 Water quality – Determine pH	–	5.5–9
MLSS	TCVN 6625:2000 Water quality – Determination of suspended solids by filtration through a fiberglass filter	mg/l	100

2.4. Determined measurement method

– Statistical method and data processing: Running a data processing model to determine the accuracy of the experiment, making tables, charts to compare and evaluate model results.

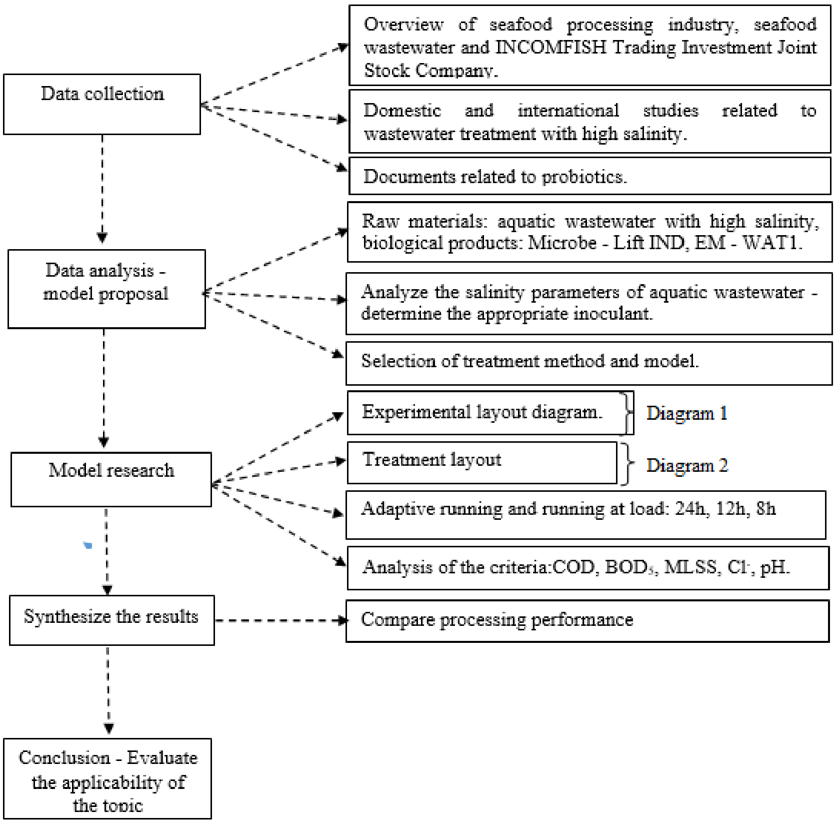

Figure 2. Research diagrams.

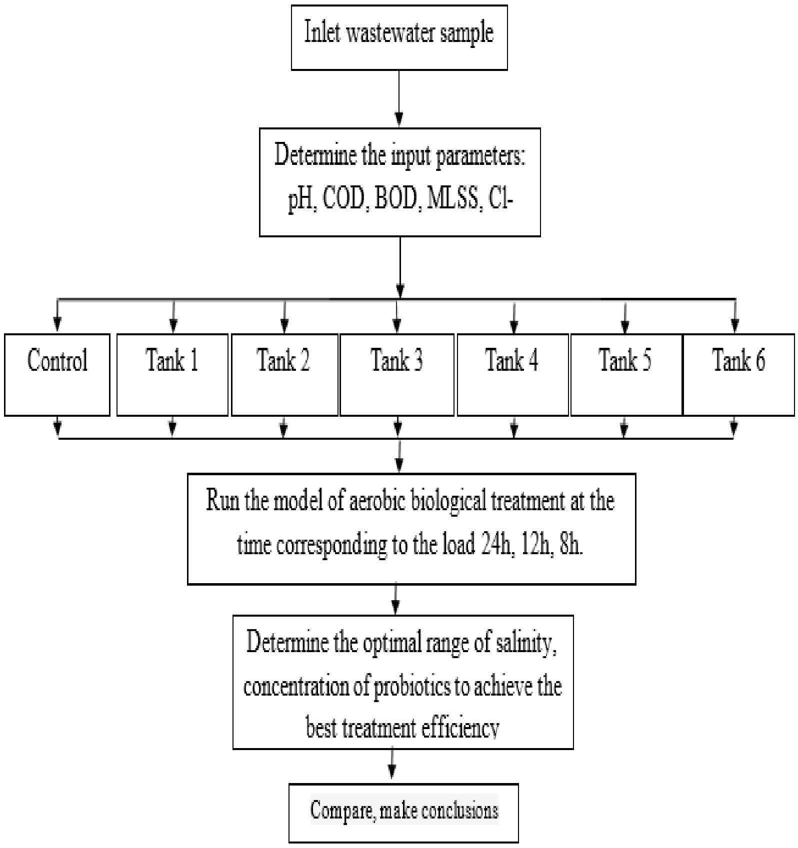

Figure 3. Experimental arrangement.

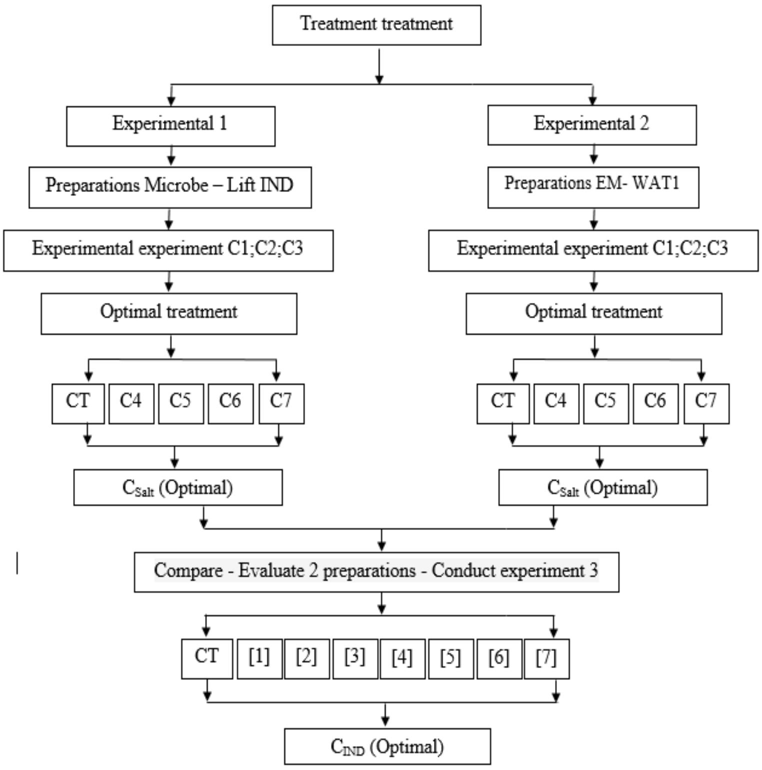

Figure 4. Experimental layout.

3. Results and discussion

To apply at a greater range wastewater sources with higher salinity, the study conducted experiments in 3 final tests corresponding to salinity of 1‰, 5‰, 10‰ and from selected the optimal processing value ranges from 6‰, 7‰, 8‰, 9‰, 10‰. From there, evaluate the treatment efficiency of the activated sludge method with bio–products and find out the optimal salinity range. Compare and select the most appropriate preparation, determine the optimal concentration of inoculants to apply in practice.

3.1. Determination of salinity value suitable for biological products

Conducting tests at 3 different salinity levels to find the most suitable treatment salinity range with the dosage of the supplement Microbe–Lift IND and EM–Wat1 recommended by the manufacturer.

The analysis results showed that Microbe–Lift IND inoculant was processed at higher salinity when compared with EM–WAT1. The evidence at 8‰ salinity, treatment efficiency after 6 days is more than 80%, approximately the treatment efficiency at salinity 6‰ and 7‰. And at 9‰ salinity the efficiency is lower than 80%. This shows that microorganisms still operate effectively at 8‰ salinity, 8‰ is chosen as the optimal salinity. Therefore, use Microbe–Lift IND probiotics to continue processing at optimal salinity to determine the most appropriate inoculant concentration. Based on research, we can choose probiotics suitable for wastewater with different salinity, to save treatment costs.

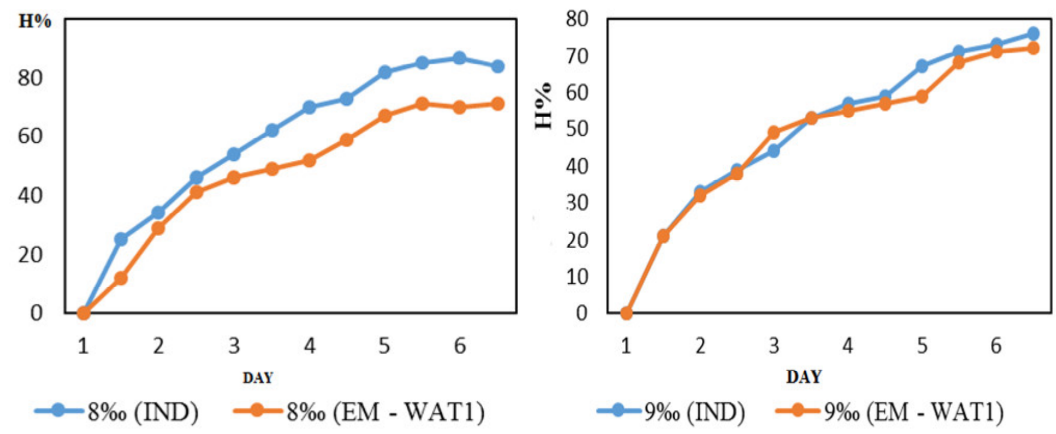

Figure 5. Processing efficiency of inoculants Microbe–Lift IND and EM–WAT1 at salinity 6‰, 7‰, 8‰, 9‰.

3.2. Test to determine the optimal concentration of the supplement at the appropriate salinity

Continue to experiment in different treatments to find out the optimal amount of probiotics: fix the salinity at 8‰, the retention time is 8 hours, added the tanks times the dosage Microbe–Lift IND supplement are 5 ml, 6 ml, 7 ml, 8 ml, 9 ml and 10 ml. Analyze the output samples, compare and conclude the dosage of probiotics to be used.

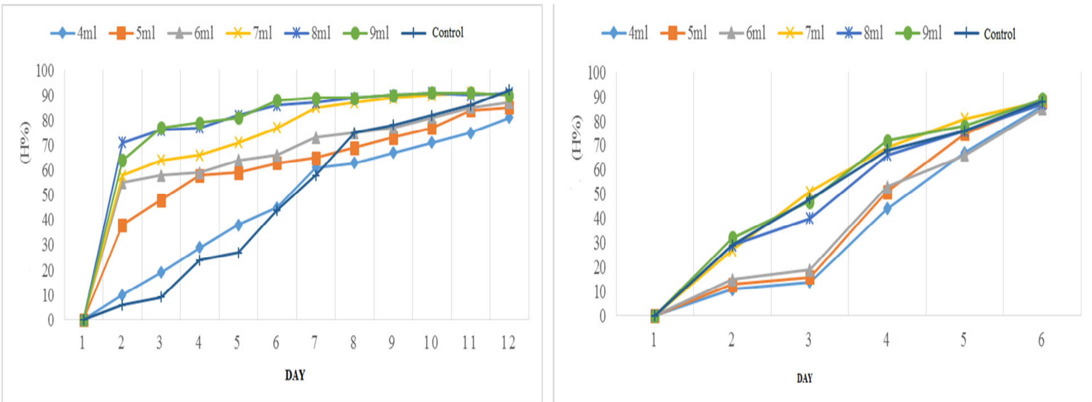

Figure 6. Evolution of COD and BOD_5 treatment efficiency by day when supplementing with Microbe – Lift IND probiotics at different dosages.

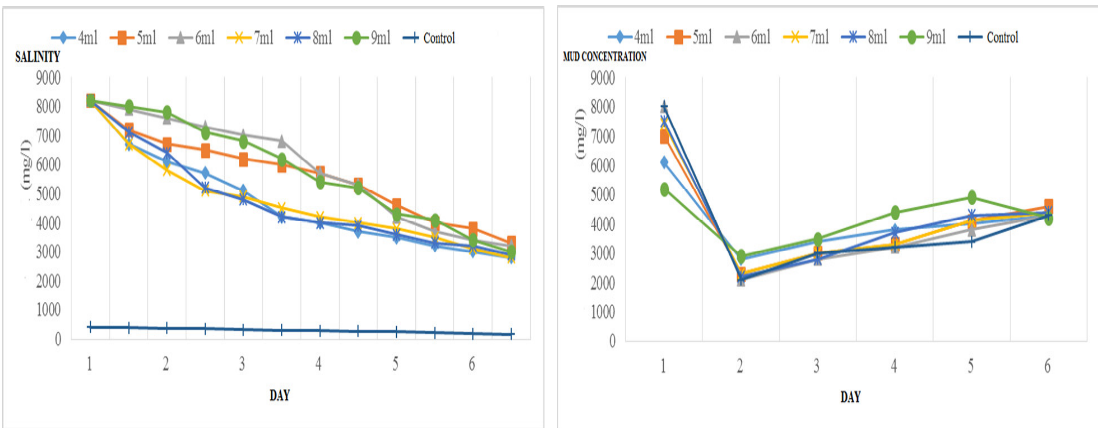

Figure 7. Performance of salinity treatment and MLSS by day when supplementing with Microbe–Lift IND probiotics at different dosages.

COD analysis results showed that the higher the dose of probiotics added, the higher the treatment efficiency. Therefore, the optimal concentration of probiotics is 0.25 ml of inoculant/L of wastewater (corresponding to 9ml/36L of study wastewater). BOD_5 analysis results show that treatment efficiency at 7 ml, 8 ml and 9 ml is better than 4 ml, 5 ml, 6 ml, in which it is at the most stable 7 ml.

Analysis results showed that the salinity in the tank decreases over time. It shows that the higher the volume of the inoculant is in proportion to the lower the salinity. The amount of sludge in the tanks increased during the first days of treatment but was corrected and remained stable at about 2000–4000 ml. The results show that microorganisms decompose organic matter present in wastewater and increase biomass and partly absorb salt from wastewater.

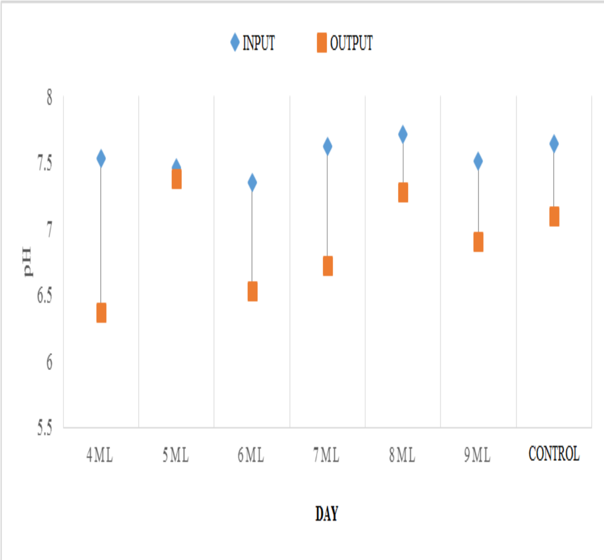

Figure 8. The evolution of pH by day when supplementing with Microbe–Lift IND at different dosages.

With low inoculant concentration, the pH range is wider. When the concentration of the inoculant is increased, the range of variation is reduced and lies at the effective level of treatment.

4. Conclusion

Compared in volumes, it was concluded that at 9 ml, wastewater treatment capacity at 8‰ salinity reach over 90% by 4 days, if the dosage supplement is low, the processing performance is not equal high dosage supplementation is expensive for the purchase of additional preparations.

Therefore, the preferred concentration of the composition is 0.25 ml of wastewater. Optimal handling load: 4.5kg COD/m^3.day for 8 hours of storage time for 2 preparations.

When running the model at 3 loads: 24–hour, 12–hour, 8–hour when the addition of 2 preparations then the 8–hour load achieves high processing performance abouve 80% at salinity 1‰ and 5‰ and 10‰ are the lowest processing efficiency.

Processing performance of Microbe–Lift IND preparations is high at salinity 6‰, 7‰ and 8‰ and decreased at salinity 9‰. The processing performance of EM–WAT1 preparations is most effective in salinity 6‰ and decreases when increasing salinity to 7‰, 8‰, 9‰. From there, it is concluded that the ability to process Microbe–Lift IND at high salinity better than EM–WAT1.

Wastewater after treatment in accordance with QCVN 11–MT: 2015/BTNMT; Column B National technical regulation on the effluent of aquatic products processing industry.

Author's contribution: Constructing research ideas: V.S.L., V.P.N.; Select research method: V.S.L., V.P.N., P.H.; Sampling: V.S.L., V.P.N.; Sampling analyze: V.S.L., V.P.N.; Data processing: V.S.L., V.P.N., P.H.; Write the draft of the article: V.S.L., V.P.N.; Article editing: V.S.L., P.H.

Conflicts of Interest: The authors declare no conflict of interest.

References

1. Ventosa, A.; Nieto, J.J.; Oren, A. Biology of Moderately Halophilic Aerobic Bacteria. *Microbiol. Mol. Biol. Rev.* **1998**, *62*, 504–544.
2. Dincer, A.R.; Kargi, F. Use of halophilic bacteria in biological treatment of saline wastewater by fed-batch operation. *Water Environ. Res.* **2000**, *72*, 170–174.
3. Dincer, A.R.; Kargi, F. Salt inhibition kinetics in nitrification of synthetic saline wastewater. *Enzyme Microb. Technol.* **2001**, *28*, 661–665.
4. He, H.; Chen, Y.; Li, X.; Cheng, Y.; Yang, C.; Zeng, G. Influence of salinity on microorganisms in activated sludge processes: A review. *Int. Biodeterior. Biodegrad.* **2017**, *119*, 520–527.
5. Johir, M.A.H.; Vigneswaran, S.; Kandasamy J.; BenAim, R.; Grasmick, A. Effect of salt concentration on membrane bioreactor (MBR) performances: Detailed organic characterization. *Desalin.* **2013**, *322*, 13–20.
6. Lefebvre, O.; Moletta, R. Treatment of organic pollution in industrial saline wastewater: a literature review. *Water. Res.* **2006**, *40*, 3671–3682.
7. Nguyen, H.N.; Phung, T.K.N. Overview of Vietnam's seafood industry. Avalable online, November 8, 2019. http://vasep.com.vn/1192/OneContent/tong–quan–nganh.htm.
8. Lefebvre, O.; Moletta, R. Treatment of organic pollution in industrial saline wastewater: A literature review. *Water Res.* **2006**, *40*, 3671–3682.
9. Das, P.; Behera, B.K.; Meena, D.K.; Azmi, S.A.; Chatterjee, S.; Meena, K.; Sharma, A.P. Salt stress tolerant genes in halophilic and halotolerant bacteria: Paradigm for salt stress adaptation and osmoprotection. *Microbiol. Appl. Sci.* **2015**, *4*, 642–658.
10. Sivaprakasam, S.; Mahadevan, S.; Sekar, S.; Rajakumar, S. Biological treatment of tannery wastewater by using salt–tolerant bacterial strains. *Microb. Cell Fact.* **2008**, *7*, 1–15.
11. Abou–Elela, S.I.; Kamel, M.M.; Fawzy, M.E. Biological treatment of saline wastewater using a salt–tolerant microorganism. *Desalin.* **2010**, *250*, 1–5.

VIETNAM JOURNAL OF
HYDROMETEOROLOGY

Research Article

Calculation of methane gas emissions (CH_4) from domestic waste water in Nhue–Day River basin

Cai Anh Tu[1*], Nguyen Thi Kim Anh[2], Le Van Quy[2], Pham Thi Quynh[2]

[1] VNU University of Science, Vietnam National University, Hanoi; caianhtu1984@gmail.com
[2] Viet Nam Institute of Meteorology, Hydrology and Climate Change; nguyenkimanh1004@gmail.com; vanquymt@gmail.com; quynhpt0310@gmail.com
* Correspondence: caianhtu1984@gmail.com; Tel.: +84–936324567
Received: 08 January 2021; Accepted: 20 February 2021; Published: 25 April 2021

Abstract: The process of domestic wastewater treatment has created a large amount of greenhouse gases (GHG). However, the measure for evaluating domestic wastewater treatment is only the treatment efficiency. Meanwhile, the factors to assess the possibility of generating GHG emissions have not been concerned. The Nhue–Day River basin plays an important role on the socio–economic development; therefore, one of the problem needs to be filled with concern is the level of GHG emissions from waste sources, including domestic wastewater. In order to contribute to forecast and evaluate the domestic wastewater impacts on the generation of GHG emissions, the study has been implemented. The main methods taken as synthesis, analysis, and inheritance of research documents and calculations are based upon the guidance of the Intergovernmental Panel on Climate Change, 2006, chapter 5,6 – Wastewater disposal and treatment and other Vietnamese studies on climate change. The study has calculated GHG emissions from wastewater in the Nhue–Day River basin through the use of septic toilets, other toilets and centralized treatment plant by aerobic technologies for the current status (2019) and the scenario in 2030. Thereby, it shows that the CH_4 gas is mainly generated from anaerobic treatment of domestic wastewater with total CH_4 emissions currently at 52,850,201.55 Gg CH_4/year (processed 49,742,761.24 Gg CH_4/year accounting for 94.12%); and for the scenario up to 2030 is 212,764,669.79 Gg CH_4/year (processed 212,700,144.64 Gg CH_4/year at 99.97%).

Keywords: Nhue–Day River basin; Methane gas emissions; Domestic waste.

1. Introduction

The Nhue–Day River basin is a dynamic economic center as well as important economic area of the North and the whole country. Especially, Hanoi under the Nhue–Day River basin is the capital, the economic, cultural and political center of Vietnam. The basin has a total area of 7,665 km^2, accounting for 10% of the entire Red River basin, in the territory of 5 provinces/cities as Hoa Binh, Hanoi, Ha Nam, Nam Dinh and Ninh Binh. Nevertheless, the environment in the Nhue–Day River basin is considered as one of high levels of pollution due to untreated wastewater discharged into the river [1]. According to different studies [1–4], the biggest source of environmental pollution for the Nhue–Day River basin is domestic wastewater, accounting for up to 70% of total wastewater in the basin. In addition to increase the pollution of river, domestic wastewater is also the source of greenhouse gas emissions, thereby leading to negative impacts on environmental quality and hman health. Over the past years, the measures of domestic wastewater treatment (septic tanks, toilets, centralized wastewater treatment plants, etc.) have achieved certain results that contribute to the improvement of environmental quality. At present, new challenges are being considered and oriented to ensure the sustainability of wastewater treatment measures in terms of economic sustainability as well as limit negative impacts on the environment. Greenhouse gas emissions from the measures of domestic wastewater treatment are one of the main factor related to the sustainability of the approach. The recent studies have identified that domestic wastewater treatment as potential sources of artificial GHG emissions contributes climate change and air pollution [5]. Methane gas (CH_4) is mainly generated by anaerobic decomposition of organic matter (sludge from wastewater treatment systems). Nevertheless, there has not been any specific study on the inventory and evaluation of GHG emission trend from domestic wastewater in the Nhue–Day River basin. Besides, due to rapid economic development, the achievement of green growth targets is currently a big challenge for Vietnam [6]. Therefore, the major objective of the study aims to assess the impact of domestic wastewater on the generation of greenhouse gas emissions and provide the first visual perception of its contribution on reduction emission target of Vietnam.

The calculation of CH_4 emission from domestic wastewater in the Nhue–Day River basin is indicated through the main subjects:

– Untreated domestic wastewater (Discharge wastewater into neighboring areas as rivers, lakes, etc.)

– Treated domestic wastewater: (i) Centralized wastewater treatment plants (CWTP), (ii) Septic tanks (ST), (iii) Other types of toilets (T).

2. Methodology

2.1. Description of study site

The Nhue–Day River basin has geographic coordinates from 20^o to 21^{o}20’ North latitude and 105^o to 106^{o}30’ East longitude, including the administrative territory of 5 provinces/cities (Table 1, Figure 1).

Table 1. The scope of Nhue–Day River basin [7].

No	Province/City	Cities, counties, districts, towns
1	Hoa Binh	Districts: Ky Son, Luong Son, Kim Boi, Yen Thuy và Lac Thuy.
2	Hanoi	Districts: Ba Dinh, Bac Tu Lirm, Cau Giay, Dong Da, Ha Dong, Hai Ba Trung, Hoan Kiem, Hoang Mai, Nam Tu Liem, Tay Ho, Thanh Xuan. Ba Vi, Chuong My, Dan Phuong, Hoai Duc, My Duc, Phu Xuyen, Phuc Tho, Quoc Oai, Soc Son, Thanh Oai, Thanh Tri, Thach That, Thuong Tin, Ung Hoa, Son Tay city.
3	Ha Nam	Phu Ly city; districts: Kim Bang, Ly Nhan, Thanh Liem, Binh Luc, Duy Tien.
4	Ninh Binh	Ninh Binh city, Tam Diep town, districts: Nho Quan, Gia Vien, Hoa Lu, Kim Son, Yen Khanh, Yen Mo.
5	Nam Dinh	Nam Dinh city, districts: Vu Ban, Y Yen, My Loc, Nam Truc, Truc Ninh, Xuan Truong, Giao Thuy, Hai Hau và Nghia Hung.

The study focuses upon domestic wastewater discharging from various households within the river basin.

2.2. Research methods

2.2.1. Methods on synthesization, analysis and inheritance of research documents

The method is used to collect, synthesize and analyze relevant data such as calculation formulas and necessary parameters. In which, the parameters include as population, percentage of people applying septic tanks and not applying domestic wastewater treatment, proportion of people using other types of toilets, capacity of wastewater treatment plants (by aerobic technology), etc. The statistic calculates for the year of 2019 based upon the Preliminary census results in 2019 from General Statistics Office. The data predicts for 2030 according to the Decision 681/QD–TTg on the Planning of drainage and wastewater treatment systems for residential and industrial areas in the Nhue–Day River basin to 2030.

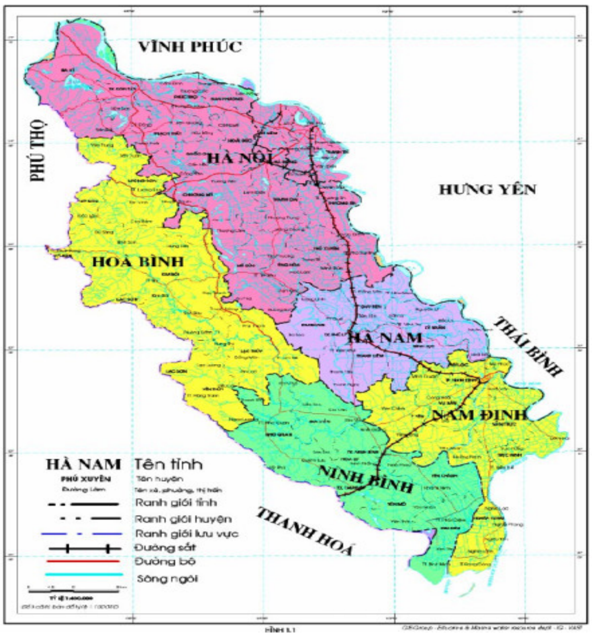

Figure 1. Location of Nhue–Day River basin.

2.2.2. Calculation methods

The calculation formulas for GHG emissions from domestic wastewater are based upon Vietnamese and international documents on GHG inventory of waste and wastewater [8,9,10]. The main formulas are applied in this study as:

Determine the total organic content in wastewater

The total organic content in waste water is determined by the formula:

$$T0W_i = P \times BOD \times I \times 365 \quad (1)$$

where $T0W_i$ is the total organic content in the wastewater (kg BOD/year); P is Population in inventory year (person); BOD is the BOD city–specific per capita BOD in inventory year (g BOD/person/day); I is the correction factor; i is the population group.

The amount of BOD generated per capita in domestic wastewater is taken according to the prescribed value of 35 g/person/day [11].

Determine the emission factor

The emission factor is calculated for each treatment method according to the formula:

$$EF_j = Bo \times MCF_j \times U_i \times T_{ij} \quad (2)$$

where EF_i is the mission factor (kg CH_4/kg BOD); B_o is the maximum CH_4 producing capacity (kg CH_4/kg BOD): 0.6; MCF_j is the CH_4 correction factor (fraction); U_i is the fraction of population group i in inventory year; T_{ij} is the degree of utilization (ratio) of treatment/discharge pathway or system, j, for each population group fraction i in inventory year; i is the population group; j is each treatment/discharge system.

Determine the total CH_4 emissions

The total CH_4 emissions are determined by the following formula [8]:

$$CH_4 = \sum i\, [(T0W_i - S_i) \times EF_i - R_i] \times 10^{-3} \quad (3)$$

where CH_4 is total CH_4 emissions (ton/year); $T0W_i$ is total CH_4 emissions (ton/year); S_i is the organic component removed as sludge (kg BOD /year); EF_i is the emission factor (kg

CH_4/kg BOD); R_i is the amount of CH_4 recovered (kg CH_4/year); i is the population groups are urban and rural. The wastewater treatment and handling system is classified as septic tanks, toilets, with/without drainage systems).

2.2. Research subjects

Basic parameters for calculation

The calculation parameters to determine CH_4 generated from domestic wastewater collected from the published papers verified by the Scientific Councils.

Table 2. Urban and rural population of provinces in Nhue–Day River basin in 2019 [7].

Province	Population (people)	Urban	Rural
		Number of people	Number of people
Hoa Binh	854,131	134,081	720,050
Hanoi	8,053,663	3,962,310	4,091,353
Ha Nam	811,126	68,466	742,660
Ninh Binh	1,780,393	339,019	1,514,093
Nam Dinh	982,487	206,524	775,963
Total	*12,481,800*	*4,710,400*	*6,527,680*

Based upon the average fertility rates according to the 2019 Local Statistical Yearbook, the urban and rural populations in the Nhue–Day River basin are determined for the year of 2030.

Table 3. Urban and rural population of provinces in Nhue–Day River basin in 2030 [7].

Province	Population (people)	Urban	Rural
		Number of people	Number of people
Hoa Binh	915,222	143,671	771,551
Hanoi	10,309,183	5,072,000	5,237,183
Ha Nam	892,217	75,311	816,906
Ninh Binh	1,483,079	332,000	1,482,747
Nam Dinh	1,097,324	230,663	866,661
Total	*14,697,025*	*5,521,977*	*9,175,048*

3. Results and discussions

3.1. Calculation on current level of methane greenhouse gas emissions from domestic wastewater

3.1.1. Results of total organic content in domestic wastewater

a) Basic parameters for calculation

The calculation parameter of total organic content in domestic wastewater is based on the guidance document on GHG inventory issued by the Intergovernmental Panel on Climate Change (IPCC) in 2006 along with a number of recent studies on environmental issues in the Nhue–Day River basin.

Table 4. Basic parameters for emission calculation [8].

Parameter	Value
I – Correction factor	= 1,25: For industrial and domestic wastewater. = 1: For domestic wastewater.
BOD g/peson/day (assumption of moderate emissions)	35
Level of wastewater treatment Tkj (%)	
– Septic tank	20
– Drainage drainage (Discharge into rivers, lakes and	10

Parameter	Value
surrounding area)	
– Centralized wastewater treatment plants (by aerobic technology)	50
– Other treatment methods (Other types of toilet)	20

The average percentage of people using a septic toilet in the Nhue–Day River basin accounts for 82% of the total population at 7,779,136 people [7]. Besides, the average rate of people using other types of toilets accounts for 10%, corresponding to 1,450,192 people. The average percentage of the population not applying any domestic wastewater treatment system is 8% at 2,008,752 people.

Accordingly, the centralized wastewater treatment plant (CWTP) using aerobic technology in the Nhue–Day River basin currently handle about 7.73% (875.7x10^3 m^3/day) of the total amount of domestic wastewater (1,333.4x10^3 m^3/day) [5,7]. Thus, it is estimated that the CWTP using aerobic technology for approximately 964,843 people and the amount of wastewater at about 11,516,957 people in the basin is not discharged into the wastewater treatment system (Table 5).

Table 5. Population rate according to the current treatment plan [7].

Type of treatment method	Urban			Rural			Total of people
	Rate (%)		Number of people	Rate (%)		Number of people	
	Value range	Average value		Value range	Average value		
Hygienic toilets in provinces	78–95	92	4,333,568	68–78	75	4,895,760	9,229,328
Average septic tanks in the provinces of the river basin (%)	75–85	82	3,862,528	55–62	60	3,916,608	7,779,136
Population using other toilets	7–12	10	471,040	10–17	15	979,152	1,450,192
Population does not apply any treatment methods for domestic wastewater	5–9	8	376,832	21–28	25	1,631,920	2,008,752
Estimated population has domestic wastewater treated in centralized wastewater treatment plants (CWTP) by aerobic technology		7.73	964,843				964,843
Estimated population has untreated domestic wastewater in CWTP							11,516,957

b) Calculation results

The calculation results in the Nhue–Day River basin show that:

– Total organic content generated in case of no domestic wastewater treatment system is 25,661,806,8 kg BOD/year.

– The total organic content generated in case of domestic wastewater treatment is 130,230,534,2 kg BOD/year as:

+ Derived from the concentrated wastewater treatment plant (CWTP) is 12,325,869 kg BOD/year.

+ Derived from the septic tank system (ST) is 99,378,462.4 kg BOD/year

+ Derived from other types of toilet (T): 18,526,202,8 kg BOD/year.

– The total organic content generated in both cases without and with wastewater treatment system in the Nhue–Day River basin is 155,892,341 kg BOD/year.

$$T0Wi \text{ (no treatment)} = 2{,}008{,}752 \text{ people} \times 35 \text{ g/person/day} \times 1 \times 365 \text{ days} = 25{,}661{,}806.8 \text{ kg BOD/year}$$

$$T0Wi \text{ (CWTP)} = 964{,}843 \text{ people} \times 35 \text{ g/person/day} \times 1 \times 365 \text{ days} = 12{,}325{,}869 \text{ kg BOD/year}$$

T0Wi (ST) = 7,779,136 people x 35 g/person/day x 1 x 365 days
= 99,378,462.4 kg BOD/year
T0Wi (T) = 1,450,192 people x 35 g/person/day x 1 x 365 days
= 18,526,202.8 kg BOD/year

3.1.2. Calculation results of emission factors

a) Basic parameters for calculation

The CH_4 emission factor is calculated based upon specific treatment cases in the Day–Nhue River basin (Tables 6 and 7).

Table 6. Correction coefficient of CH_4 (MCF_j) for domestic wastewater [9].

Case	CH_4 value	
No treatment method		
– No treatment for domestic wastewater	0.1	0–0.2
Treatment method		
Centralized wastewater treatment plants by aerobic technology – Good management	0	0–0.1
Centralized wastewater treatment plants by aerobic technology – Mismanagement	0.3	0.2–0.4
Septic tanks	0.5	0.5
Other types of toilets	0.7	0.7–1.0

Table 7. Basic parameters for emission calculation [11].

Parameter	
Amount of CH_4 recovered (kg CH_4/year)	Since the sludge treatment is currently only carried out in wastewater treatment plants at a very low rate, this value thereby could be ignored.
Ri–Amount of CH_4 recovered (kg CH_4/year)	Since there is no mandatory regulation to recover CH_4 gas during the sludge treatment, this value is 0.

b) Calculation results

The results indicate that the CH_4 emission factor in case of not applying any measures for domestic wastewater treatment is 12,052.51 kg CH_4/kg total BOD.

The CH_4 emission factor for domestic wastewater treatment system at a concentrated wastewater treatment plant (by aerobic technology) is 86,835.87 kg CH_4/kg total BOD.

The CH_4 emission factor in case of using a septic tank is 466,748.16 kg CH_4/kg total BOD, and is 121,816.13 kg CH_4/kg total BOD for other toilets.

Thus, the total CH_4 emission factor for all cases with and without treatment measures is 687,452.67 kg CH_4/kg total BOD.

EF_j (no treatment) = 0.6 kg CH_4/kg BOD x 0.1 x 2,008,752 people x 10%
= 12,052.51 kg CH_4/kg total BOD
EF_j (CWTP) = 0.6 kg CH_4/kg BOD x 0.3 x 964,843 people x 50%
= 86,835.87 kg CH_4/kg total BOD
EF_j (ST) = 0.6 kg CH_4/kg BOD x 0.5 x 7,779,136 people x 20%
= 466,748.16 kg CH_4/kg total BOD
EF_j (T) = 0.6 kg CH_4/kg BOD x 0.7 x 1,450,192 people x 20%
= 121,816.13 kg CH_4/kg total BOD

3.1.3. Calculation results of total CH4 emission

a) Basic parameters for calculation

The basic parameter for the identification of total CH_4 emission is based upon the calculation from:

– Total organic content in domestic wastewater;

– Emission factors.

b) Calculation results

CH_4 (no treatment) = 25,661,806.8 kg BOD/year x 1,205.251 kg CH_4/kg total BOD x 10^{-3}
= 30,928,918 tons CH_4/year

CH_4 (CWTP) = 12,325,869 kg BOD/year x 86,835.87 kg CH_4/kg total BOD x 10^{-3}
= 1,070,327,558 tons CH_4/year

CH_4 (ST) = 99,378,462.4 kg BOD/year x 466,748.16 kg CH_4/kg total BOD x 10^{-3}
= 46,384,714,469 tons CH_4/year

CH_4 (T) = 18,526,202.8 kg BOD/year x 121,816.128 kg CH_4/kg total BOD x 10^{-3}
= 2,256,790,292 tons CH_4/year

Therefore, the total CH_4 emission from domestic wastewater in the Nhue–Day River basin is 49,742,761,237 tons CH_4/year corresponding to 49,742,761.24 Gg CH_4/year.

Table 8. Results of total organic value, correction coefficient and total CH_4 emission in domestic wastewater in the Nhue–Day River basin in 2019.

Treatment method		Symbol	Total organic content (kg BOD/year)	Correction coefficient CH_4 (kg CH_4/ kg total BOD)	Total CH_4 emission (ton CH_4/year)
No treament method	Discharge wastewater into the surrounding area (river, lake, etc.)	No treatment	25,661,806.8	1,205.251	30,928,918
Treament method	Centralized wastewater treatment plants (by aerobic technology)	CWTP	12,325,869	86,835.87	1,070,327,558
	Septic tank system	ST	99,378,462.4	466,748.16	46,384,714,469
	Other treatment methods (Other types of toilets)	T	18,526,202.8	121,816.128	2,256,790,292
	Total treatment measures		130,230,534.2	675,400.16	49,711,832,319
	Total		155,892,341	676.605.41	49,742,761,237

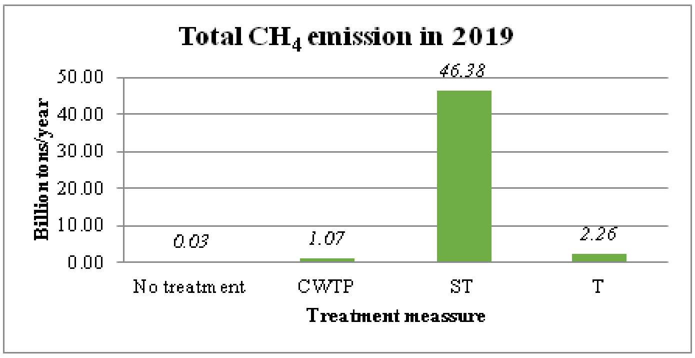

Figure 2. Total CH_4 emission in the Nhue–Day River basin in 2019.

Table 8 and Figure 1 show the calculation results of total organic content, the correction coefficient and total CH_4 emission in domestic wastewater in the Nhue–Day River basin such as:

– Total organic content: 155,892,341 kg BOD/year.

– Correction coefficient: 676,605.41 kg CH_4/kg total BOD.

– The total emissions are 49,742,761,237 tons CH_4/year corresponding to 49,742,761.24 Gg CH_4/year. CH_4 greenhouse gas mainly comes from the anaerobic decomposition of domestic wastewater in septic tanks and other types of toilets. Specifically, CH_4 gas generated from anaerobic decomposition (septic tank systems and other toilets) accounts for 97.85% (equivalent to 48,641,504,761 kg CH_4/kg total BOD) compared to total amount of emissions in case of applying treatment measures (corresponding to 49,711,832,319 kg CH_4/kg total BOD).

3.2. Calculation on the level of methane greenhouse gas emissions from domestic wastewater in 2030

3.2.1. Results of total organic content in domestic wastewater

Pursuant to the Decision 681/QD–TTg on the Planning of drainage and wastewater treatment systems for residential and industrial areas in the Nhue–Day River basin to 2030 and the plan of the Hanoi People's Committee on environmental protection in Nhue–Day River basin until 2020, the CWTP by aerobic technology in the Nhue–Day River basin will be able to handle about 43% by 2030 (from 875.7 x 10^3 m^3/day at present to 1,182.5 x 10^3 m^3/day according to Decision 681/QD–TTg) [12]. Therefore, it is estimated that the CWTP with aerobic technology for about 6,319,721 people in the basin and the amount of wastewater is not discharged into the wastewater treatment system at approximately 8,377,304 people. Additionally, the average proportion of people using a septic toilet account for 92% of total population in the Nhue–Day River basin at 13,521,263 people. The average rate of people using other types of toilets accounts for 8% corresponding to 1,175,762 people. Besides, there are no households that do not apply any measures of domestic wastewater treatment by 2030.

Table 9. Population rate according to the treatment plan in 2030.

Type of treatment method	Urban		Rural		Total of people
	Average value (%)	Number of people	Average value (%)	Number of people	
Hygienic toilets in provinces	100	5,521,977	90	8,257,543	13,779,520
Average septic tanks in the provinces of the river basin (%)	92	8,080,219	70	6,422,534	14,502,753
Population using other toilets	8	441,758	20	1,835,010	2,276,768
Population does not apply any treatment methods for domestic wastewater	0	0	10	917,505	917,505
Estimated population has domestic wastewater treated in centralized wastewater treatment plants (CWTP) by aerobic technology	43				6,319,721
Estimated population has untreated domestic wastewater in CWTP					8,377,304

Calculation results

T0Wi (no treatment) = 917,505 people x 35 g/person/day x 1 x 365 days
= 11,721,126.38 kg BOD/year

T0Wi (CWTP) = 6,319,721 people x 35 g/person/day x 1 x 365 days
= 80,734,435.78 kg BOD/ year

T0Wi (ST) = 14,502,753 people x 35 g/person/day x 1 x 365 days
= 185,272,669.58 kg BOD/year

T0Wi (T) = 2,276,768 people x 35 g/person/day x 1 x 365 days
= 29,085,711.2 kg BOD/year

– Total organic content generated in case of no domestic wastewater treatment system is 11,721,126.38 kg BOD/year.

– Total organic content generated in case of domestic wastewater treatment system is 295,092,816.56 kg BOD/year as:

+ Derived from the concentrated wastewater treatment plant (CWTP) is 80,734,435.78 kg BOD/year.

+ Derived from the septic tank system (ST) is 185,272,669.58 kg BOD/year.

+ Derived from other types of toilet (T) is 29,085,711.2 kg BOD/year.

– The total organic content generated in both cases without and with wastewater treatment system in the Nhue–Day River basin is 306,813,942.94 kg BOD/year.

3.2.2. Calculation results of emission factors

Calculation results

The results indicate that the CH_4 emission factor in case of not applying any measures for domestic wastewater treatment is 5,505.03 kg CH_4/kg total BOD.

The CH_4 emission factor for domestic wastewater treatment system at a CWTP (by aerobic technology) is 568,774.89 kg CH_4/kg total BOD.

The CH_4 emission factor in case of using a septic tank is 870,165.18 kg CH_4/kg total BOD, and is 191,248.51 kg CH_4/kg total BOD for other toilets.

Thus, the total CH_4 emission factor for all cases with and without treatment measures is: 1,635,639.61 kg CH_4/kg total BOD.

E_j (no treatment) = 0.6 kg CH_4/kg BOD x 0.1 x 917,505 people x 10%
= 5,505.03 kg CH_4/kg total BOD

E_j (CWTP) = 0.6 kg CH_4/kg BOD x 0.3 x 6,319,721 people x 50%
= 568,774.89 kg CH_4/kg total BOD

E_j (ST) = 0.6 kg CH_4/ kg BOD x 0.5 x 14,502,753 people x 20%
= 870,165.18 kg CH_4/kg total BOD

EF_j (T) = 0.6 kg CH_4/kg BOD x 0.7 x 2,276,768 people x 20%
= 191,248.51 kg CH_4/kg total BOD

3.2.3. Calculation results of total CH_4 emission

a) Basic parameters for calculation

The basic parameter for the identification of total CH_4 emission is based upon the calculation from:

– Total organic content in domestic wastewater;

– Emission factors.

b) Calculation results

CH_4 (no treatment) = 11,721,126.38 kg BOD/year x 5,505.03 kg CH_4/kg total BOD x 10^{-3}
= 64,525,152 tons CH_4/year

CH_4 (CWTP) = 80,734,435.78 kg BOD/year x 568,774.89 kg CH_4/kg total BOD x 10^{-3}
= 45,919,719,830 tons CH_4/year

CH_4 (ST) = 185,272,669.58 kg BOD/year x 870,165.18 kg CH_4/kg total BOD x 10^{-3}
= 161,217,825,874 tons CH_4/year

(T) = 29,085,711.2 kg BOD/year x 191,248.51 kg CH_4/kg total BOD x 10^{-3}
= 5,562,598,930 tons CH_4/year

Therefore, the total CH_4 emission from domestic wastewater in the Nhue–Day River basin is 212,764,669,786 tons CH_4/year corresponding to 212,764,669.79 Gg CH_4/year.

Table 10. Results of total organic value, correction coefficient and total CH_4 emission in domestic wastewater in the Nhue–Day River basin in 2030.

Treatment method		Symbol	Total organic content (kg BOD/year)	Correction coefficient CH_4 (kg CH_4/kg total BOD)	Total CH_4 emission (ton CH_4/year)
No treament method	Discharge wastewater into the surrounding area (river, lake, etc.)	No treatment	11,721,126.38	5,505.03	64,525,152

Treatment method		Symbol	Total organic content (kg BOD/year)	Correction coefficient CH_4 (kg CH_4/kg total BOD)	Total CH_4 emission (ton CH_4/year)
Treament method	Centralized wastewater treatment plants (by aerobic technology)	CWTP	80,734,435.78	568,774.89	45,919,719,830
	Septic tank system	ST	185,272,669.58	870,165.18	161,217,825,874
	Other treatment methods (Other types of toilets)	T	29,085,711.2	191,248.51	5,562,598,930
	Total treatment measures		295,092,816.56	1,630,188.58	212,700,144,634
Total				1,635,693.61	212,764,669,786

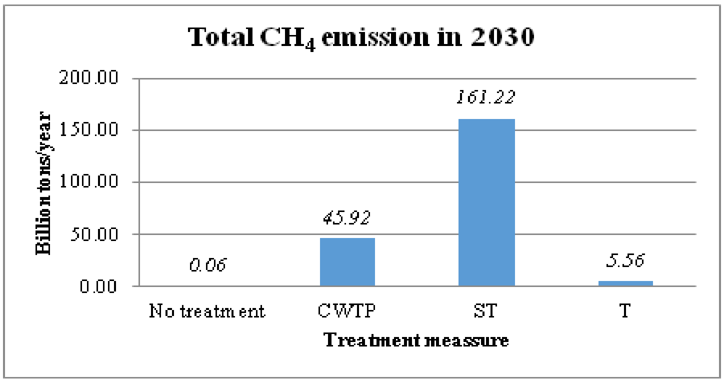

Figure 3. Total CH_4 emission in the Nhue–Day River basin in 2030.

Table 10 and Figure 2 describe that the calculation results of total organic content, the correction coefficient and total CH_4 emission in domestic wastewater in the Nhue–Day River basin by 2030 as:

– Total organic content: 306,813,942.94 kg BOD/year.

– Correction coefficient: 1,635,693.61 kg CH_4/kg total BOD.

– The total emissions are 212,764,669,786 tons CH_4/year corresponding to 212,764,669.79 Gg CH_4/year. CH_4 greenhouse gas mainly comes from the anaerobic decomposition of domestic wastewater in septic tanks and other types of toilets. Specifically, CH_4 gas generated from anaerobic decomposition (septic tank systems and other toilets) accounts for 78.41% (equivalent to 166,780,424,804 kg CH_4/kg total BOD) compared to total amount of emissions in case of applying treatment measures (corresponding to 212,700,144,634 kg CH_4/kg total BOD).

4. Conclusion

The study has indicated that the total amount of gas emissions from domestic wastewater reach at 52,850,201.55 Gg CH_4/year in 2019 and 212,764,669.79 Gg CH_4/year by 2030. CH_4 greenhouse gas mainly comes from the application of anaerobic treatment measures for domestic wastewater. In 2019, the total emissions are 49,742,761.24 Gg CH_4/year. Specifically, CH_4 gas generated from anaerobic digestion (septic tank systems and other types of toilets) accounts for 97.85% of the total emissions in case of applying treatment measures. In 2030, CH_4 gas from anaerobic decomposition only remains at 78.41% of the total emissions when applying the measures; meanwhile aerobic treatment efficiency in plants has increased from 7.73% in 2019 to 43% by 2030.

Accordingly, among with the requirement on waste management to limit the GHG generation through anaerobic measures, it is necessary to encourage the use of environmentally friendly technologies in centralized wastewater treatment plants [13]. The study proposes that, when the operational efficiency of waste treatment technologies is considered, it should take into account the level of GHG generation besides the factors of wastewater treatment efficiency [14]. Moreover, it is necessary to have further specific studies on other GHG emissions in the Nhue–Day River basin.

Author Contributions: Conceptualization, C.A.T.; Data sets, C.A.T., L.V.Q.; Methodology, C.A.T., P.T.Q.; Verification of results, C.A.T., N.K.A., L.V.Q., P.T.Q.; Writing–original draft preparation, C.A.T., N.K.A., L.V.Q., P.T.Q.; Writing–review and editing, C.A.T., N.K.A., L.V.Q., P.T.Q.

Conflicts of Interest: The authors declare no conflict of interest.

References

1. Ho, M.D.; Nguyen, T.T.H. Assessment on the current status of greenhouse gas emissions, environmental classification and proposal of solutions to develop green industries in Long An province. *J. Sci. Technol*. **2017**, 1–20.
2. World Bank, Japan International Cooperation Agency (JICA), German Development Bank (KfW). Assessment of Urban Wastewater Management in Vietnam, 2013.
3. Thang, N.T. Water quality assessment and loading capability of Nhue–Day River in the context of climate change and socio–economic development, National University of Hanoi, 2014.
4. Hung, N.Q. Environmental pollution in the Nhue–Day River basin and completion of penalty policy in the environmental field. *J. Legislative Stud.* **2015**, *286*, 1–6.
5. Tu, C.A. Proposal on scientific basis and river water quality zoning according to usage purposes. *J. Environ.* **2018**, 37–43.
6. Ministry of Natural Resources and Environment. Technical Report: Intended Nationally Determined Contribution of Viet Nam, Hanoi, 2015.
7. General Statistics Office. Preliminary census results in 2019.
8. JICA (Japan International Cooperation Agency). Guidance Document on City–Level Greenhouse Gas Inventory. Project on Support the Planning and Implementation of NAMAs in a MRV Manner, 2017.
9. Intergovernmental Panel on Climate Change. Guidelines for Volume 5, Chapter 6 – Waste Water Disposal and Treatment, 2016.
10. Intergovernmental Panel on Climate Change. Guidelines for National Greenhouse Gas Inventories. Volume 5: Waste, 2015.
11. Nguyen, L.H.; Kensuke, F. Calculation of greenhouse gas from domestic wastewater. Sustainable Science Integrated Research Institute–School of Urban Engineering and University of Tokyo, Japan. Faculty of Environmental Engineering–University of Civil Engineering, 2018.
12. Government. Decision 681/QD–TTg on the Planning of drainage and wastewater treatment systems for residential and industrial areas in the Nhue–Day River basin to 2030, 2013.
13. Gupta, D.; Singh, S.K. Greenhouse Gas Emissions from Wastewater Treatment Plants: A Case Study of Noida. *J. Water Sustainability* **2012**, *2*, 131–139.
14. Campos, J.L.; Valenzuela–Heredia, D.; Pedrouso, A.; Val del Río, A.; Belmonte, M.; Mosquera–Corral, A. Greenhouse Gases Emissions from Wastewater Treatment Plants: Minimization, Treatment, and Prevention. *J. Chem*. **2016**, 1–12. https://doi.org/10.1155/2016/3796352.

VIETNAM JOURNAL OF HYDROMETEOROLOGY

Research Article

Assessing land use change in the context of climate change and proposing solutions: Case study in Gia Lai province, Vietnam

Nguyen Ninh Hai[1], Nguyen Tuan Anh[1], Nguyen Minh Ky[1]*, Bach Quang Dung[2]*, Nguyen Thi Nhu Huong[3], Nguyen Hoang Dieu Minh[1], Nguyen Thi Ly[1]

[1] Nong Lam University of Ho Chi Minh City, Gia Lai campus, Tran Nhat Duat Street, Dien Phu Ward, Pleiku City, Gia Lai Province, Vietnam.
[2] Viet Nam Meteorological and Hydrometeorological Administration, Ha Noi, Vietnam.
[3] Pleiku High School, Gia Lai Province, Vietnam.
*Correspondence: nmky@hcmuaf.edu.vn; dungmmu05@gmail.com;
Tel.: +84–384321415.
Received: 10 March 2021; Accepted: 15 April 2021; Published: 25 April 2021

Abstract: The study presents the results of the assessment of land use change in the period 2014–2019 in Chu Pah district, Gia Lai province and proposed solutions. The research used the methods including data collection, spatial analysis, stakeholder and expert analysis. Remote sensing imagery (Google Earth) is employed to interpret, and the conducted field survey to verify in 14 communes and towns in order to create the current map of land use with high accuracy. For instance, the group of agricultural land changes the largest with the conversion of annual crop land into perennial crops. The area of residential land increases due to the increasing demand of residential land and the population growth. In addition, the group of unused land decreased relatively high mainly to meet the needs of cultivation and afforestation. The negative impacts of climate change also contribute to change the purpose and status of land resources in Chu Pah district. The results are meaningful in providing database for establishing land use status quo map and making decisions on sustainable socio–economic development.

Keywords: Land use change; Land management; Climate change; Google Earth; Remote sensing.

1. Introduction

Studying land use change is to clarify changes and use land resources effectively in specific areas using modern technologies such as remote sensing and geographic information systems [1–3]. Many studies showed that land cover change is an important factor in environmental change. Therefore, research on land use change is considered by scientists and managers to analyze the causes. In fact, there are many methods of determining the process of land use changes such as applying experimental models to assess changes in land cover by remote sensing [3–6]. However, this approach is unsuccessful in explaining human behavior leading to land use change. According to another approach, spatial modeling can be used to determine the process of land use changes based on the Google Earth satellite images [7–9]. Advantages of using Google Earth can provide high spatial resolution satellite imagery. Google Earth provides images at different times and is therefore very useful in the process of urban planning development and in determining land use and land cover changes. High resolution Google Earth satellite imagery can observe visual objects such as residential areas, construction works, transport systems, water surface, etc. to integrate into GIS to create the current land use map [9]. These changes will then be used to assess impacts related to policy and other factors. In addition, statistical analysis method is a useful tool due to the ability to test hypotheses, rank factors, test hypothesis rigor. However, the process requires a combination of spatial, temporal and analytical data, so there are still obstacles and challenges to achieving the accuracy results [10].

Chu Pah district is an important gateway in the northern economic corridor of Gia Lai province and Pleiku city. Chu Pah is located in an important position and has exchange advantages to promote local socio–economic development [11]. Meanwhile, the process of economic development and urbanization has caused many problems in the management and use of land resources such as degradation, inappropriate use of resources, and land disputes [12]. According to the scenarios of climate change and sea level rise for Vietnam, compared with the period of time 1980–1999, the average temperature will be increased around 2 to 3°C at the end of this century [13]. Also, with the current negative impacts of climate change in the Central Highlands region is significant. Land use change is a research process related to the way people use land. It alters the availability of various resources including vegetation, soil, and water. Water resources management could be affected by land–use change such as the amount of evapotranspiration, groundwater infiltration and overland runoff [14]. In addition, climate patterns, natural hazards also could be affected negatively on a global and local scale [15]. Climate change is the change of the climate system such as hydrosphere, biosphere and lithosphere by natural and artificial causes. According to research [16] showed that the impacts of climate change have changed agricultural activities. Similarly, the research showed that many areas of Gia Lai province are affected by variations in temperature, precipitation, and extreme weather events such as droughts and floods. In agriculture, there should be many synchronous solutions, in which the change of crop structure needs to be suitable with the weather conditions of the area [17]. There is an urgent problem to be addressed in the state management of land resources.

Therefore, it is important to assess land use change and propose solutions for effective land use and management, providing detailed and accurate information for policy making. At the same time, the results also support the management of rational and efficient use of land resources, meeting the use demands of economic, cultural and security and defense sectors.

2. Methods

2.1. Study area

Located in the north of Gia Lai province, Chu Pah district has a natural area of 97,457.68 ha, bordering Kon Tum province in the North; Dak Doa district in the East; Ia Grai district in the west; Pleiku city and Ia Grai district in the south. Climate characteristics of Chu Pah district are characterized by the Central Highlands, the humid tropical climate of the south Vietnamese monsoon, there is a distinct difference and contrast between the two seasons. The dry season is from November to April each year with low rainfall, and the rainy season is hot, humid, and rainy, from May to October.

2.2. Methods

2.2.1. Secondary data collection

This method is used to collect data and documents including topographic and hydrological maps [18]; Report on the results of the review and adjustment of 3 forest types in Gia Lai province to 2025 and a vision to 2030 and other relevant documents on administrative boundaries [11].

2.2.2. Mapping and spatial analysis

To analyze and determine the spatial change of land use categories in the period 2014–2019, the study used MicroStation V8i software to establish and edit maps based on Google Earth satellite images (Landsat 8, 30x30 m). In addition, the area of land units are calculated by automatic topology using TK Desktop software Version 3.6.

2014 2019 The status quo map 2019

Figure 1. Mapping and status quo map.

For Google Earth satellite image data (*.TIF), the study used as of 2014 and 2019 (Google Earth Engine: A planetary–scale platform for Earth science data & analysis. URL: https://earthengine.google.com), then converted the WGS84 satellite image coordinates to the VN2000 standard map coordinate system. This study used the coordinate transformation between world geodetic system (WGS84) and Vietnam geodetic system (VN2000) for calculating process [19]. The formula converts the pixel's x–coordinate to the longitude and the y–coordinate of a pixel to latitude, using equations (1) and (2), respectively.

$$\mathrm{x} = \left[2^{z+7}\left(1 + \frac{\text{longitude}}{180}\right) \right] \ (1); \ y = 2^{z+7}\left(1 - \frac{1}{2\pi}\log\left(\frac{1+\sin\left(latitude\frac{\pi}{180}\right)}{1-\sin\left(latitude\frac{\pi}{180}\right)} \right) \right) \quad (2)$$

In which, x is pixel's x–coordinate to the longitude; y is the y–coordinate of a pixel to latitude; and z is ellipsoidal height. After downloading and merging Google Earth images with Universals Map Downloader version 9.10 software. Google Earth images will be referenced to the MicroStation V8i software using manual image interpretation method based on the satellite image interpretation keypad. Specifically, in order to perform the satellite imagery interpretation process, the study establishes image interpretation patterns and is described in Table 1. These image interpretation patterns are consistent and followed as land management standards.

Table 1. Google Earth imagery interpretation.

Objective	Pattern	Color	Size	Shape	Topographic
Perennial crops		Dark blue, black	Large	Large, very large cluster	Flat or sloping
Stream and river		Bright, milky white	Unstable	Meandering	Lowlands, valleys
Residential land	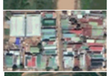	Green gray	Small	Rectangular, square	Flat land, small slope
Aquaculture land		Blue	Small	Rectangular, square	Flat, sunken
Paddy land	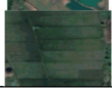	Green	Unstable	Polygons, plots	Low–lying, riverine

Objective	Pattern	Color	Size	Shape	Topographic
Transport land	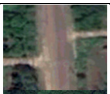	Greyish	Unstable	Linear form	Flat, sloping land
Forest land		Black blue	Very large	Very large cluster	Hilly
Water surface		Dark green	Medium, large	Cluster, round shape	Lowlands, lower
Unused land		Red gray	Medium, large	Large, very large cluster	Hilly, large slope

2.2.3. Accuracy assessment

The method of accuracy assessment aims to confirm the accuracy and acceptance of the satellite image interpretation [20–21]. In order to assess reliability, the study conducted field survey and recorded GPS location, and create a matrice to calculate Overall Accuracy and Kappa (K), which is to verify the results of satellite image interpretation [21–22]. Kappa can be used in accuracy assessment and determine the values of error matrix. Kappa is computed as equation (3).

$$K = \frac{N\sum_{j=1}^{r} x_{ii} - \sum_{j=1}^{r}\left(x_{i+} * x_{+i}\right)}{N^2 - \sum_{j=1}^{r}\left(x_{ii} * x_{+i}\right)} \quad (3)$$

where r is the number of rows of the matrix; x_{ii} is the number of observations of row and column i; x_{i+} and x_{+i} are respectively the marginal totals of row and column i; and N is the total number of observations [22]. In this study, the field survey took 123 random samples of target groups (Figure 2) including perennial crop land (15 samples), stream and river land (9 samples), residential land (9 samples), aquaculture land (12 samples), paddy land (21 samples), transportation land (12 samples), forestry land (15 samples), water surface land (9 samples), and unused land (12 samples). The results of the calculation comparing the satellite image interpretation and the control samples are the basis for evaluating accuracy of the study.

2.2.4. Stakeholder and expert analysis

To clarify the level of stakeholders' involvement in the process of implementing the research to propose land resource use and management solutions, the study determines the approaches for the cooperation and participation of stakeholders [23–24]. After collecting secondary data, a list of stakeholders is fully listed. Following the semi–structured interview method with staff, leaders involved in managing land use change. Next, potential stakeholders were identified, and then conducted semi–structured interviews of experts. A final list of stakeholders is used to classify. Based on the stakeholder power–interest matrix, the stakeholders were subsequently divided into four basic groups including Keep informed, Maintain interest, Active consultation, Key players. After classifying stakeholders, it is important to decide how to involve the stakeholders. Stakeholder analysis clarified the roles and functions and interactions between the parties. This method is significant in making the appropriate solutions recommendation [25–26]. In addition, to solidify the basis of proposing solutions for effective land for resource use management, the research conducted an expert interview based on the Likert scale [27]. Accordingly, the group of experts is explored and will evaluate the score of choosing the solutions based on professional knowledge and experience. Thus, the making solutions are proposed based on the methodological framework and is shown in Figure 3.

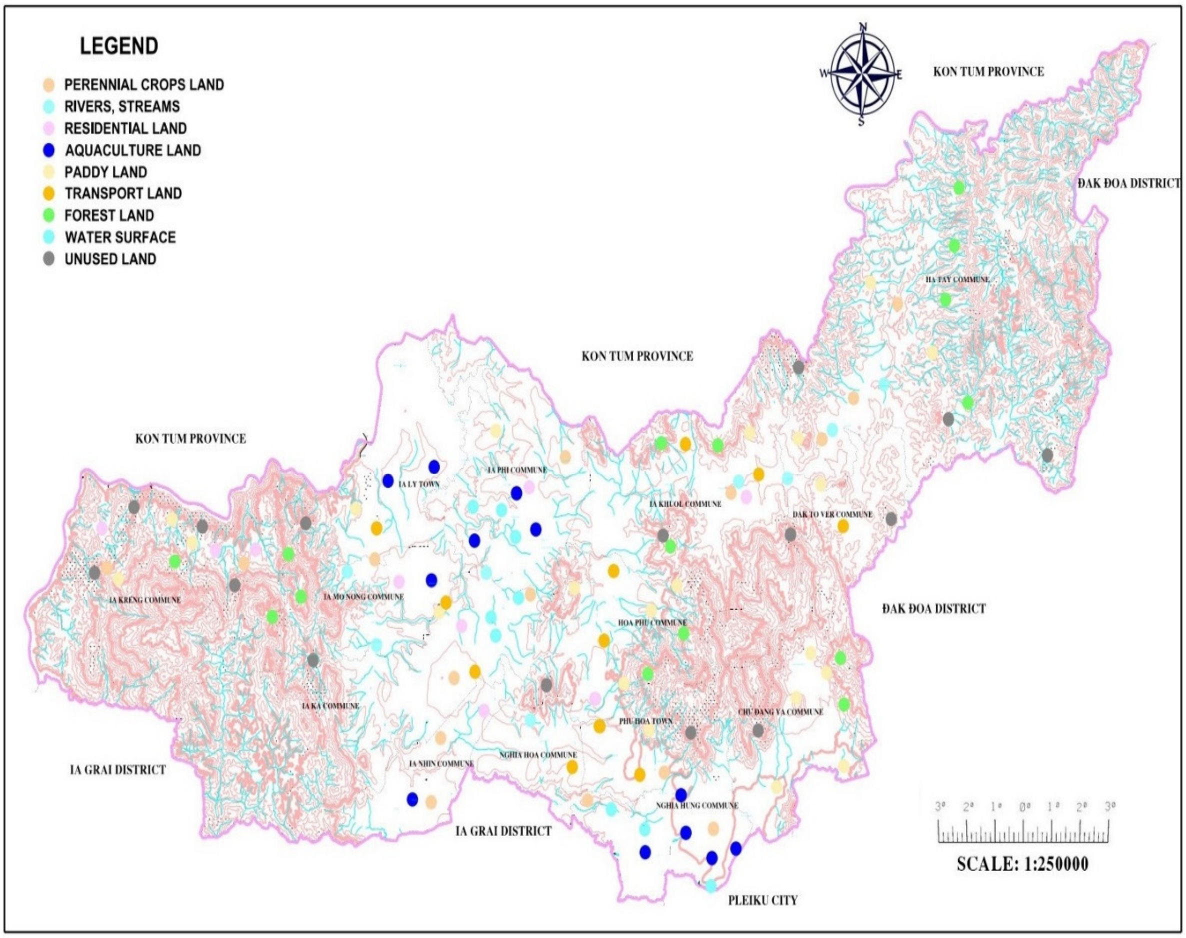

Figure 2. Map of field sampling to verify image classification.

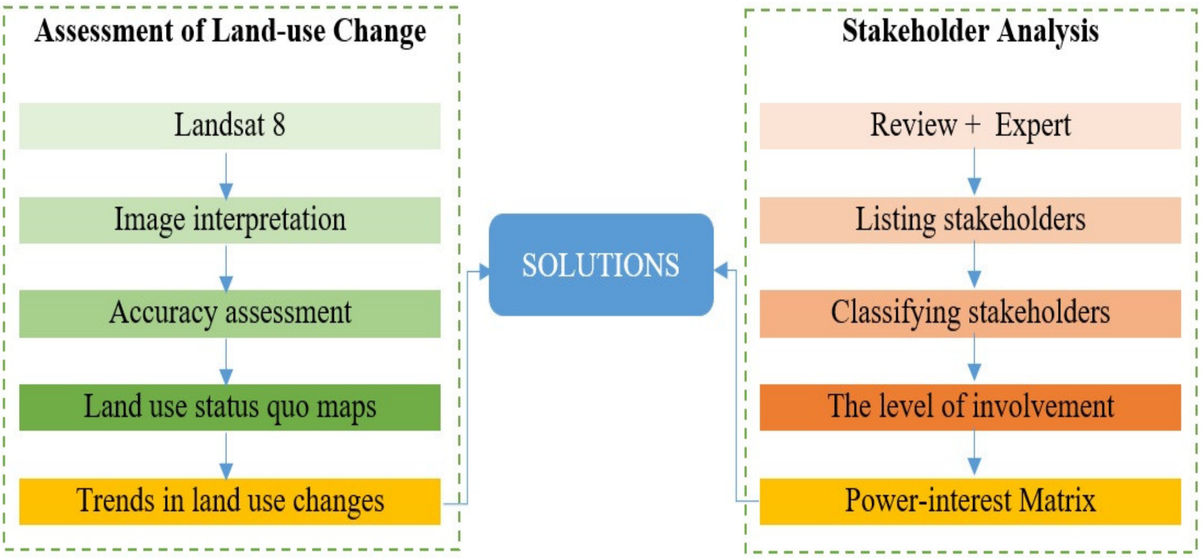

Figure 3. Methodological framework.

2.2.5. Statistical method

The data are calculated average (mean), standard deviation (SD) and analyzed using the softwares of M. Excel 2013 and SPSS V.13.0 for Windows.

3. Results and discussion

3.1. Land use change in Chu Pah district in the context of climate change

3.1.1. The current status of land use change

The use of satellite imagery (ie., Landsat 5, 7 and 8) from Google Earth demonstrations the effective application in processing and assessing changes in land resources [7] by the spatial interpretation and analysis. In 2019, the area of natural land in Chu Pah district was 97,221.37 ha, lower than that in 2014 (97,457.68 ha) with the decline of 236.30 ha (Figures 5 and 6). The reason is due to the change of administrative boundaries between Gia Lai and Kon Tum provinces, which was determined according to Resolution No. 113/NQ–CP [28].

3.1.2. Change of land use categories

In 2019, the results illustrate that agriculture land was 86,160.44 ha and witnessed an increase of 1,085.22 ha (an average rise of 217.04 ha/year, corresponding to the rate of 0.25%/year) in the period 2014–2019 (Table 2). Obviously, the negative impact of climate change has caused difficulties for human activities such as the poor, vulnerable communities in rural areas [18, 29]. This is a hug reason lead to change of land use in developing countries as Vietnam. The results found the highest increase is perennial crop land with 9,120.62 ha from annual crop land and unused land in the communes of Ha Tay, Ia Khuol, Ia Mo Nong and Ia Ka. In addition, the area of forest land increases 1,224.21 ha due to the area of planted forests in Ia Ly protection forest management unit (subdivision 215–Ia Kreng Commune) and Bien Ho protection forest management unit (subdivision 253–Hoa Phu commune). The current situation of rice land changes showed an increase of 329.30 ha due to the adjustment of paddy land along rivers and streams for the effective management and use of land resources in the communes of Ha Tay, Ia Khuol, and Ia Mo Nong. It can be seen that the assessment of the current state of changes in agricultural land resources plays an important role in proposing solutions to the effective management and use of local resources.

Table 2. Changes in agricultural land in the period 2014–2019.

ID	Land use categories	Area (ha)		Change (ha)	Rate (%/year)
		2019	2014		
1	Paddy land	4,657.97	4,328.67	+329.30	+1.41
2	Annual crop land	13,440.22	21,990.47	–8,550.25	–12.72
3	Land for perennial crops	38,339.22	29,218.60	+9,120.62	+4.76
4	Forest land	29,541.67	29,391.35	+150.32	+0.04
5	Aquaculture land	150.28	115.28	+35.00	–0.05
6	Other agricultural land	31.10	30.85	+0.25	+4.66
	Total	86,160.44	85,075.22	+1,085.22	+0.25

Figure 4 shows the fluctuation of non–agricultural land group in the period 2014–2019 in Chu Pah district. Notably, residential land increased by 22.44 ha, corresponding to an increase of 0.56%/year due to the needs of infrastructure development in the context of rapid population growth. The results show similarities with previous studies on the causes of urban expansion in the Central Highlands [30].

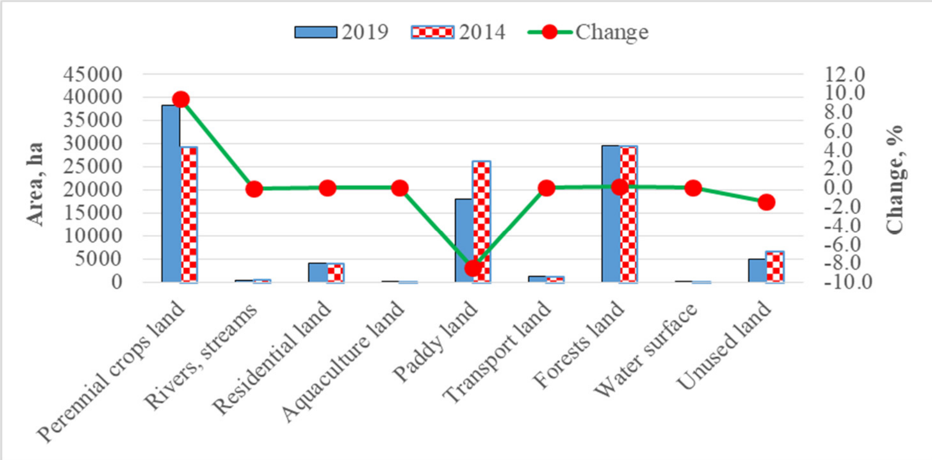

Figure 4. Changes in agricultural land in the period 2014–2019.

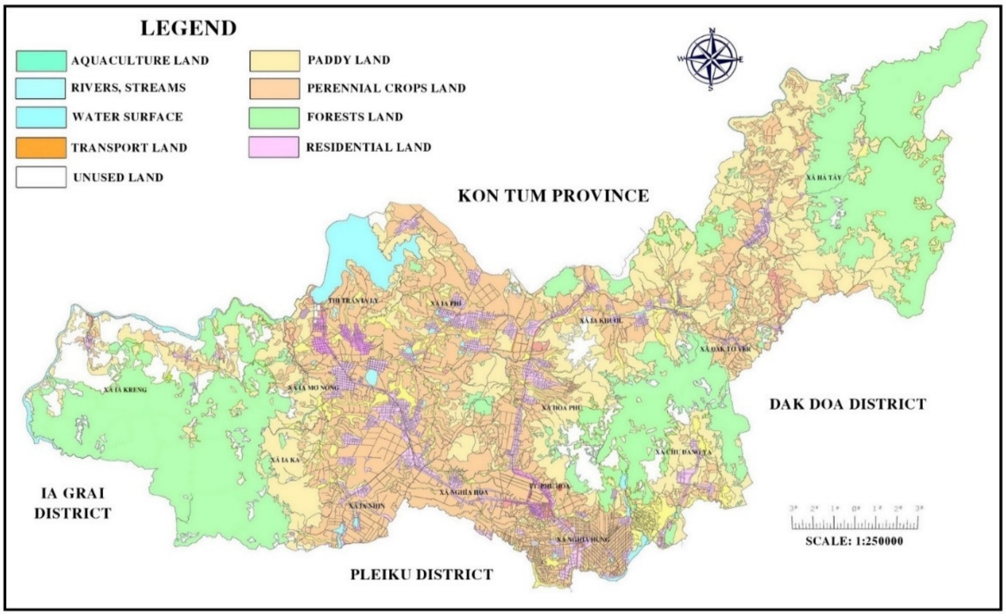

Figure 5. Current land use map in Chu Pah district in 2014.

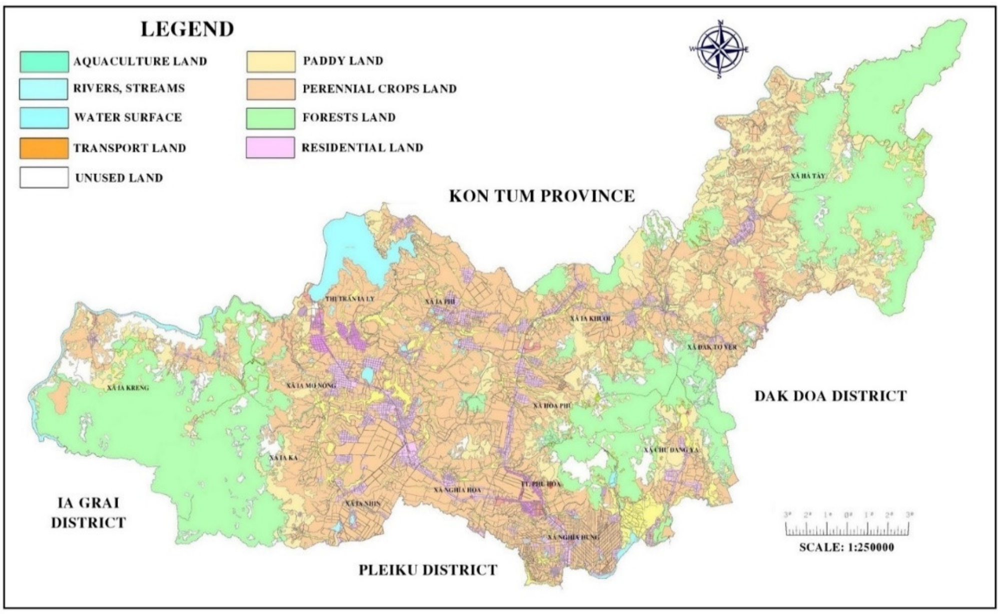

Figure 6. Current land use map in Chu Pah district in 2019.

3.1.3. Evaluate the reliability

Evaluating the reliability of satellite imagery interpretation has an important role and confirmed the acceptability levels [30–31]. During random field sampling, matrix studies compute the accuracy level through Overall Accuracy and Kappa's index. Table 3 shows that the accuracy level in the image classification process is high with the lowest rate corresponding to 75.0% (for example: aquaculture land, unused land). In contrast, the groups such as residential land, transportation, rivers and streams have very high accuracy. Normally, the accuracy of over 75.0% Google Earth satellite image interpretation is satisfactory and acceptable. In this study, the Overall Accuracy was 87.8% and Kappa index was 86.3% represents high reliability. Thus, the results of the study showed that the Overall Accuracy in the process of creating land use maps of Chu Pah district and the Kappa index is acceptable. It can be seen that the imagery interpretation process to assess land use change in Chu Pah district is effective and meets the criteria of imagery classification.

Table 3. Matrix of accuracy evaluation after imagery classification.

	Field–proven by GPS									
Land classify	**Perennial crops land**	**Rivers, streams**	**Residen tial land**	**Aquacul ture land**	**Paddy land**	**Trans port land**	**Forest land**	**Water surface**	**Unused land**	**Sum**
Perennial crops land	12	0	0	0	3	0	0	0	0	15
Rivers, streams	0	9	0	0	0	0	0	0	0	9
Residential land	0	0	18	0	0	0	3	0	0	21
Aquaculture land	0	0	0	6	0	0	0	0	0	6
Paddy land	0	0	0	0	18	0	0	0	3	21
Transport land	0	0	0	0	0	12	0	0	0	12
Forests land	3	0	0	0	0	0	12	0	0	15
Water surface	0	0	0	3	0	0	0	9	0	12
Unused land	0	0	0	3	0	0	0	0	9	12
Sum	15	9	18	12	21	12	15	9	12	123

3.2. Analyze stakeholders and propose effective management solutions

Stakeholder analysis is a useful tool based on a coordinated and supportive approach to sustainable land resource management [32–33]. In this study, the matrix would examines the interest and influence with 3 levels (low–medium–high), which are classified into 4 groups (Figure 7).

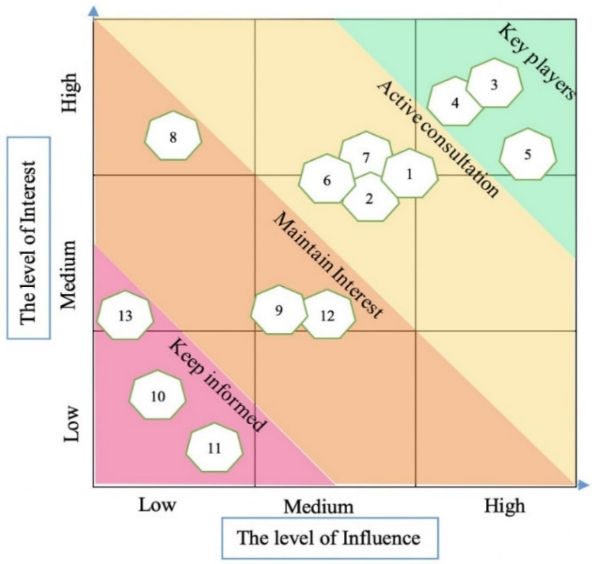

No.	Stakeholders
1	Provincial People's Committee
2	Department of Natural Resources and Environment
3	Chu Pah District People's Committee
4	Division of Natural Resources and Environment
5	Communal People's Committee
6	Provincial Land Use Right Registration Office
7	District Land Use Right Registration Office
8	Experts and professionals
9	Organizations related to land use rights; and Departments related to land resource management
10	Communities
11	Household business
12	Associations
13	Media

Figure 7. Matrix of stakeholder analysis.

The process of analyzing stakeholders specifically classifies: (i) The group of key stakeholders that are direct participants (high level of importance and influence) includes: The Division of Natural Resources and Environment is a specialized agency to advise and assist the Chu Pah District People's Committee in performing the state management function in the field of natural resources and environment; At the commune level, cadastral and environmental officers are responsible for advising and performing tasks to assist the communal People's Committee to organize the implementation in the fields of land use management, environmental resources, construction, urban, transport, agriculture; (ii) A group of stakeholders that requires proactive consultation (medium to high impact and low to moderate interest) including the Department of Natural Resources and Environment to advise and assist the Provincial People's Committee and coordinating with the Land Use Right Registration Office at the provincial and district level); (iii) A group of stakeholders that need to maintain an interest (medium to high level of interest, low influence) including experts and professionals (consultants, expert advisors, policy); organizations related to land use rights; and departments related to land resource management; (iv) A group of stakeholders who should exchange information (low interest and low influence) including residential communities, household business, and media.

On the other hand, based on the current situation as well as the analysis and grouping of stakeholders, combine with expert survey in the context of climate change, the study proposed some solutions for effective land use resource management in Chu Pah according to the priority categories.

Table 4. Proposal on solutions for efficient management and use of land resources.

Code	Recommended solution	Values[1]	Ranking
GP_1	Develop and implement programs to support sustainable livelihoods, stabilize life and economic development.	4.724±0.578	I
GP_2	Strengthen inspection and supervision of the use of land resources; strictly handle violations of approved land use plannings.	4.451±0.285	II
GP_3	Investment in the documents for land resource management such as cadastral mapping, certificate of land use rights.	4.037±0.963	III
GP_4	Policy of improving unused land resources, improving the efficiency of agricultural and forestry land exploitation to meet development needs in the sustainability and protection of the ecological environment.	3.831±0.321	IV

Notes: GP_{1-4}: Solutions from 1 to 4. [1]Values: Mean±SD of 5–point Likert scale.

In general, strengthening sustainable land use management should be aimed at using land ecology efficiently [34], thereby contributing to reducing the global consequences in the exploitation and use of land resources [35]. Survey results with priority order: developing and implementing a sustainable livelihood support program > monitoring the implementation of land use > developing documents for resource land management resource > improving unused land resources and the efficiency of agricultural land exploitation. In which, the average value of the expert assessment is to build and implement the sustainable livelihood support program (GP_1) with the highest result of 4.724 (SD = 0.578). Similarly, the solutions of GP_2, GP_3, GP_4 with the average values are 4.451 (SD = 0.285); 4.037 (SD = 0.963) and 3.831 (SD = 0.321) respectively. Therefore, it is recommended to pay attention to solutions to improve the efficiency of agricultural and forestry land exploitation in order to meet the needs of sustainable development and protection of the ecological environment.

4. Conclusions

The results of applying Google Earth satellite imagery interpretation approach to establish land use maps help illustrate the distribution of land–use space in Chu Pah district. The Overall Accuracy and Kappa index were respectively 87.8% and 86.3%, representing high reliability. From our study of the land use changes in Chu Pah district showed that the conversion from annual crop land into perennial crop land was outstanding in the period 2014–2019. Analysis of the use of non–agricultural land groups can be seen that the residential land area has increased significantly (22.44 ha) to serve the needs of transforming economic development and responding to population growth. In addition, the negative impact of climate change can be caused change of land use in developing countries. The negative impact of climate change has been caused difficulties for human as well as agricultural activities in Chu Pah district. The results also found that the cooperation and participation of stakeholders is the foundation for effective management of land resources use on the basis of accountability and coordination. In order to limit the situation of self–conversion of land use categories not according to planning the specialized agency should consider relevant recommendations. However, limitations of the current study can be existed by the pixels in the affected highland areas, which cannot be detected as well as other zones (e.g. plain areas). The difference between this study and land inventory status quo might be occurred in the small scope. In the future, we should be used the higher–resolution images to investigate these changes.

Acknowledgments: The authors would like to thank the Chu Pah District People's Committee, Chu Pah Department of Natural Resources and Environment for research funding and providing key information for this study.

Author contributions: Constructing research ideas: N.N.H., N.T.A.; Select research method: N.T.A., N.N.H., N.M.K.; Survey, sampling and analysis: N.N.H., N.T.A., N.M.K., N.H.D.M., N.T.L., N.T.N.H.; Data processing: N.N.H., N.T.A., N.M.K., B.Q.D.; Writing–original draft preparation: N.N.H., N.T.A., N.M.K.; Writing–review and editing: N.N.H., N.T.A., N.M.K., B.Q.D.

Conflicts of Interest: The authors declare no conflict of interest.

References

1. Chauhan, H.; Nayak, S. Land Use/Land Cover Changes near Hazira Region, Gujarat Using Remote Sensing Satellite Data. *J. Indian Soc. Remote Sens.* **2005**, *33*, 413–420.
2. Ky, N.M.; Thuong, N.T.L.; Phu, B.K.; Dang, T.L.H. Remote Sensing and GIS Technology Application to Assess a Forest Resources Fluctuation in ChuProng District, Gia Lai Province. *An Giang Uni. J. Sci.* **2019**, *22*, 67–80.
3. LaGro, J.A.; DeGloria, S.D. Land Use Dynamics within an Urbanizing Non–Metropolitan County in New York State (USA). *Landsc. Ecol.* **1992**, *7*, 275–289.
4. Andersen, L.E. The Causes of Deforestation in the Brazilian Amazon. *J. Environ. Dev.* **1996**, *5*, 309–328.
5. Mallupattu, P.K.; Sreenivasula Reddy, J.R. Analysis of Land Use/Land Cover Changes Using Remote Sensing Data and GIS at an Urban Area, Tirupati, India. *Sci. World J.* **2013**, *2013,* pp. 6. https://doi.org/10.1155/2013/268623.
6. Mertens, B.; Lambin, E.F. Spatial Modelling of Deforestation in Southern Cameroon: Spatial Disaggregation of Diverse Deforestation Processes. *Appl. Geogr.* **1997**, *17*, 143–162.
7. Huang, H.; Chen, Y.; Clinton, N.; Wang, J.; Wang, X.; Liu, C.; Gong, P.; Yang, J.; Bai, Y.; Zheng, Y. Mapping Major Land Cover Dynamics in Beijing Using All Landsat Images in Google Earth Engine. *Remote Sens. Environ.* **2017**, *202*, 166–176.
8. Jacobson, A.; Dhanota, J.; Godfrey, J.; Jacobson, H.; Rossman, Z.; Stanish, A.; Walker, H.; Riggio, J. A Novel Approach to Mapping Land Conversion Using Google Earth with an Application to East Africa. *Environ. Model. Softw.* **2015**, *72*, 1–9.

9. Malarvizhi, K.; Kumar, S. V.; Porchelvan, P. Use of High Resolution Google Earth Satellite Imagery in Landuse Map Preparation for Urban Related Applications. *Proc. Technol.* **2016**, *24*, 1835–1842.
10. Munroe, D.K.; Müller, D. Issues in Spatially Explicit Statistical Land–Use/Cover Change (LUCC) Models: Examples from Western Honduras and the Central Highlands of Vietnam. *Land Use Policy* **2007**, *24*, 521–530.
11. GL. PPC. Resolution No. 100/NQ–HDND dated 7/12/2017 on Approving the Results of Reviewing and Adjusting the Planning of 3 Forest Types to 2025 and a Vision to 2030 in Gia Lai Province. Gia Lai Provincial People's Committee: Gia Lai, 2017.
12. MONRE. National State of the Environment Report 2016: Urban Environment; Vietnam Publishing House of Natural Resources, Environment and Cartographic, 2017.
13. MONRE. Climate Change, Sea Level Rise Scenarios for Vietnam. Publisher of Map and Environment Resources: Hanoi, 2012.
14. Akpoti, K.; Antwi, E.O.; Kabo–bah, A.T. Impacts of Rainfall Variability, Land Use and Land Cover Change on Stream Flow of the Black Volta Basin, West Africa. *J. Hydrol.* **2016**, *3*, 26.
15. Chakilu, G.; Moges, M. Assessing the Land Use/Cover Dynamics and Its Impact on the Low Flow of Gumara Watershed, Upper Blue Nile Basin, Ethiopia. *Hydrol. Current Res.* **2017**, *7*, 268.
16. Hang, L.T.; Hung, N.T.Q.; Ky, N.M. Impacts of climate change and public awareness of coffee production activities in Gia Lai province. *J. Agric. Rural Dev.* **2017**, *20*, 21–28.
17. Khoa, N.P. Developing Climate Change Response Map for the Agricultural Sector of Gia Lai Province in 2013, with an Orientation to 2020 and a Vision to 2030. *HueUni–JARD*, **2015**, *108* (9). https://doi.org/10.26459/jard.v108i9.2923.
18. CP.DPC. Report on Land Inventory Results and Land Use Status Quo Map in 2019 – Chu Pah District. Chu Pah District People's Committee, 2020.
19. MONRE. Using the coordinate transformation between world geodetic system WGS84 and national geodetic system VN2000. Ministry of Environment and Resources: Hanoi, 2007.
20. Mohammed, N.Z.; Ghazi, A.; Mustafa, H.E. Positional Accuracy Testing of Google Earth. *IJMSE* **2013**, *4*, 6–9.
21. Tilahun, A.; Teferie, B. Accuracy Assessment of Land Use Land Cover Classification Using Google Earth. *Am. J. Environ. Prot.* **2015**, *4*, 193–198.
22. Congalton, R.G. A Review of Assessing the Accuracy of Classifications of Remotely Sensed Data. *Remote Sens. Environ.* **1991**, *37*, 35–46.
23. Brown, G.; de Bie, K.; Weber, D. Identifying Public Land Stakeholder Perspectives for Implementing Place–Based Land Management. *Landsc Urban Plan.* **2015**, *139*, 1–15.
24. Reed, M.S.; Graves, A.; Dandy, N.; Posthumus, H.; Hubacek, K.; Morris, J.; Prell, C.; Quinn, C.H.; Stringer, L.C. Who's in and Why? A Typology of Stakeholder Analysis Methods for Natural Resource Management. *J. Environ. Manage.* **2009**, *90*, 1933–1949.
25. Anh, N.T.; Hai, N.N.; Trang, T.T.T; Dung, B.Q.; Ky, N.M. Analyzing Stakeholder Involvement in Urban Domestic Water Supply System – Case Study in Central Highland of Vietnam. *VN J. Hydrometeorol.* **2019**, *2-1*, 56–65. https://doi.org/10.36335/VNJHM.2019(2-1).56-65.
26. Bryson, J.M. What to Do When Stakeholders Matter: Stakeholder Identification and Analysis Techniques. *Public Manag. Rev.* **2004**, *6*, 21–53.

27. Joshi, A.; Kale, S.; Chandel, S.; Pal, D.K. Likert Scale: Explored and Explained. *Curr. J. Appl. Sci. Technol.* **2015**, *7*, 396–403.
28. Vietnamese Government. Resolution No. 113/NQ–CP dated December 5, 2019 on the Determination of the Administrative Boundaries between Kon Tum and Gia Lai Provinces in Three Historical Regions, Hanoi, 2019.
29. Thang, L.V.; Ky, N.M. Assessing the study of climate change trend in Vietnam: A case study in Danang City. *HUJOS – Earth Sci. Environ.* **2017**, *126*, 19–28.
30. Hai, N.N.; Anh, N.T.; Khuong, T.N.L.; Dung, B.Q.; Ky, N.M. Research on Urban Sprawl Trends and Landscape Change in Pleiku City, Gia Lai Province. *VN J. Hydrometeorol.* **2019**, *2-1*, 37–47. https://doi.org/10.36335/VNJHM.2019(2-1).37-47.
31. Tilahun, A.; Teferie, B. Accuracy Assessment of Land Use Land Cover Classification Using Google Earth. *Am. J. Environ. Prot.* **2015**, *4*, 193–198.
32. Schwilch, G.; Bachmann, F.; Valente, S.; Coelho, C.; Moreira, J.; Laouina, A.; Chaker, M.; Aderghal, M.; Santos, P.; Reed, M.S. A Structured Multi–Stakeholder Learning Process for Sustainable Land Management. *J. Environ. Manage.* **2012**, *107*, 52–63.
33. Wang, J.; Aenis, T. Stakeholder Analysis in Support of Sustainable Land Management: Experiences from Southwest China. *J. Environ. Manage.* **2019**, *243*, 1–11.
34. Deng, X.; Gibson, J. Sustainable Land Use Management for Improving Land Eco–Efficiency: A Case Study of Hebei, China. *Ann. Oper. Res.* **2020**, *290*, 265–277.
35. Foley, J.A.; DeFries, R.; Asner, G.P.; Barford, C.; Bonan, G.; Carpenter, S.R.; Chapin, F.S.; Coe, M.T.; Daily, G.C.; Gibbs, H.K. Global Consequences of Land Use. *Sci.* **2005**, *309*, 570–574.

VIETNAM JOURNAL OF HYDROMETEOROLOGY

Rerearch paper

Prediction of potential for greenhouse gas mitigation and power recovery from a municipal solid waste landfill case in Tien Giang province, Vietnam

Long Ta Bui[1,2*], Phong Hoang Nguyen[1,2]

[1] Ho Chi Minh City University of Technology; longbt62@hcmut.edu.vn; nhphongee407@gmail.com
[2] Vietnam National University Ho Chi Minh City
*Corresponding author: longbt62@hcmut.edu.vn; Tel.: +84–918017376
Received: 27 February 2021; Accepted: 15 April 2021; Published: 25 April 2021

Abstract: Research on landfill gases (LFGs) collection mainly consisting of CH_4 and CO_2 gases, is not only a solution to decrease environmental risks but also to utilize and generate an alternative clean power source of coal. Many typical landfill cases in Vietnam, which install a recovery system and remove captured CH_4 by the flaring methods, are able to contribute to reducing significantly greenhouse gas (GHG) emissions with roughly 0.25 tCO_2–eq/tons being equivalent to 7.8 million tons of CO_2–eq/year. Furthermore, a wide range of LFG recovery projects financed by the World Bank was conducted on 27 landfills in 19 cities of Vietnam, which generated a potential of GHG emission reduction up to 1,116,068 tCO_2–eq/year. However, quantification of biogas emissions for each landfill as a basis in order to design and construct a suitable recovery system always has to face many challenges. The purpose of this study to propose an integrated system including a database combined with mathematical models in a Web–based packaged software named EnLandFill to be able to accurately quantify the emission load of GHGs and estimate electricity production generating from recovered LFGs. On a case study of Tien Giang province, total maximum cumulative emissions of LFGs, CH_4, and CO_2, which is around 279 million m^3, 145 million m^3, and 134 million m^3 respectively, have been forecasted in scenario 1 for the period of 2021–2030. Additionally, the annual electricity generation potential is highest in scenario 2, estimating a total value of over 800 million kWh.

Keywords: Landfill; Munticipal Solid Waste; Methane; Models; Energy recovery potential.

1. Introduction

Recovery of CH_4 gas from municipal solid waste (MSW) landfills with the aim of utilizing to generate biogas has been mentioned since the 70s of last century [1]. According to the Intergovernmental Panel on Climate Change (IPCC), the recovery of CH_4 from landfills is the key to reduce GHGs from landfill [2]. The European Union (EU) countries already have regulations and strategies to encourage restrictions on landfill of biodegradable wastes, increasing the utilization of waste to decrease LFG emissions [3–5]. Many EU directives and IPCC guidelines have encouraged the use of energy from LFG [2, 6]. From there, the task of evaluating the recovery efficiency of LFG (E%) is necessary, to estimate the maximum recovery potential of CH_4 gas collection system [7], as well as to use the recovered gas generating electricity and heat whilst contributing to GHG emissions reduction, bringing about economic benefits [8]. The United States and many European countries have led the remarkable achievements in creating energy from landfill biogas in the late 20th century [9].

The problem of generating power source from MSW has attracted the attention of organizations and researchers around the world [9]. In the US, MSW landfill–the 2nd largest source of artificial CH_4 emissions with an estimated 30 million tons of CO_2–eq in 2006 [10]. Since 1994, the Landfill CH_4 Outreach Program (called LMOP) has been launched by the US EPA with the goal of reducing GHGs from landfills through the recovery and use of LFG as a renewable energy source [11]. As of December 2007, an estimated 450 LFG (or LFGE) power projects have been operated throughout the United States, producing approximately 1,380 MW of electricity per year and providing about 235 million ft^3 of LFG/day to direct use [12].

In China, India, and some developed nations in ASEAN such as Thailand or Malaysia almost have focused on mining the common benefits from LFG recovery projects. Many facilities to accommodate LFG recovery have been built in the period of 2005–2010 [9]. In India, [13] determined the CH_4 emission load from landfills in Delhi, respectively 1,288.99 Gg; 311.18 Gg; 779.32 Gg in the period 1984–2015 and corresponding energy generating potential reached $4.16\times10^8 - 9.86\times10^8$ MJ for Ghazipur landfill; $2.08\times10^8 - 4.06\times10^8$ MJ for landfill Okhla and $3.42\times10^8 - 8.11\times10^8$ MJ for landfill Bhalswa [13]. The research team in Thailand evaluated the complex benefits of LFG energy recovery process for the Bang Kok area [14]. Life–cycle assessment (LCA) method has been applied to determine the GHG emission loads with a mitigation potential of 471,763 tCO_2–eq over a 10–year LFG recovery period, equivalent to 12% of the total CH_4 gas is generated.

According to the assessment of experts' Vietnam, if the recycling technologies are applied well, the gas recovery systems can contribute to reducing GHG emissions up to about 0.68t CO_2/ton of waste [15]. The World Bank–funded study forecasts 27 different landfills in the whole of Vietnam that implement LFG recovery projects [16]. In case of flaring GHGs, the potential reduction is about 1,116,068 tCO_2–eq/year for the baseline landfill and 646,824 tCO_2–eq/year for the new one. In the case of utilizing LFG to generate electricity, the total potential for mitigation is estimated at 2,006,969 tCO_2–eq/year. Particularly for My Tho City, Tien Giang with the total potential to minimize is forecasted at around 53,083 tCO_2–eq/year [16]. In Hanoi, many given studies to recover and use LFG gas under the name of "Clean Development Mechanism (CDM)" [17] has been implemented in Nam Son landfill in Soc Son District and Tay Mo landfill in Tu Liem District. Baseline scenario results show that while LFG is recovered through collection and flaring system, it will significantly reduce environmental risks as well as contribute to GHG emissions reduction around 2,600,000 tCO_2–eq in the period 2010 – 2017, an average of 373,696 tCO_2–eq/year [17].

As a good example at Go Cat landfill, Ho Chi Minh City has efficiently deployed an LFG recovery system with 21 vertically recovered wells [18]. Approximately 879,650 tons of LFG [18] have been collected, generating a total electricity capacity of about 2.43 MW and annual electricity output of 16 GWh [17]. Furthermore, two other CDM–based LFG collection projects have aslo been conducted in Phuoc Hiep and Dong Thanh landfills [15]. At Nam Binh Duong landfill since 2018, the power plant operating on recovered CH_4 gas has been operated with a total power supply capacity of 9.1 million kVA, by 2019 the total power supply has increased to 11.4 million kVA [19].

This study is carried out towards the determination of GHG recovery potential, towards the creation of renewable energy sources for local/national socio–economic goals. Selected objects for specific calculation are the Tan Lap 1 landfill in Tien Giang province, computing scenarios applying the EnLandFill Web–based software with consideration of LFG recovery and utilization of power generation are performed. The simulating results are also validated by monitoring data in order to evaluate the efficiency of the software. The specific study aims to find the most practical solution to allow local/national governments to recover energy, control, and reduce GHG emissions in the period of 2021–2030. Moreover, this research is also carried out within the framework of a Scientific research project at the National University of Ho Chi Minh City.

2. Methods and data

2.1. Study area

Tien Giang is a province in the Mekong Delta region, one of eight provinces/cities in the Southern Key Economic Region; within the range of coordinates from 10º12'20" to 10º35'26" north latitude and from 105º49'07" to 106º48'06" east longitude. The whole province has a natural area of about 2,510.61 km^2, accounting for 0.76% of the country's area and accounting for 6.2% of the entire Mekong Delta region [20]. Along with promoting socio–economic development, environmental issues, especially activities MSW management and treatment are being paid attention. The Department of Construction, together with the Department of Natural Resources and Environment, are the two focal points for MSW management in the province. Management has faced many challenges because most of them are open landfills, or landfill is unhygienic and always overloaded [20]. Currently, there are 8 active landfills in Tien Giang province, of which the Thanh Nhut landfill has only recently been operating, and 2 closed landfill sites including the Tan Thuan Binh landfill in Cho Gao District and the Binh Phu landfill in Cai Lay District [20].

Figure 1 presents a map of the study area, specifying the geographical location and the scope of the waste treatment area in Tan Lap 1 landfill. The total existing area of landfill is 14.88 ha in Tan Phuoc District, Tien Giang province, operating since 1999 [20]. The current landfill with an average treatment capacity of 340 tons/day, mainly treats waste by burial methods [20].

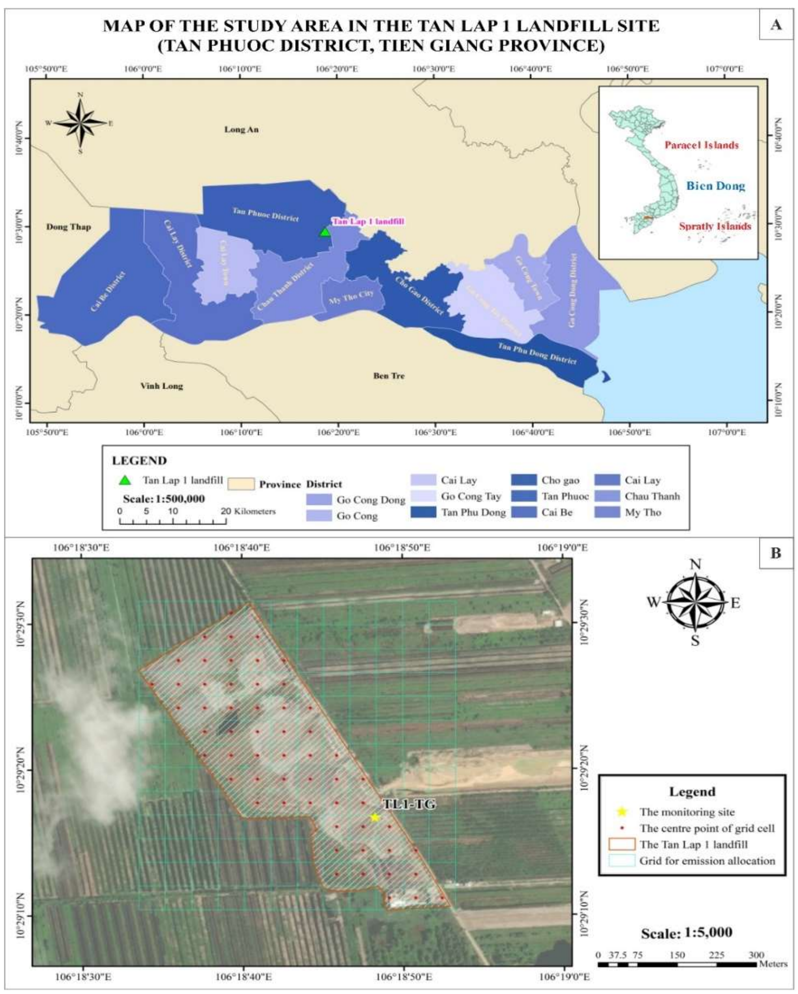

Figure 1. The study area at the Tan Lap 1 landfill in Tien Giang province, Vietnam (a) and (b).

2.2. Research framework

The framework of this study is divided into six parts clearly. In particular, firstly, both the potential CH_4 generation capacity parameter ($L_{0,\ opt(x)}$, m^3/ton) and the optimal CH_4 generation rate coefficient (k_{opt}, year^{-1}) is determined as the input data of models. Secondly, the volume estimation of MSW (ton/year) is forecasted in the 2021–2030 period, which is based on prediction levels of the population as well as population growth rate in the study area and MSW generation potential rate. Thirdly, the annual LFG emission load (m^3/year or ton/year) from the Tan Lap 1 landfill is also estimated in the same period using gathered data of buried MSW volume (ton/year) from 1999 to 2020 combined with the MSW volume predicting for the 2021–2030 period. Fourthly, a basis of LFG collection efficiency (E, %), lower heating value of CH_4 (MJ/m^3), landfill peak coating oxidation coefficient (OX,%), power generation efficiency (δ, %), and power factor (ε, %) are applied to assess the electricity production potential from the recovery of LFGs in the Tan Lap 1 landfill. Fifthly, the values of annual electricity production potential (kWh/year), the number of hours operating power stations throughout the year (D_{hr}, hours), and the number of days operating power station in a year (γ) is used to calculate expected capacity of the electricity generation stations (MW) from the captured LFGs. Finally, the effective assessment of recovered LFG usage as an alternative power source to traditional coal sources is performed through the amount of CO_2 emission reduced in the future and the released GHGs emission mitigation according to different computing scenarios based on the Global Warming Potential (GWP) index.

The EnLandFill [21] software was selected to perform the first and third calculating steps. The approach applying in EnLandfill has been widely used in many parts of the world due to its simplicity and accuracy [22–24]. Additionally, this software has been automated processing in the form of packaged multi–modules applicable to specific conditions of Vietnam.

Building simulation scenarios, forecasting emission load of LFGs, consisting of total LFG (TLFG), CH_4, and CO_2 in the period of 2021–2030 based on Decision No. 1635/QĐ–UBND dated 24/05/2019 of People's Committee of Tien Giang province about Solid Waste Management Plan in Tien Giang province for the period 2011–2020, vision to 2030 [25]. Three detailed calculation scenarios are set up, including:

Scenario 1 (S1): All MSW generated from My Tho City, Cai Be Town and 04 districts in the study area including: Cai Lay, Chau Thanh, Tan Phuoc and Cho Gao are collected, partly transported, about 60% to 02 new treatment zones, the Eastern treatment area and the Western treatment area in Binh Xuan commune, Go Cong Town and Thanh Hoa commune, Tan Phuoc District, Tien Giang province. The remaining volume of solid waste, about 40%, will be completely treated by burial method. In the period 2025–2030, a generation of generated gas collection system will be arranged, efficiency of 75%, all collected gas will be served for electricity generation;

Scenario 2 (S2): All 100% of MSW generated from My Tho City, Cai Be Town and 04 districts in the study area, Cai Lay, Chau Thanh, Tan Phuoc and Cho Gao is collected, transported and processed completely by burial method. In the period of 2021–2030, a generation gas collection system will be arranged with the collection efficiency of 75% for the period from 2021–2025 and 90% for the period from 2026–2030; At the same time, all collected gas will be served for electricity generation;

Scenario 3 (S3): All 100% of MSW generated from the whole study area is collected and transported to landfill treatment about 85% of the volume and 15% of the volume treated by combustion method. In the forecasting period of 2021–2030, a generation gas collection system will be arranged with the collection efficiency of 75% for the period from 2021 to 2025 and 90% for the period from 2026–2030; At the same time, all collected gas will be served for energy generation.

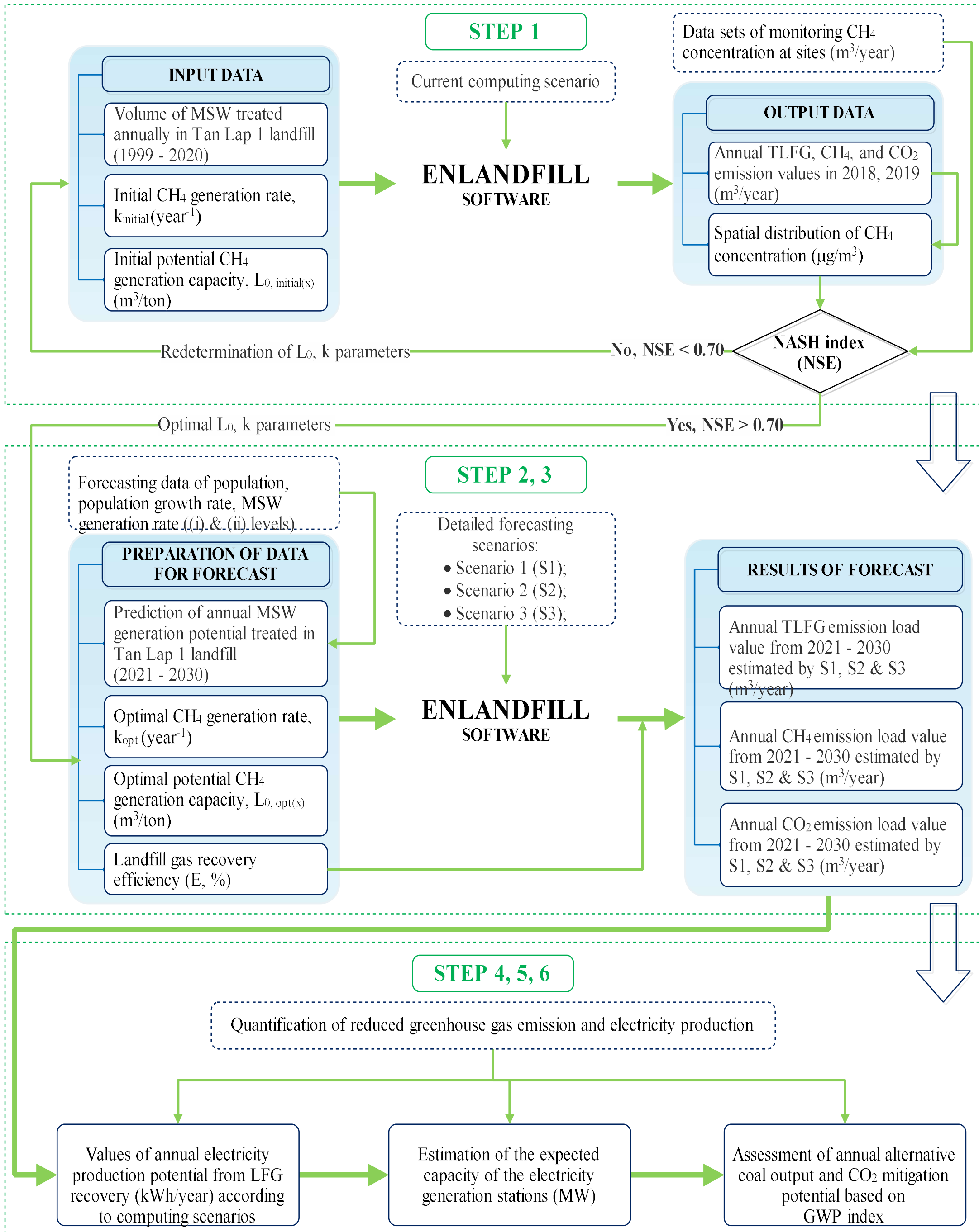

Figure 2. Conceptual framework of the applied methodology in this study.

2.3. Models

2.3.1. EnLandFill software

The results of experimental calculation through iteration calculations using EnLandFill software gave an estimated result of the potential coefficients of gas generation CH_4 (L_0) and the optimal gas rate constant (k) for research area. The Nash–Sutcliffe Statistical Index (NSE) is used to assess the optimal level of the set of coefficients (L_0, k). Monitoring data of CH_4 concentration was collected from reports of Tien Giang Department of Natural Resources and Environment, which was measuring times at 9.00 am on 25/03/2018, 8.00 am on

10/06/2018, at 11.00 am on 10/09/2018 and at 9.00 am on days 25/03/2019, 10/06/2019, 10/09/2019, 11/11/2019 at the TL1–TG monitoring position, Figure 1, are within the study area [26–27]. The EnLandFill software has been developed and tested based on meteorological data sets, mathematical models, and typical parameters with any landfill since the year 2019, which is applied to estimate LFG emission from MSW landfills of many Southern provinces [21].

2.3.2. Estimation of electricity generation potential from the recovered landfill gas

The electricity generation potential of MSW landfills depends on the total volume of CH_4 recovered from LFG collection systems [23–24]. The FOD (First–Order Decay) model in the EnLandFill software can be used to determine LFG emissions for each year in this research area. It should be noted that only a fraction of the CH_4 gas volume produced from organic matter degradable processes in landfills is able to be captured for electricity generation [24]. Therefore, the LFG recovery efficiency (E, %) assumed in the period of 2021–2030 is around 75% to 90% [25]. The total generated CH_4 gas volume from landfill captured to produce energy can be estimated as (1):

$$CAP_{CH_{4Yeari}} = E \times (1 - OX) \times \sum_{i=1}^{n} \sum_{j=0.1}^{1} k_{opt} L_{0,opt(x)} \left[\frac{M_i}{10} \right] e^{-k_{opt} t_{ij}} \times D_{CH_4} \quad (1)$$

The electricity generation potential, $EP_{LFG,yeari}$ (unit: kWh/year) from the total captured CH_4 gas volume estimated for each operating year can be obtained as (2) [9, 13]:

$$EP_{LFG,yeari} = \frac{CAP_{CH_{4Yeari}} \times LHV_{CH_4} \times \delta \times \varepsilon}{\phi} \quad (2)$$

where LHV_{CH_4} is the Lower Heating Value (LHV) of CH_4 gas (unit: MJ/m^3), and the LHV_{CH_4} value is about from 35.0 MJ/m^3 to 37.2 MJ/m^3 [23, 28, 29]; δ is the capacity factor of the entire recovered CH_4 combustion process to generate energy source, the common δ value is roughly 85% [23, 30]; ε is the electricity generation efficiency of the gas turbine engine, and is given a range of 30–35% [13, 31]; ϕ is the conversion factor from MJ to kWh, and ϕ value is taken as 3.6 [23–24]. The energy plant size from captured CH_4 gas of landfill ($LFGTE_{(size)}$) assuming it is able to operate throughout the year is calculated in kW or MW as (3) below [9, 23]:

$$LFGTE_{(size)} = \frac{EP_{LFG,yeari}}{D_{hr} \times \gamma} \quad (3)$$

where D_{hr} is the number of hours in a day (unit: hours), and γ is the number of days that power plant is worked in a year (unit: days).

2.3.3. Calculating the amount of coal replaced and CO_2 reduced from landfill gas

Type of coal and oil thermal power generation accounts for the largest proportion of 38% with 20,056 MW of total power system capacity in Vietnam [32]. The proportion of imported coal for electricity production tends to rise from 3.9% in 2016 to 65.6% in 2030 [32], which is able to lead to financial risks, pressures on infrastructure costs and investment costs, along with energy security, environmental risks and public health [33].

Electricity production from the recovered LFG is a type of fuel instead of coal sources, thereby reducing the local dependence on imported coal as well as adding a clean energy souce. The mass flow rate of coal (unit: kg/hour) used as a fuel that is replaced by the captured CH_4 gas through an LFG collection system can be calculated as (4) follows [34–35]:

$$m_{Coal} = \frac{EP_{LFG,yeari}}{LHV_{Coal} \times \eta \times \tau} \quad (4)$$

where $EP_{Coal,yeari}$ is the electrical power generated from coal (unit: MJ/year); $EP_{LFG,yeari}$ is the electrical power produced from recovered LFG (unit: MJ/year); m_{Coal} is the mass flow rate of coal consumed or equivalent instead (unit: kg/hour); LHV_{Coal} is the Lower Heating Value of coal (unit: MJ/kg); η is the boiler efficiency (unit: %), and τ is the operating time (unit: hour).

2.3.4. Assessment of GHGs emission reduction potential from MSW landfills

The MSW generation and treatment in landfills commonly including rapidly biodegradable waste that increased significantly GHG emissions releasing into the atmosphere [36], whilst LFG is mainly composed of CH_4 and CO_2 gases [37–39] contributing about 45–60% and 40–60% respectively [40]. Both CH_4 and CO_2 gases are the main GHGs because of their capacity to trap solar energy [41].

The Global Warming Potential (or "GWP") can be understood as a certain amount of GHG, released into the atmosphere causes a warming effect on the Earth [42] over a given period of time (normally 100 years) [41, 43]. GWP is an index, with CO_2 gas having the index value of 1, and the GWP for all other GHGs is the number of times more warming they cause compared to CO_2 [41]. The GWP values used to convert the GHG emissions from different unit to homogeneous unit called CO_2 equivalent or CO_2–eq shown in Table 1 [42]. The GHG emissions can be compared directly through a calculation based on (5) follows [41, 43]:

$$Emission_{GHGi,CO_2-eq} = Emission_{GHGi} \times GWP_{index,i} \quad (5)$$

where $Emission_{GHGi,CO_2-eq}$ is the emission of GHG i converted to the unit of CO_2–eq; $Emission_{GHGi}$ is the emission of GHG i estimated in the unit of ton or kg, and $GWP_{index,i}$ is the Global Warming Potential of GHG i that can be referenced from Table 1 below.

Table 1. The GWP index values for CO_2 and CH_4 gases from the Report Assessment of IPCC.

Greenhouse Gas (GHGs)	GWP values for 100–year time horizon			
	Second Assessment Report (AR2)	Third Assessment Report (AR3)	Fourth Assessment Report (AR4)	Fifth Assessment Report (AR5)
Carbon Dioxide (CO_2)	1	1	1	1
Methane (CH_4)	21	23	25	28

To calculate the total value of GHG emission reduction potential generated from landfills for each year based on the computing scenario plan having biogas recovery to produce power generation can be shown in (6) [36, 44].

$$\sum RE_{GHGs,yeari} = Q'_{CH_{4Yeari}} \times GWP_{CH_4} + Q'_{CO_{2Yeari}} \times GWP_{CO_2} \quad (6)$$

where $\sum RE_{GHGs,yeari}$ is the total GHGs emission reduction potential of the year i (unit: tCO_2–eq/year); $Q'_{CH_{4Yeari}}$ and $Q'_{CO_{2Yeari}}$ is the emissions of CH_4 and CO_2 gases generated from landfill in the year i can be decreased; GWP_{CH_4} and GWP_{CO_2} is the Global Warming Potential (GWP) values of CH_4 and CO_2 gases.

3. Results and discursion

3.1. Assessment of potential solid waste generation, 2021–2030

From the population data in 2019 [45] and the forecast of the average population growth rate per year according to [46], the estimated results of population and generated solid waste volume potential will be collected and treated in the period of 2021–2030 in the Tan Lap 1 landfill, based on the studies [47] calculated and shown in Table 2. At the same time, based on [25], the rate of solid waste collected in the period from 2021–2025 in My Tho City, Cai Be Town is P_{pre} = 90% and 4 other districts in the study area are P_{pre} = 85%; Then, in the period from 2026–2030, the planned collection rate for the whole province will be P_{pre} = 100%.

Table 2. Prediction of population and MSW generation potential, in the period of 2021–2030.

Year	Population, Unit: people			Solid waste generation potential, Unit: ton		
	My Tho City	Cai Be District	Other Districts	My Tho City	Cai Be District	Other Districts
2021	230,340	295,601	716,738	82,023	105,262	241,047
2022	231,463	297,043	720,234	82,423	105,775	242,223
2023	232,593	298,492	723,747	82,825	106,291	243,404
2024	233,727	299,948	727,278	83,229	106,810	244,591
2025	234,466	300,896	729,575	83,492	107,147	245,364
2026	235,206	301,846	731,880	102,505	131,548	318,961
2027	235,949	302,800	734,193	102,829	131,963	319,968
2028	236,695	303,756	736,512	103,154	132,380	320,979
2029	237,443	304,716	738,839	103,480	132,798	321,993
2030	237,937	305,350	740,377	103,695	133,075	322,664
Total	**2,345,818**	**3,010,448**	**7,299,372**	**929,654**	**1,193,049**	**2,821,195**

The above results show that, MSW in the period 2021–2030 tends to increase continuously as follows: (i) in the period of 2021–2025, the estimated total volume of generated solid wastes collected and treated at the landfill is 2,161,905 tons (average 1,184.6 tons/day) and level (ii) in the period 2026–2030, the total volume of generated solid waste that can be treated is 2,781,993 tons (average 1,524.4 tons/day). In which, the largest generated solid waste is concentrated in Cai Be Town with a total volume of about 531,285 tons (average of 291.1 tons/day) according to the level (i) of the period 2021–2025 and about 661,764 tons (average 362.6 tons/day), according to the level (ii) of the period 2026–2030; followed by in Chau Thanh District with a total volume of about 451,527 tons (average 247.4 tons/day) according to the level (i) of the period 2021–2025 and about 595,501 tons (average 326.3 tons/day) according to level (ii) of the period 2026–2030.

3.2. Assessment of greenhouse gas emission load

Assuming that the composition of buried solid waste at landfill is not much different, in the period 1999–2020, from the composition of solid waste, the mass ratio (W_i, %) and fixed carbon composition (DOC_i, %) is shown in Table 3 and determined DOC, L_0 values based on studies [21, 44, 48].

Table 3. Synthesis of buried solid waste components of Tan Lap 1 landfill.

Solid waste component	W_i, mean (%)	Range of DOC_i (%)	DOC_i, mean (%)	W_i * DOC_i
Organic matter	77.53	20 – 50	38	0.294614
Paper	3.89	40 – 50	42	0.016338
Rubber	3.19	47	46	0.014674
Textiles	1.40	25 – 50	28	0.003920

Solid waste component	W_i, mean (%)	Range of DOC_i (%)	DOC_i, mean (%)	$W_i * DOC_i$
Nappies	0.17	44 – 80	58	0.000986
Garden and park waste	4.50	45 – 55	48	0.021600
Metal	0.23	–	–	–
Glass	0.21	–	–	–
Ceramic and brick	2.14	–	–	–
Hazardous waste	0.06	–	–	–
Plastics	3.18	–	–	–
Other wastes	3.50	–	–	–
Total	**100.00**	**–**	**–**	**0.352132**

Similarly, it is assumed that the composition of solid waste treated at landfill is little different from year to year, continues to remain unchanged in the period 2021–2030. Combined with parameters $DOC_f = 0.48$; the correction coefficient for gas CH_4, $MCF_{Tan\ Lap1} = 0.6$ [48], the F ratio of CH_4 gas in the total generated gas is valued from 50–53%, the optimal F is determined to be 52%. The results of estimating the potential value of CH_4 gas generation are from 106.137–112.505 m^3/tons of solid waste with an optimal $L_{0,opt(x)}$ value of 110.3826 m^3/tons of solid waste. The optimal input CH_4 (k_{opt}) generated rate constant for the LFG emission load forecasting model is determined by the experimental method based on the initial range of k values. The result of running calculation iterations determines the load, the concentration of the contagant at the measuring locations have been compared and verified to have determined the optimal k_{opt} value for landfill is $k_{opt} = 0.23$ $year^{-1}$. Note that the range of k values set in EnLandFill software for landfill is $k_{min} = 0.17$ [49].

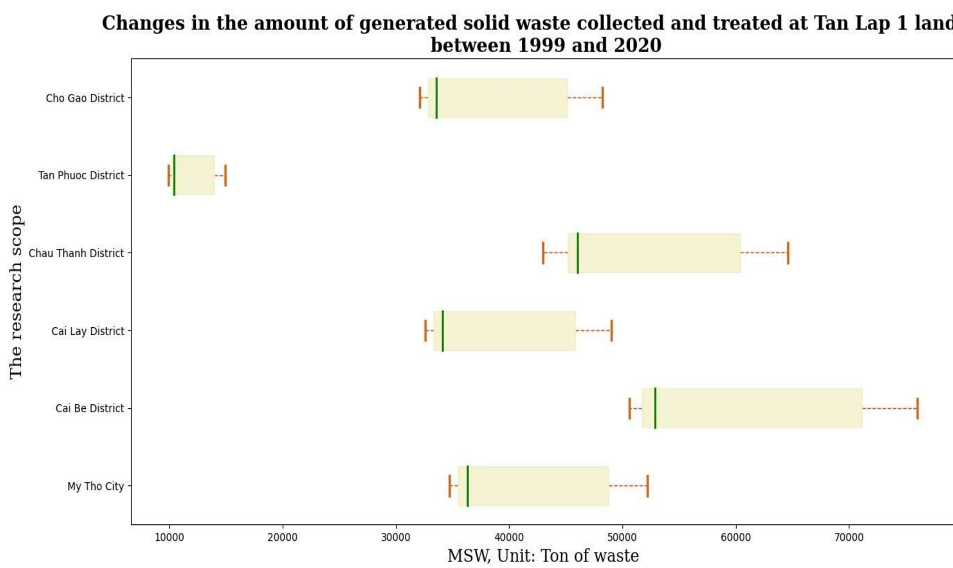

Figure 3. The diagram of changes in the solid waste generation which was collected and treated in the period of 1999–2020.

Based on the current data on the current volume of waste generated, collected and treated in the period 1999–2020 (Figure 3), it is found that in 2020 the total volume of collected and disposed urban MSW is estimated at 305,010.9 tons; in which the amount of solid waste generated in Cai Be Town is the highest with the volume of 76,034.6 tons, followed by Chau Thanh District and My Tho City with 64,569.4 tons and 52,190.5 tons respectively. The volume of solid waste generated is lowest in Tan Phuoc District with only 14,944.7 tons. The total volume of solid waste that has been buried and treated in the landfill in the period from 1999–2020 is 5,273,628.8 tons with the total volume of solid waste treated in Cai Be Town being the highest with 1,310,862.7 tons and the lowest is in Tan Phuoc District with 257,652.1 tons.

3.2.1. Scenario 1 (S1)

Figure 4 shows the CH_4, CO_2 and total landfill gas (TLFG) emissions load, from 2000–2030 under scenario 1. Figures 4a and 4b show that emissions of CH_4, CO_2, TLFG gases tend to increase significantly, specifically with optimal parameters $L_{0, opt(x)}$ = 110.38 m^3/tons solid waste (with F = 52%) and k_{opt} = 0.23 year^{-1} determine the total accumulated CH_4 and CO_2 gas loads are 435.3 million m^3 and 401.8 million m^3 respectively out of a total of 837.0 million m^3 TLFG. In particular, the highest CH_4 and CO_2 emissions are in 2020 with a load value of 30.9 million m^3 CH_4/year and 28.5 million m^3 of CO_2/year with maximum TLFG emissions of 59.4 million m^3/year. Compared with the results using the k_{min} and k_{max} parameters with the calculated parameter the optimal $L_{0, opt(x)}$ did not change, it was found that the estimated result had a significant difference. Specifically, the total accumulated CH_4 gas load reaches 395.2 million m^3/760.0 million m^3 of TLFG (k_{min} case) and 512.0 million m^3/984.7 million m^3 of TLFG (k_{max} case). Meanwhile, for CO_2, the total cumulative load reached 364.8 million m^3/760.0 million m^3 TLFG (in case of k_{min}) and 472.6 million m^3/984.7 million m^3 TLFG (in the case of k_{max}).

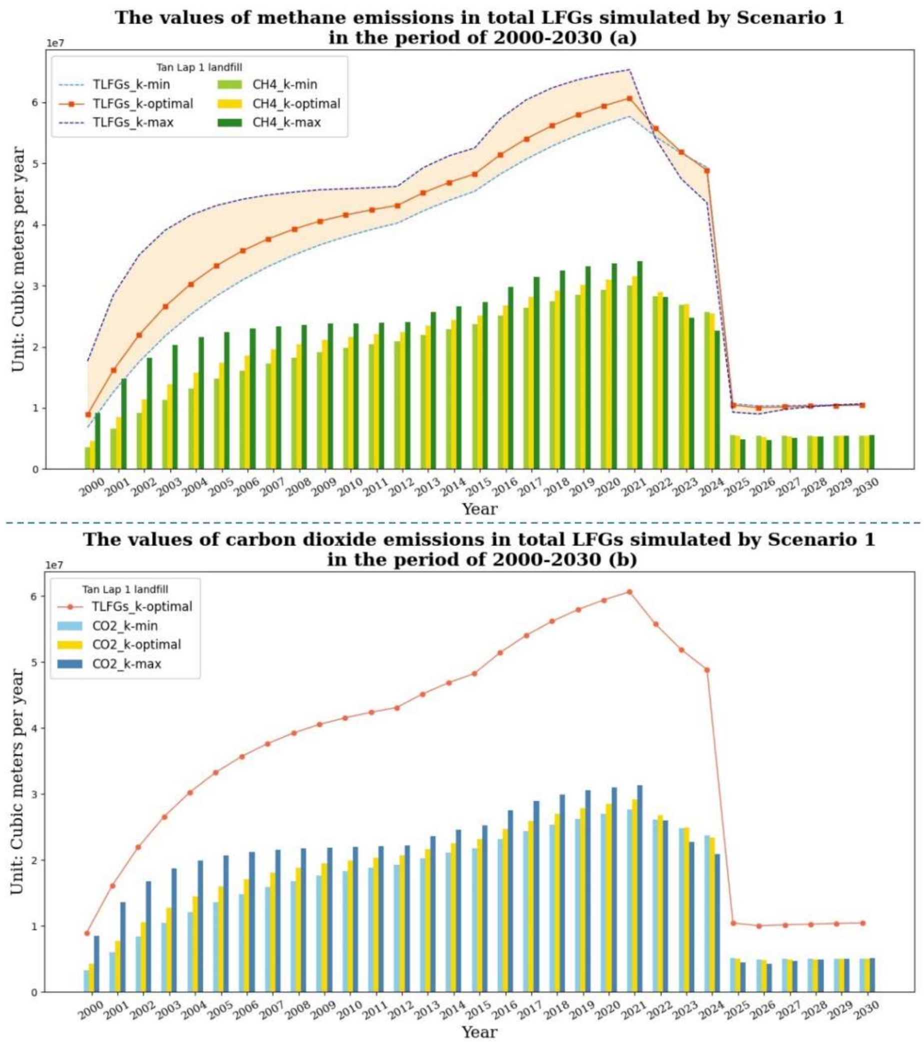

Figure 4. Emission load values of CH_4 (a) & CO_2 (b) according to scenario 1 in the period of 2000–2030.

In the period 2021–2030, GHG emissions tend to decrease significantly, especially in the period 2021–2025. Specifically, from 2021 to 2025 with optimal parameters $L_{0, opt (x)}$ and k_{opt} identified the total cumulative load of CH_4 and CO_2 gases is 118.4 million m^3/227.7

million m^3 of TLFG and 109.3 million m^3/227.7 million m^3 of TLFG, respectively. In the period 2025–2030, GHG emissions tend to be stable, with little variation when landfill is installed with LFGs collection system with gas recovery efficiency of E = 75%, and considering the oxidation in surface coating with an oxidation index (OX) of 10%. With CH_4, the total cumulative emissions are 26.7 million m^3 and with CO_2 of 24.7 million m^3 out of a total of 51.4 million m^3 of cumulative TLFG emissions, a decrease of 77.4% compared to the period 2021–2025. In the entire forecast period, the maximum generated TLFG emission load occurs at the beginning of the period in 2021 with the value of 60.7 million m^3/year, of which CH_4 and CO_2 are generated the highest is 31.6 million m^3/year and 29.1 million m^3/year, respectively.

3.2.2. Scenario 2 (S2)

Calculation results under scenario 2 are shown in Figure 5, showing the emission load of CH_4, CO_2 gases and TLFG in the period 2000–2030. From Figures 5c and 5d show that the trend and emission load of LFGs is similar to results from scenario 1, 2000–2020, calculated based on parameters $L_{0,\ opt\ (x)}$ optimal, optimal k_{opt}, k_{min} and k_{max}. The results show that emissions are maximized in 2020 with TFLG reaching 59.4 million m^3/year, of which CH_4 reaches 30.9 million m^3/year and CO_2 reaches 28.5 million m^3/year.

In the period of 2021–2030, the amount of GHGs emissions (CH_4 and CO_2) tends to decrease significantly compared to the current state, total accumulation of TLFG decreases by about 85.32% compared to the period 2000–2020. Specifically, in the first half of the period from 2021 to 2025, emissions tended to increase slightly, from 2025 to 2026, emissions decreased sharply, then maintained almost stable until the end of the period in 2030. Maximum emissions of the entire period The forecast section occurs in 2025 with 18.0 million m^3 TLFG/year, 9.4 million m^3 CH_4/year and 8.6 million m^3 CO_2/year, 3.37 times lower than scenario 1. The period from 2021 to 2025 when the LFGs collection system is installed with the gas recovery efficiency of E = 75% and the oxidation in the surface coating with an oxidation factor (OX) of 10%; together with the optimal parameters $L_{0,\ opt\ (x)}$ and k_{opt}, identified the total cumulative load of CH_4 and CO_2 gases of 41.7 million m^3 CH_4/80.2 million m^3 TLFG and 38.5 million m^3 of CO_2/80.2 million m^3 TLFG, respectively, 2.84 times lower than scenario 1. In the period 2025–2030, GHGs emissions tend to be stable, with little fluctuation when the LFGs collection system increases gas recovery efficiency to E = 90%. With CH_4, the total cumulative emission load is 22.2 million m^3 and for CO_2 gas is 20.5 million m^3 out of a total of 42.7 million m^3 of accumulated TLFG emissions, a decrease of 46.8% compared to the period 2021–2025 and 1.21 times lower than scenario 1.

3.2.3. Scenario 3 (S3)

The emission load of CH_4, CO_2 gases and TLFG for the period 2000–2030 under scenario 3 is shown in Figure 6. Figures 6e and 6f show that the emission trend of LFGs is similar to the simulation results of scenario 1 as well as scenario 2. Cumulative emissions generated in the period 2000–2020 with TFLG reaching 837.0 million m^3, 77.1 million m^3 higher for the case of k_{min} and 147.6 lower million m^3 in the case of k_{max}; of which CH_4 reached 435.3 million m^3, higher than 40.1 million m^3 with the case of k_{min} and lower than 76.8 million m^3 with the case of k_{max} and for CO_2, 37.0 higher million m^3 for k_{min} case and lower than 70.9 million m^3 for k_{max} case.

In the period of 2021–2030, the value of GHGs emission load of CH_4 and CO_2 tends to decrease significantly compared to the current state, the total accumulation of TLFG decreases by about 86.59% compared to the period 2000–2020. Specifically , in the first half of the period from 2021–2025, emissions tended to increase slightly, from 2025 to 2026, emissions decreased sharply, then maintained almost stable until the end of the period in 2030. Considering the entire forecast period, the maximum emissions will occur in 2025 with

16.1 million m^3 of TLFG/year, 8.4 million m^3 of CH_4/year and 7.7 million m^3 of CO_2/year, 1.12 times lower than the scenario 2, 3.77 times compared to scenario 1. In the first half of the forecast period from 2021 to 2025, LFGs collection system is installed with the gas recovery efficiency of E = 75% and oxidation in the surface coating with an oxidation coefficient (OX) of 10%; together with the optimal parameters $L_{0,\ opt\ (x)}$ and k_{opt}, identified the total cumulative CH_4 and CO_2 loads is 39.0 million m^3 CH_4/75.0 million m^3 TLFG and 36.0 million m^3 CO_2/75.0 million m^3 TLFG, respectively, 1.07 times lower than scenario 2 and 3.04 times lower than scenario 1. In the second half period from 2025 to 2030, GHGs emissions tend to be stable, there is an increase but less variation when the LFGs collection system increases gas recovery efficiency to E = 90%. With CH_4, the total cumulative emission load is 19.3 million m^3 and with CO_2 is 17.8 million m^3 out of a total of 37.2 million m^3 of accumulated TLFG emissions, a decrease of 50.4% compared to the period 2021–2025, 1.15 times lower than scenario 2 and 1.38 times lower than scenario 1.

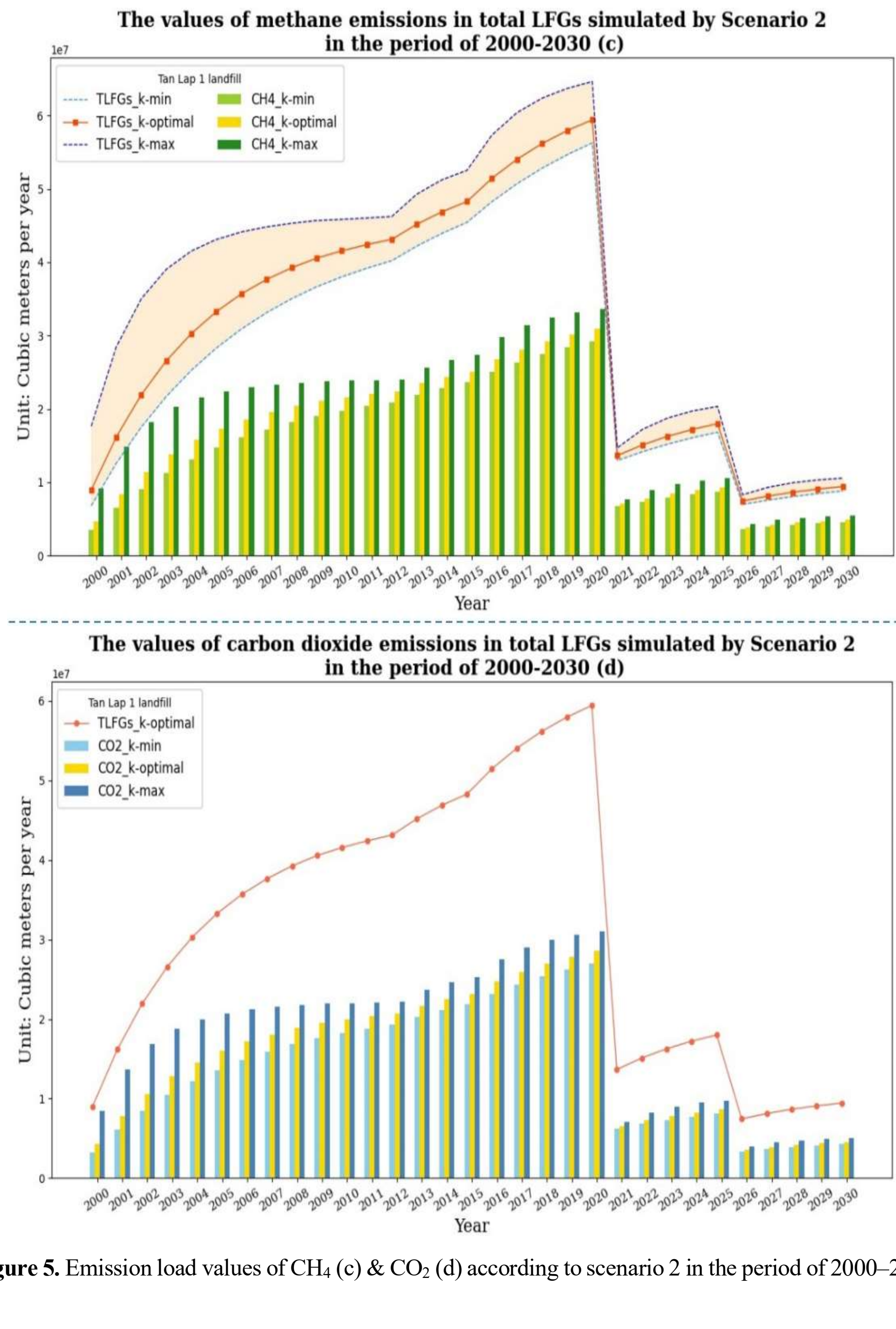

Figure 5. Emission load values of CH_4 (c) & CO_2 (d) according to scenario 2 in the period of 2000–2030.

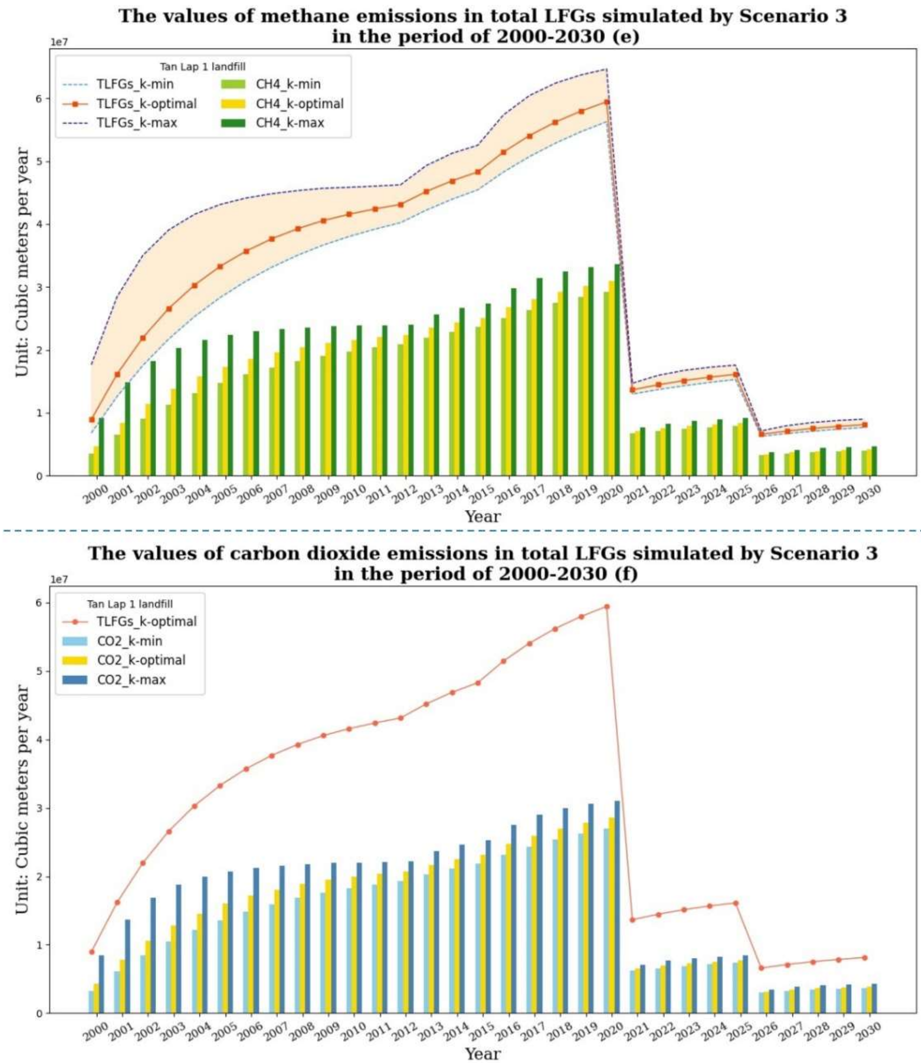

Figure 6. Emission load values of CH_4 (e) & CO_2 (f) according to scenario 3 in the period of 2000–2030.

3.3. Assessing the potential for electricity creation

3.3.1. Electricity output from recovered biogas in the period 2021–2030

The result of estimation of total CH_4 emission load recovered from the collection system with recovery efficiency E = 75–90% under scenarios 1–3, potential value of annual electricity generation $EP_{LFG,yeari}$ (kWh/year) was estimated using formula (2) shown in Table 4. Comment that, the annual electricity generation potential, 2021–2030, is highest in scenario 2, with a total value of 806.16–999.64 million kWh, 3.37 times higher than scenario 1 and 1.12 times higher than scenario 3. The greatest potential for electricity generation is in 2030 with an estimated 109.46–135.72 million kWh/year. The total value of electricity generated annually in scenarios 1 and 3 is 239.11–296.50 million kWh, 721.59–894.77 million kWh, respectively. The lowest power generation potential can be seen in scenario 1, about 3.02 times lower than scenario 3. The largest power generation potential in scenarios 1 and 3 is in 2030, estimated to be 40.48–50.20 million kWh/year (scenario 1) and 94.24–116.85 million kWh/year (scenario 3).

The size of the generating station ($LFGTE_{(size)}$) is calculated according to the formula (3) from CH_4 with the assumption that the power station is capable of operating throughout the year with D_{hr} = 24 hours/day, the number of days the power station operates in a year γ = 365 days. Thus, with the above assumptions, in scenario 1, the scale of the power station will gradually increase from 4,620 to 5,728 MW in 2025, it can reach 4,621–5,730 MW in 2030. For scenario 2, the scale of the power station from 6,028–7,475 MW in 2021 has increased significantly by about 2.07 times by the end of the period, estimated at 12,495–15,494 MW by 2030. Similarly for scenario 3, the size of power station tends to increase gradually in the whole period, from 6,028–7,475 MW (in 2021) up to 10,757–13,339 MW, by 2030.

Table 4. Estimated electricity generated potential results in the period 2021–2030.

Year	$CAP_{CH_{4Yeari}}$ (million m^3/year)	**Electricity generation potential, Unit: million kWh/year**			
		LHV = 35 MJ/m³ ε = 30%	**LHV = 35 MJ/m³ ε = 35%**	**LHV = 37.2 MJ/m³ ε = 30%**	**LHV = 37.2 MJ/m³ ε = 35%**
Scenario 1					
2021	0.000	0.000	0.000	0.000	0.000
2022	0.000	0.000	0.000	0.000	0.000
2023	0.000	0.000	0.000	0.000	0.000
2024	0.000	0.000	0.000	0.000	0.000
2025	16.323	40.467	47.212	43.011	50.179
2026	15.670	38.848	45.323	41.290	48.172
2027	15.876	39.358	45.918	41.832	48.805
2028	16.050	39.791	46.423	42.292	49.341
2029	16.200	40.161	46.855	42.686	49.800
2030	16.329	40.483	47.230	43.027	50.199
Total (million kWh)	**96.447**	**239.109**	**278.960**	**254.138**	**296.495**
Scenario 2					
2021	21.299	52.804	61.605	56.123	65.477
2022	23.556	58.399	68.132	62.070	72.415
2023	25.381	62.924	73.412	66.880	78.026
2024	26.864	66.601	77.701	70.787	82.585
2025	28.075	69.603	81.203	73.978	86.307
2026	34.870	86.449	100.857	91.882	107.196
2027	37.982	94.164	109.857	100.082	116.763
2028	40.487	100.374	117.103	106.683	124.464
2029	42.510	105.389	122.954	112.013	130.682
2030	44.150	109.455	127.697	116.335	135.724
Total (million kWh)	**325.174**	**806.160**	**940.520**	**856.833**	**999.639**
Scenario 3					
2021	21.299	52.804	61.605	56.123	65.477
2022	22.561	55.932	65.254	59.448	69.356
2023	23.591	58.486	68.234	62.162	72.523
2024	24.437	60.583	70.681	64.391	75.123
2025	25.137	62.319	72.705	66.236	77.275
2026	30.853	76.491	89.239	81.299	94.849
2027	33.249	82.430	96.169	87.612	102.213
2028	35.180	87.218	101.754	92.700	108.150
2029	36.742	91.090	106.272	96.816	112.952
2030	38.011	94.236	109.942	100.159	116.852
Total (million kWh)	**291.061**	**721.589**	**841.854**	**766.946**	**894.770**

3.3.2. Assessment of annual alternative coal output and CO_2 mitigation

Using recovered CH_4 gas as a fuel source for electricity production is an alternative to coal material, while reducing the amount of CO_2 caused (Table 5), calculated by formula (4). The assumption of the lower heating values of coal, $LHV_{coal(wet\ basis)}$ = 22.732 MJ/kg [35, 50, 51]; Boiler efficiency from coal burning can be achieved as η = 75% [50] and operating time is τ = 24 hours provided that the boiler operates throughout 365 days/year. On the one hand, results from scenario 1 show that the output of replaced coal is estimated at 18,429–22,851 tons in the period of 2021–2030 (average about 1,843–2,285 tons/year), specifically increasing from 2025 with about 3,119–3,867 tons/year up to 3,120–3,869 tons/year in 2030. For scenario 2, there are about 62,132–77,044 tons of coal (average about 6,213–7,704 tons/year) saved when using LFG instead in the period of 2021–2030, the trend of gradually increasing from 4,070 to 5,046 tons/year (by 2021) up to 8,436–10,460 tons/year (in 2030). Similarly for scenario 3, the potential reduction of coal used in the above period is estimated at 55,614–68,962 tons (average about 5,561–6,896 tons/year) and gradually increasing in the period from 2021 with 4,070–5,046 tons/year to 7,263–9,006 tons/year by 2030.

On the other hand, the total amount of carbon dioxide (CO_2) avoided when emissions into the atmosphere due to the amount of coal replaced is also evaluated for the period 2021–2030; accordingly, the total value is approximately 67,571–83,789 tons of CO_2 for scenario 1 (average about 6,757–8,379 tons of CO_2/year), about 222,819–282,495 tons of CO_2 for scenario 2 (average about 22,782–28,250 tons of CO_2/year) and about 203,919–252,860 tons of CO_2 for scenario 3 (average about 20,392–25,286 tons of CO_2/year).

Table 5. Estimated alternative coal and CO_2 minimization potential results in the period 2021–2030.

Year	Scenario 1		Scenario 2		Scenario 3	
	m_{coal} (Unit: ton/year)	**CO_2 reduction** (Unit: ton/year)	**m_{coal}** (Unit: ton/year)	**CO_2 reduction** (Unit: ton/year)	**m_{coal}** (Unit: ton/year)	**CO_2 reduction** (Unit: ton/year)
2021	0,000	0,000	5,046	18,504	5,046	18,504
2022	0,000	0,000	5,581	20,464	5,345	19,600
2023	0,000	0,000	6,014	22,050	5,589	20,495
2024	0,000	0,000	6,365	23,338	5,790	21,230
2025	3,867	14,181	6,652	24,390	5,956	21,838
2026	3,713	13,613	8,262	30,293	7,310	26,804
2027	3,761	13,792	8,999	32,997	7,878	28,885
2028	3,803	13,944	9,593	35,173	8,335	30,563
2029	3,838	14,073	10,072	36,930	8,705	31,920
2030	3,869	14,186	10,460	38,355	9,006	33,022
Total	**22,851**	**83,789**	**77,044**	**282,495**	**68,962**	**252,860**

3.3.3. Greenhouse gas emission reduction potential

To evaluate the potential for GHG emission reduction, including CH_4 and CO_2, the index of GWP is considered. The estimated results are detailed in Figure 7.

For scenario 1, GHG emission reduction potential is calculated with recovery efficiency E = 75% because in the period of 2021–2024, recovery of generated LFGs has not been considered. Total estimated mitigation potential $\sum RE_{GHGs,re}$ = 1,962.61 thousand tons of CO_2–eq compared with without recovery of LFG is $\sum RE_{GHGs,no-re}$ = 2,910.54 thousand tons of CO_2–eq, increasing from 2025 to 2030 with 319.19 thousand tons of CO_2–eq/year up to 332.62 thousand tons of CO_2–eq/year. With scenario 2, the total GHG emission reduction potential for the entire period 2021–2030 $\sum RE_{GHGs,re}$ = 6,623.74 thousand tons of CO_2–eq compared to without recovering LFG is $\sum RE_{GHGs,no-re}$ = 8,807.04 thousand tons of CO_2–eq, increasing Gradually from 2021 with 433.86 thousand tons of CO_2–eq/year up to 899.32 thousand tons of CO_2–eq/year by 2030. Under scenario 3, the total GHG emission reduction potential for the entire period of 2021–2030: $\sum RE_{GHGs,re}$ = 5,928.87 thousand tons of CO_2–eq compared to without recovering LFG is $\sum RE_{GHGs,no-re}$ = 7,908.18 thousand tons of CO_2–eq; GHG emission reduction potential increases from 433.86 thousand tons CO_2–eq/year (in 2021) to 774.28 thousand tons of CO_2–eq/year (in 2030).

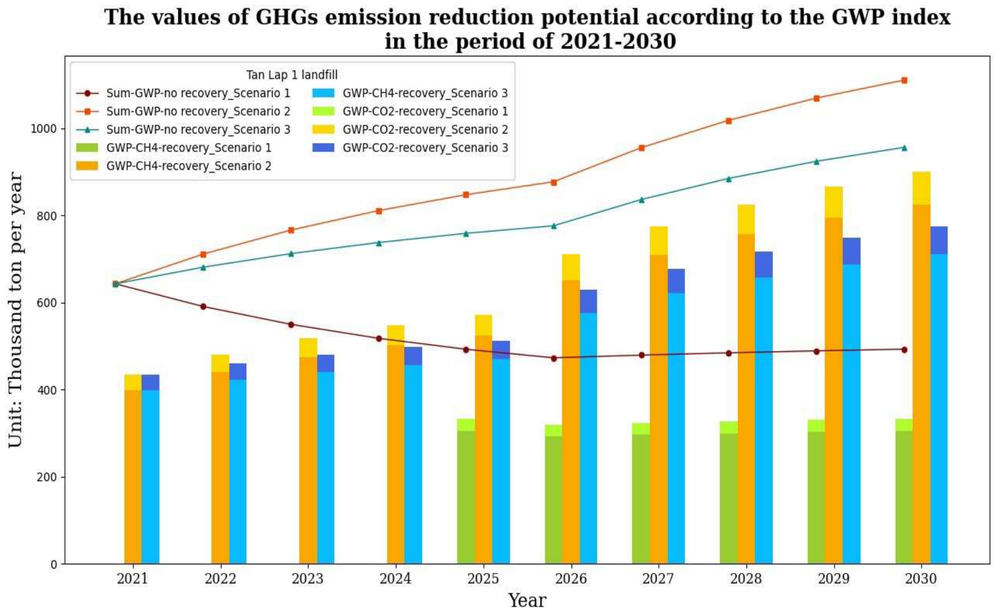

Figure 7. Potential value of GHG emission reduction, period 2021–2030 through GWP index.

3.4. EnLandFill model validation

The results of the calculation of the Nash–Sutcliffe index (NSE) show the simulation efficiency of EnLandFill ver. 2019 software in determining the emission load of generated gases, TLFG, CH_4 and CO_2 from the study area. The NSE is estimated based on the monitoring results of CH_4 gas concentrations collected at 08:00–11:00 on 25/03, 10/06, 10/09, 11/11 of 02 years 2018 and 2019 from [26–27] at the TL1–TG monitoring position within the scope of the research area. The results of simulations of the spread of CH_4 gas at the above calculation times from the study area based on the estimation results from the emission load module (scenarios 1, 2 and 3) in the EnLandFill software (Figure 8) were also extracted respectively at locations and at the same time of respective assessment.

With the Nash–Sutcliffe index (NSE), for simulation as $NSE_{TanLap\ 1}$ = 0.836 > 0.7, respectively, showed that the simulation results by EnLandFill software were at a good level with the condition that NSE > 0.7 was satisfied. Table 6 and Figure 9 show the comparison between the results of CH_4 gas concentration between monitoring and simulated CH_4 concentration using EnLandFill software.

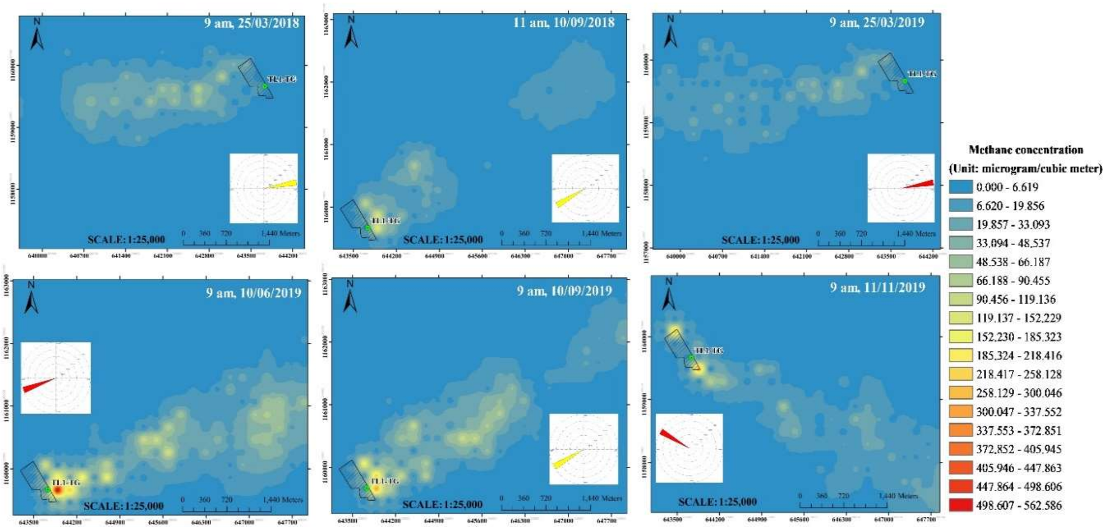

Figure 8. Maps of simulating CH_4 concentration dispersion levels and scope for several different times in 2018 and 2019.

Table 6. Table comparing CH_4 concentrations between monitoring and simulation using the EnLandFill software.

Signs	Coordinates of monitoring stations X (m)	Coordinates of monitoring stations Y (m)	Monitoring time, (hour)	Simulating CH_4 concentration by EnLandFill, (μg/m^3)	Monitoring CH_4 concentration, (μg/m^3)
TL1–TG	643733.41	1159665.13	9 am–25/03/2018	72.73	80.00
TL1–TG	643733.41	1159665.13	8 am–10/06/2018	93.09	83.00
TL1–TG	643733.41	1159665.13	11 am–10/09/2018	29.33	58.90
TL1–TG	643733.41	1159665.13	9 am–25/03/2019	16.74	9.80
TL1–TG	643733.41	1159665.13	9 am–10/06/2019	16.78	11.80
TL1–TG	643733.41	1159665.13	9 am–10/09/2019	16.76	13.60
TL1–TG	643733.41	1159665.13	9 am–11/11/2019	16.76	9.50

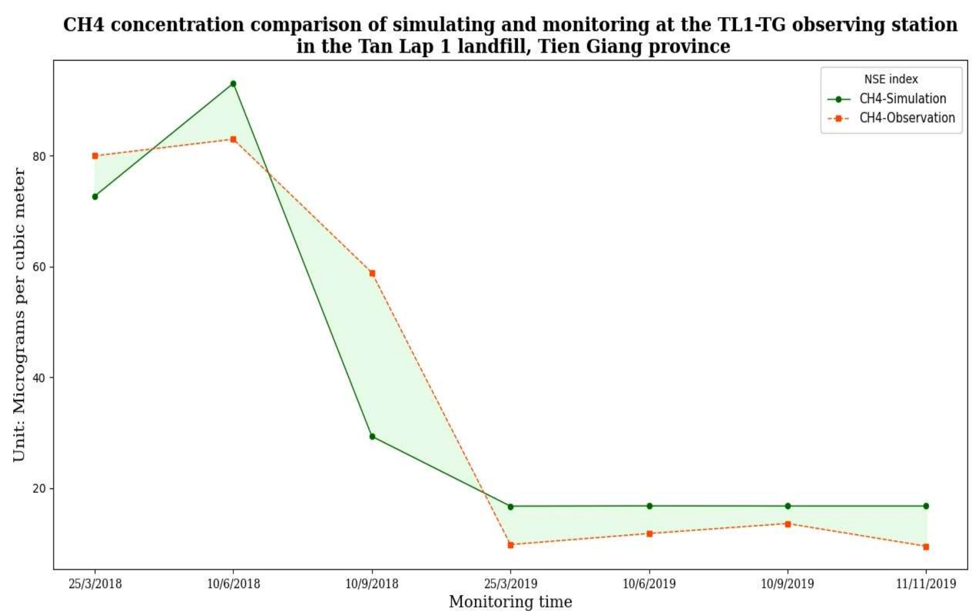

Figure 9. Comparison of CH_4 concentrations between monitoring and simulation at measuring locations.

4. Conclusion

The study identified the optimal calculation parameters and quantified the load of LFG emissions, including total LFGs, CH_4 and CO_2, forecast for the period 2021–2030, carried out for case studies in Tien Giang province. The main results of this paper are shown as follows.

In the period of 2021–2030, landfill is considered to have the lowest accumulation of GHG, CH_4 and CO_2 emissions in scenario 3, estimated about 58 million m^3 CH_4 and 53 million m^3 CO_2, showing the potential of mitigation GHG emissions according to the GWP index are approximate 6 million tons of CO_2–eq. The predicted maximum emission year is 2025 with a load of 8.4 million m^3 CH_4/year and 7.7 million m^3 of CO_2/year with a GWP of over 750 thousand tons of CO_2–eq. The highest accumulated GHG emissions are in scenario 1, estimated roughly 150 million m^3 CH_4 and 134 million m^3 of CO_2, indicating that GWP index reaches around 2 million tons of CO_2–eq. The maximum emission year is 2021 with a discharge of over 30 million m^3 CH_4/year and 29 million m^3 of CO_2/year with a GWP of about 650 thousand tons of CO_2–eq. The research results also show that with gas recovery efficiency generated from 75–90% designed for 3 scenarios, in the period of 2021–2030, it is expected to generate a total potential electricity production capacity estimated up to 990 million kWh is equivalent to the potential of replacing coal fuel source, from about 18,500–77,000 thousand tons and about 67,500–283,000 thousand tons of CO_2 avoided from coal burning.

The study results show that planning according to scenario 3 will be optimal for the treatment of MSW in Tien Giang province. This is the scenario with the lowest cumulative GHG emissions and also potentially significant power generation in the study area, 2021–2030. In addition, the simulation efficiency of the software is quite good with the NSE statistic index above 0.80. However, insufficient measurement data is one of the important reasons affecting the predictive errors of the model. Thus, future studies will continue to use the latest monitoring data to verify the simulation results by careful take into consideration background concentrations and pollution contributions from other areas in the treatment area, in order to make more accurate forecast results of the emission load of LFGs, in special attention, is paid to CH_4 gas.

Author contribution statement: Conceived and designed the experiments; Analyzed and interpreted the data; contributed reagents, materials, analysis tools or data; manuscript editing: B.T.L.; Performed the experiments; contributed reagents, materials, analyzed and interpreted the data, wrote the draft manuscript: N.H.P.

Acknowledgements This research was funded by the Viet Nam National University Ho Chi Minh City (VNU–HCM), grant No: B2019–20B–01. The authors would also like to thank the members of the Laboratory for Environmental Modelling, Ho Chi Minh City University of Technology for discussions that improved the quality of the publication.

Competing interest statement The authors declare no conflict of interest.

References

1. Berenyi, E.B.; Gould, R.N. Methane recovery from municipal landfills in the USA. *Waste Manag. Res.* **1986**, *4*, 189–196.
2. IPCC. Climate Change 2007: Synthesis Report. *Intergov. Panel Clim. Chang.* **2007**, pp. 1–104.
3. EU Commission. Taking Sustainable use of resources forward: A Thematic Strategy on the prevention and recycling of waste, Brussels, Belgium, 2005.
4. Huhtinen, K.; Lilja, R.; Sokka, L.; Salmenperä, H.; Runsten, S. The National Waste Plan to the Year 2016 – Background Document, 2007.
5. Finland Ministry of the Environment. Towards a Recycling Society e National Waste

Plan until 2016 (in Finland), 2010.
6. Niskanen, A.; Värri, H.; Havukainen, J.; Uusitalo, V.; Horttanainen, M. Enhancing landfill gas recovery. *J. Clean. Prod.* **2013**, *55*, 67–71.
7. Aghdam, E.F.; Fredenslund, A.M.; Chanton, J.; Kjeldsen, P.; Scheutz, C. Determination of gas recovery efficiency at two Danish landfills by performing downwind methane measurements and stable carbon isotopic analysis. *Waste Manag.* **2018**, *73*, 220–229.
8. Spokas, K.; Bogner, J.; Chanton, J.P.; Morcet, M.; Aran, C.; Graff, C.; Golvan, Y.M.L.; Hebe, I. Methane mass balance at three landfill sites : What is the efficiency of capture by gas collection systems?. *Waste Manage.* **2006,** *26*, 516–525.
9. Cudjoe, D.; Han, M.S.; Nandiwardhana, A.P. Electricity generation using biogas from organic fraction of municipal solid waste generated in provinces of China: Techno–economic and environmental impact analysis. *Fuel Process. Technol.* **2020**, *203*, 106381.
10. US EPA. Landfill Methane Outreach Program: Accomplishments, 2008.
11. US EPA. Landfill Methane Outreach Program: Basic Information, 2008.
12. US EPA. Landfill Methane Outreach Program: Energy Projects and Candidate Landfills, 2008.
13. Ghosh, P. et al. Assessment of methane emissions and energy recovery potential from the municipal solid waste landfills of Delhi, India. *Bioresour. Technol.* **2019**, 611–615.
14. Menikpura, S.N.M.; Sang–Arun, J.; Bengtsson, M. Climate co–benefits of energy recovery from landfill gas in developing Asian cities: A case study in Bangkok. *Waste Manag. Res.* **2013**, *31*, 1002–1011.
15. Duc, N.H. Current status, solid waste management policy in Vietnam and potential for energy recovery from solid waste, Ho Chi Minh City, 2014.
16. World Bank. Background Paper–Potential climate change mitigation opportunities in waste management sector in Vietnam, 2009.
17. UNFCCC. Report Landfill gas recovery and utilization in Nam Son, Tay Mo landfills in Hanoi (Clean Development Mechanism – CDM) – Project 3733, 2018.
18. Schneider, P.; Anh, L.H.; Wagner, J.; Reichenbach, J.; Hebner, A. Solid waste management in Ho Chi Minh City, Vietnam: Moving towards a circular economy?. *Sustain.* **2017**, *9*, 1–20.
19. Biwase, Make electricity from waste, Binh Duong Water – Environment Joint Stock Company (Biwase), 2020.
20. People's Committee of Tien Giang Province. Report on solid waste management in Tien Giang, Tien Giang Province, 2019.
21. Long, B.T.; Phong, N.H. Integrated model for methane emission and dispersion assessment from landfills: A case study of Ho Chi Minh City, Vietnam. *Sci. Total Environ.* **2020**, *738*, 139865.
22. Lima, R.M. et al. Spatially distributed potential of landfill biogas production and electric power generation in Brazil. *Waste Manag.* **2018**, *74*, 323–334.
23. Cudjoe, D.; Han, M.S. Economic and environmental assessment of landfill gas electricity generation in urban districts of Beijing municipality. *Sustain. Prod. Consum.* **2020**, *23*, 128–137.
24. Cudjoe, D.; Han, M.S.; Chen, W. Power generation from municipal solid waste landfilled in the Beijing–Tianjin–Hebei region. *Energy* **2021**, *217*, 119393.
25. People's Committee of Tien Giang Province. Planning of Solid waste management in Tien Giang Province for the period 2011 – 2020, vision to 2030, Tien Giang Province, 2013.
26. Tien Giang Department of Natural Resources and Environment. Report on the results

of environmental monitoring in Tien Giang province in 2018, Tien Giang province, 2018.
27. Tien Giang Department of Natural Resources and Environment. Report on the results of environmental monitoring in Tien Giang province in 2019. Tien Giang province, 2019.
28. Scarlat, N.; Motola, V.; Dallemand, J.F.; Monforti–Ferrario, F.; Mofor, L. Evaluation of energy potential of Municipal Solid Waste from African urban areas. *Renew. Sustain. Energy Rev.* **2015**, *50*, 1269–1286.
29. Ayodele, T.R.; Ogunjuyigbe, A.S.O.; Ekoh, E.E. Outlook of Agricultural Sector in the Face of Changing Global Climate: The Case of Nigeria. *Agric. Res. Technol. Open Access J.* **2017**, *5*, 68–71.
30. Ogunjuyigbe, A.S.O.; Ayodele, T.R.; Alao, M.A. Electricity generation from municipal solid waste in some selected cities of Nigeria: An assessment of feasibility, potential and technologies. *Renew. Sustain. Energy Rev.* **2017**, *80*, 149–162.
31. Ayodele, T.R.; Ogunjuyigbe, A.S.O.; Alao, M.A. Economic and environmental assessment of electricity generation using biogas from organic fraction of municipal solid waste for the city of Ibadan, Nigeria, *J. Clean. Prod.* **2018**, *203*, 718–735.
32. Anh, T.T. Evaluation of coal types used for thermal power plants, Ha Noi, 2019.
33. Vietnam Business Forum (VBF). The Energy Plan for Manufacturing in Vietnam (Version 2.0). Research on Vietnam's capacity to concentrate MSW resources to encourage investment in clean, safe and affordable energy production, 2019.
34. Surroop, D.; Mohee, R. Power generation from landfill gas, in 2011. Proceeding of 2nd International Conference on Environmental Engineering and Applications, **2011**, *17*, 237–241.
35. Purmessur, B.; Surroop, D. Power generation using landfill gas generated from new cell at the existing landfill site. *J. Environ. Chem. Eng.* **2019**, *7*, 103060.
36. Yaman, C.; Anil, I.; Alagha, O. Potential for greenhouse gas reduction and energy recovery from MSW through different waste management technologies. *J. Clean. Prod.* **2020**, *264*, 121432.
37. Williams, P.T. Waste Treatment and Disposal–Second Edition. 2005.
38. Rafiq, A.; Rasheed, A.; Arslan, C.; Tallat, U.; Siddique, M. Estimation of greenhouse gas emissions from Muhammad wala open dumping site of Faisalabad, Pakistan. *Geol. Ecol. Landscapes* **2018**, *2*, 45–50.
39. Fallahizadeh, S.; Rahmatinia, M.; Mohammadi, Z.; Vaezzadeh, M.; Tajamiri, A.; Soleimani, H. Estimation of methane gas by LandGEM model from Yasuj municipal solid waste landfill, Iran. *MethodsX* **2019**, *6*, 391–398.
40. Tchobanoglous, G.; Theisen, H.; Vigil, S.A. Integrated solid waste management: engineering principles and management issues. New York, USA: McGraw–Hill series in water resources and environmental engineering, 1993.
41. Brander, M. Greenhouse Gases, CO_2, CO_2–eq, and Carbon: What Do All These Terms Mean?. *Ecometrica*, 2012, pp. 3.
42. Climate Leadership Group – C40 Cities, Workshop on developing city–level greenhouse gas inventory activities – Technical manual for participating experts, Ho Chi Minh city, 2018.
43. Green House Protocol. Global Warming Potential Values, 2015.
44. IPCC. CH_4 Emissions from Solid Waste Disposal. IPCC Good Pract. Guid. Uncertain. Manag. *Nat. Greenh. Gas Invent.* **2006**, 419–439.
45. Central Population and Housing Census Steering Committee. The 2019 Vietnam population and housing census, Ha Noi Capital, 2019.
46. General Statistics Office. Vietnam Population Forecast 2014–2049, Ha Noi Capital, 2016.

47. Talaiekhozani, A.; Nematzadeh, S.; Eskandari, Z.; Dehkordi, A.A.; Rezania, S. Gaseous emissions of landfill and modeling of their dispersion in the atmosphere of Shahrekord, Iran. *Urban Clim*. **2018**, *24*, 852–862.
48. Pipatti, R. et al. Chapter 3: Solid Waste Disposal, in 2006 IPCC Guidelines for National Greenhouse Gas Inventories, IPCC, **2006**, pp. 1–40.
49. Alexander, A.; Burklin, C.; Singleton, A. Landfill Gas Emissions Model (LandGEM) Version 3.02 User's Guide, 2005, pp. 56.
50. Amrehn, T.S.J. The electricity from garbage, Ha Noi Capital, 2014.
51. ESSOM Co. LTD. Heating Values of Hydrogen and Fuels, 2019.

VIETNAM JOURNAL OF HYDROMETEOROLOGY

Research Article

Green space study in 12 urban districts of Ha Noi using remote sensing data

Hai Khuong Van[1*], Trang Tran Huong[2]

[1] Water Resources Institute; khuongvanhai@gmail.com
[2] Ha Noi University of Natural Resources and Environment; tranhuongtrang2608gmail.com
* Correspondence: khuongvanhai@gmail.com; Tel.: +84–974183835
Received: 22 February 2021; Accepted: 15 April 2021; Published: 25 April 2021

Abstract: Today, the environmental situation in urban areas becoming polluted, people are increasingly interested in and want to live in green cities. This paper uses the satellite image Landsat 8 and the method of calculating the vegetation index (NDVI) combined with the multivariate regression analysis to study and evaluate the change of greenery area for the inner districts of Hanoi period 2013–2016. The study results show that the greenery area is strongly correlated in the central districts and the average correlation in districts with high urbanization or agricultural areas. The green tree density in Ha Noi city is quite different between the central districts and suburbs. In the suburb such as Long Bien, Ha Dong, Nam Tu Liem, North Tu Liem, Tay Ho, Hoang Mai the green tree density in the people is quite high, exceeding TCVN 9257:2012. To be specific, Long Bien district has the highest green tree density, with 134.2 m2/person up to 11 times national standards. Meanwhile, central districts such as Dong Da, Hai Ba Trung, Ba Dinh, Hoan Kiem, Thanh Xuan have very low green tree density, lower than the minimum standard of TCVN 9257: 2012. To be specific, Dong Da is the lowest green tree density with 2.5 m^2/person, lower than the TCVN 9257:2012 (> 12 m^2/person) to 4.8 times national standards.

Keywords: NDIV; Green tree; Remote sensing; GIS; Ha Noi City.

1. Introduction

Urban inhabitants are expected to reach 70 % of the world population by 2050 which is likely to lead to an array of environmental problems in cities such as increasing air pollution and climatic perturbations. Urban green spaces are defined as all natural, semi–natural, and artificial systems within, around and between urban areas of all spatial scales [1]. Urban green spaces promote multiple effects such as health, wellbeing and aesthetic benefits to urban dwellers [2]. Therefore, data on Urban green spaces are crucial to a range of issues in urban science such as planning, management and public health.

In the past decades, remote sensing technologies have occupied an important place in the study of Urban green spaces as they can generate repeated and complete coverage at different spatial scales and for different seasons [3]. Based on recent advances such as high spatial resolution imagery and free data access policies, remote sensing is providing a valuable set of tools which are able to minimize the need for field survey, even in highly heterogeneous and complex urban settings. For instance, remote sensing has proven to be effective for mapping street trees [4], detecting species within Urban green spaces [5], mapping invasive shrubs in Urban green spaces [6] and assessing vegetation health within Urban green spaces [7]. Furthermore, current remote sensing programs such as Copernicus [8] and Landsat not only provide historical time–series data but also facilitate access to recently acquired data [9].

Green plants have a decisive role in Urban green spaces. They are considered as urban lungs, play a role in harmonizing the natural, human and social factors, improve the microclimate, the quality of living environment and create urban landscapes. Currently in Vietnamese cities, there are two methods of urban greenery management, including: land use map (used by departments). Stumps distribution map (used extensively in tree companies). Both methods of management have a common disadvantage that do not calculate the actual green plant cover.

Hanoi is a special urban area, is the brain center of politics–economy–culture of the country, has the highest urbanization rate in Vietnam [10–11]. The rapid urbanization rate has expanded the urban area, forming spontaneously developed residential areas with dense residential density, increasing construction density means vacant land is scarce, and Hanoi cabinet is increasingly "less" green. Therefore, the assessment of the current urban greenery in the city is very necessary to understand the current urban greening situation, as a tool for the State, the local government at all levels, and the people to work together to formulate policies. policies and implementation of measures to maintain and improve urban green coverage.

One of the most powerful tools to support green plant research is Remote sensing and GIS [12–14]. Remote sensing is one of the achievements of aerospace science and it is widely applied in many fields, from meteorology, hydrology, geology, environment, ...[15–17]. This paper uses remote sensing and GIS to study the urban green area fluctuation to assess the distribution and variation of urban green trees, support the management and planning of green plants in Ha Noi.

2. Materials and methods

2.1. Data collection

Using landsat 8 images with 30m resolution of United States Geological Survey (USGS) [18]. Additional Criterial tool is used to select 10% less cloud cover to ensure the best image, clear and cloudless in the study area. Information about Landsat 8 images collected and processed is given in Table 1.

Table 1. List statistics of Landsat 8 images were used in the study.

No.	Image code	Location	Date	Time (GMT +7)
1	LC81270452013160LGN00	127/45	09/06/2013	10h25’
2	LC81270452013352LGN00	127/45	18/12/2013	10h24’
3	LC81270452014019LGN00	127/45	19/01/2014	10h24’
4	LC81270452015022LGN00	127/45	22/01/2015	10h23’
5	LC81270452015150LGN00	127/45	30/05/2015	10h22’
6	LC81270452015182LGN00	127/45	01/07/2015	10h22’
7	LC81270452015230LGN00	127/45	18/08/2015	10h23’
8	LC81270452016137LGN00	127/45	16/05/2016	10h22’
9	LC81270452016153LGN00	127/45	01/06/2016	10h23’
10	LC81270452016265LGN00	127/45	21/09/2016	10h23’
11	LC81270452016281LGN00	127/45	07/10/2016	10h23’
12	LC81270452016345LGN00	127/45	10/12/2016	10h23’

Survey data was collected during the survey on 7th January 2017, which was used as a model for independent sampling. Survey sites are stable location, less variable locations of trees in the period from 2013 to 2016. Independent sites are randomly selected, but spread over the area. The number of survey sites are 45 points with 30 features for classification and 15 random points for checking the accurate classification. The map of the survey sites is shown in the Figure 1.

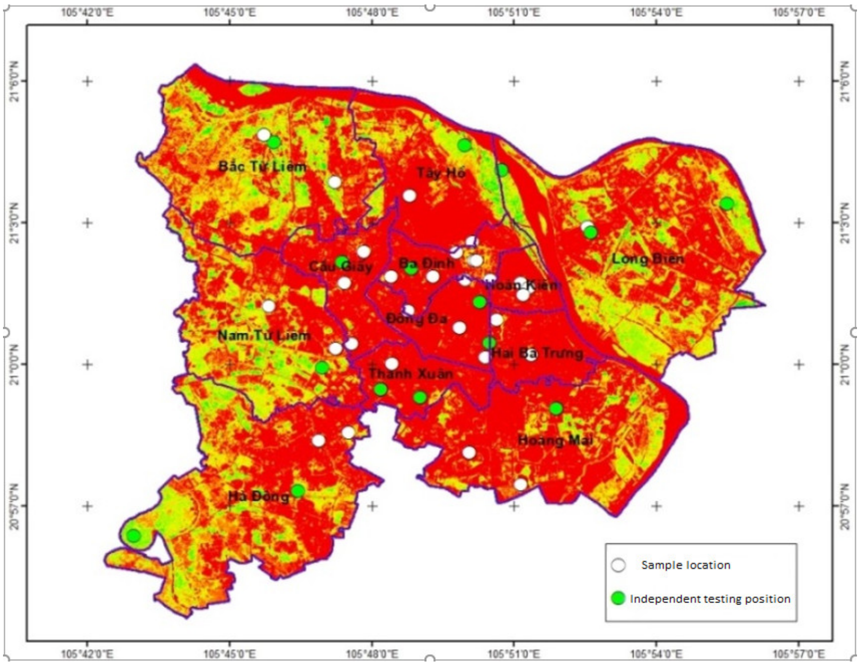

Figure 1. The survey locations in the research area.

2.2 Methodology

The steps of reseach and evaluation the variation of green plant area in the study include: 1) collecting satellite imagery data; 2) Filter and select images that are reliable; 3) Survey, identify the objects; 4) Calculate the NDVI vegetation index from the satellite images and compare with the sample from the survey; 5) Verification of NDVI index from independent samples; 6) Development of green plant distribution maps based on NDVI; 7) Evaluate the variation of tree area by multivariate regression. The method details of the steps are presented in Figure 2.

2.2.1. The normalized difference vegetation index (NDVI)

The normalized difference vegetation index (NDVI) is widely used to determine the distribution of vegetation, assess the growth and development crops, as a basis for forecasting drought, yield and product. The vegetation index is determined based on the different reflexes of the object between the visible and near infrared.

$$NDVI = \frac{\mathrm{IR-R}}{\mathrm{IR+R}} \quad (1)$$

where R is the reflection value of near infrared (NIR); R is the reflection value of the red wave length.

2.2.2. Multivariate Linear Regression

The development of plants associated with four weather conditions in the year. Therefore, the change of vegetation layer is often associated with the characteristics of climate such as rainfall, temperature, and humidity .... In the study, the authors have pointed out the relationship between NDVI and climatic factors that affect the density of green trees in urban areas [19–21].

The authors observed that the variation of vegetation area was strongly correlated with three climatic factors including temperature, humidity and rainfall. The general linear regression equation with three independent variables is of the form:

$$Y = b_0 + b_1 \times X_1 + b_2 \times X_2 + b_3 \times X_3 \quad (2)$$

where Y is the dependent variable (variable plant area); X_1, X_2, X_3 are independent variables (climate variables); b_0 is the original pitch; b_1 is the slope coefficient of Y following by X1 while keeping X_2, X_3 constant; b_2 is the slope coefficient of Y following by X_2 while keeping X_1, X_3 constant; b_3 is the slope coefficient of Y following by X_3 while keeping X_1, X_1 constant.

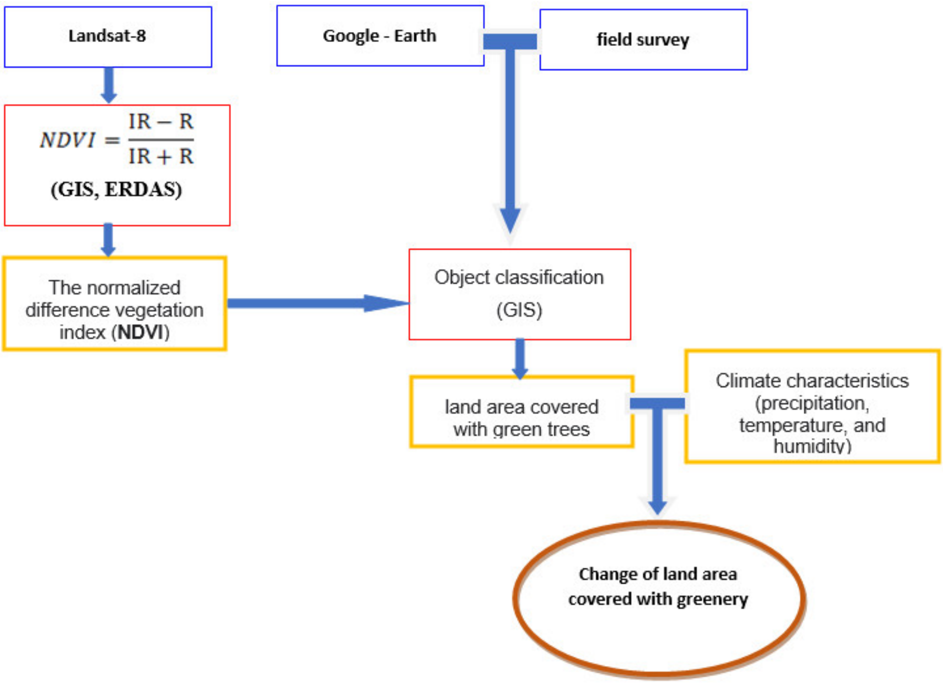

Figure 2. Overview diagram describing the steps taken.

3. Results and disscusion

The NDVI method is used to evaluate the plant index from satellite imagery. Initial results from satellite images show that NDVI in the inner of Ha Noi ranged from 0 to 0.48 (Figure 3).

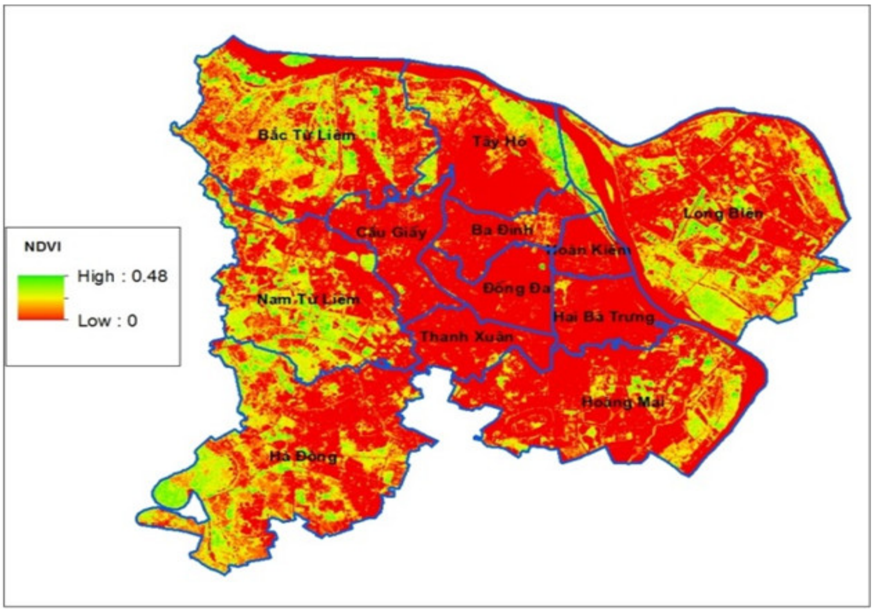

Figure 3. NDVI for the inner city on Octorber 7, 2016.

In order to eliminate non–vegetative sites, the initial NDVI results did not evaluate, 30 survey sites with 16 sites of the vegetation class, 5 points of the water surface, 2 points traffic class and 7 points in residential, commercial areas that has been used to accurate vegetation classification. Figure 4 shows the results of vegetation classification of some survey sites. The results of the calibration show that areas with a NDVI value of ≥ 0.18 are vegetation cover, whereas areas with a NDVI value < 0.18 are non–plants: traffic; water surface; residential areas; commercial center. The NDVI in this area is set to 0.

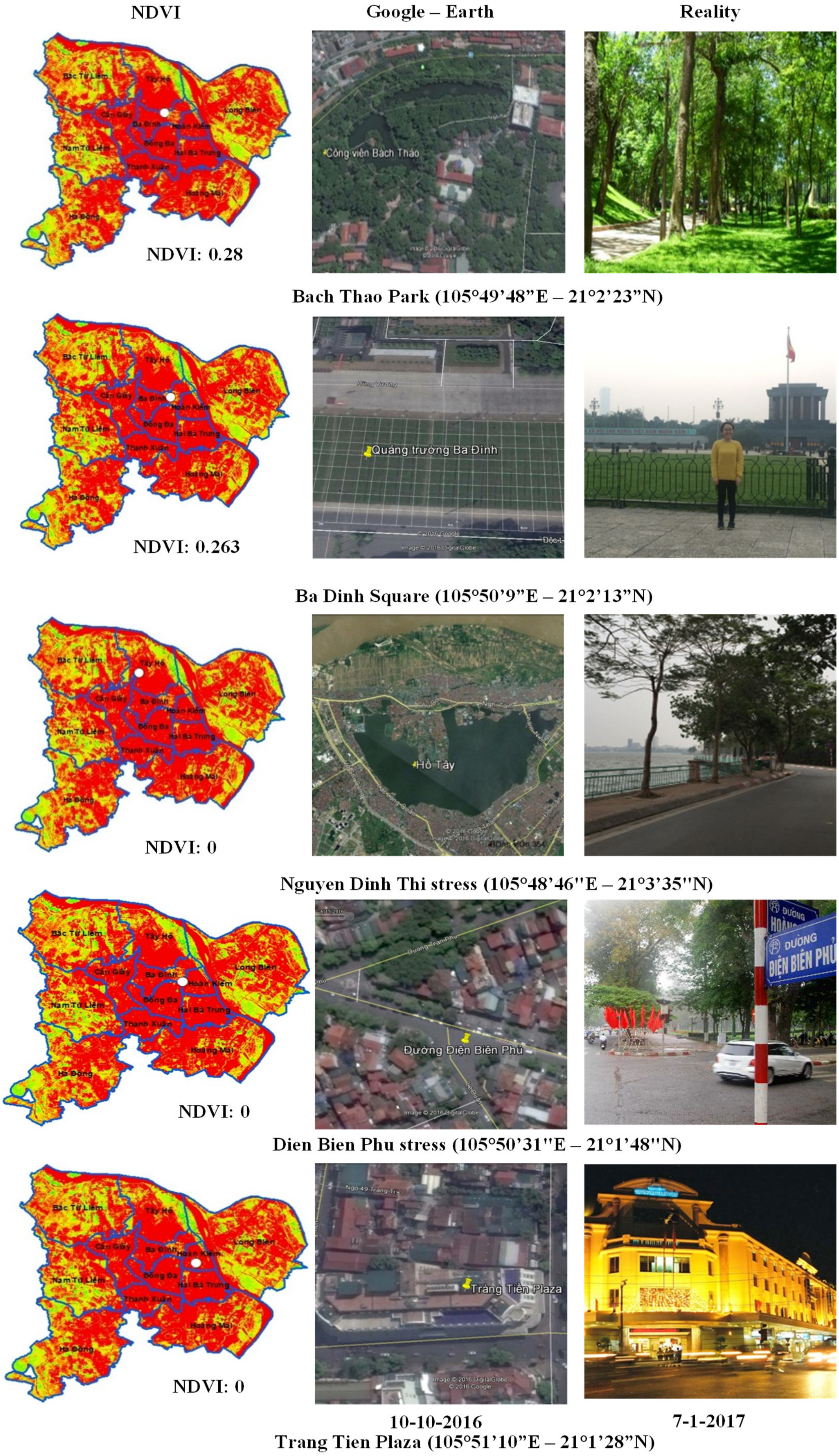

Figure 4. Results of vegetation classification at some survey sites.

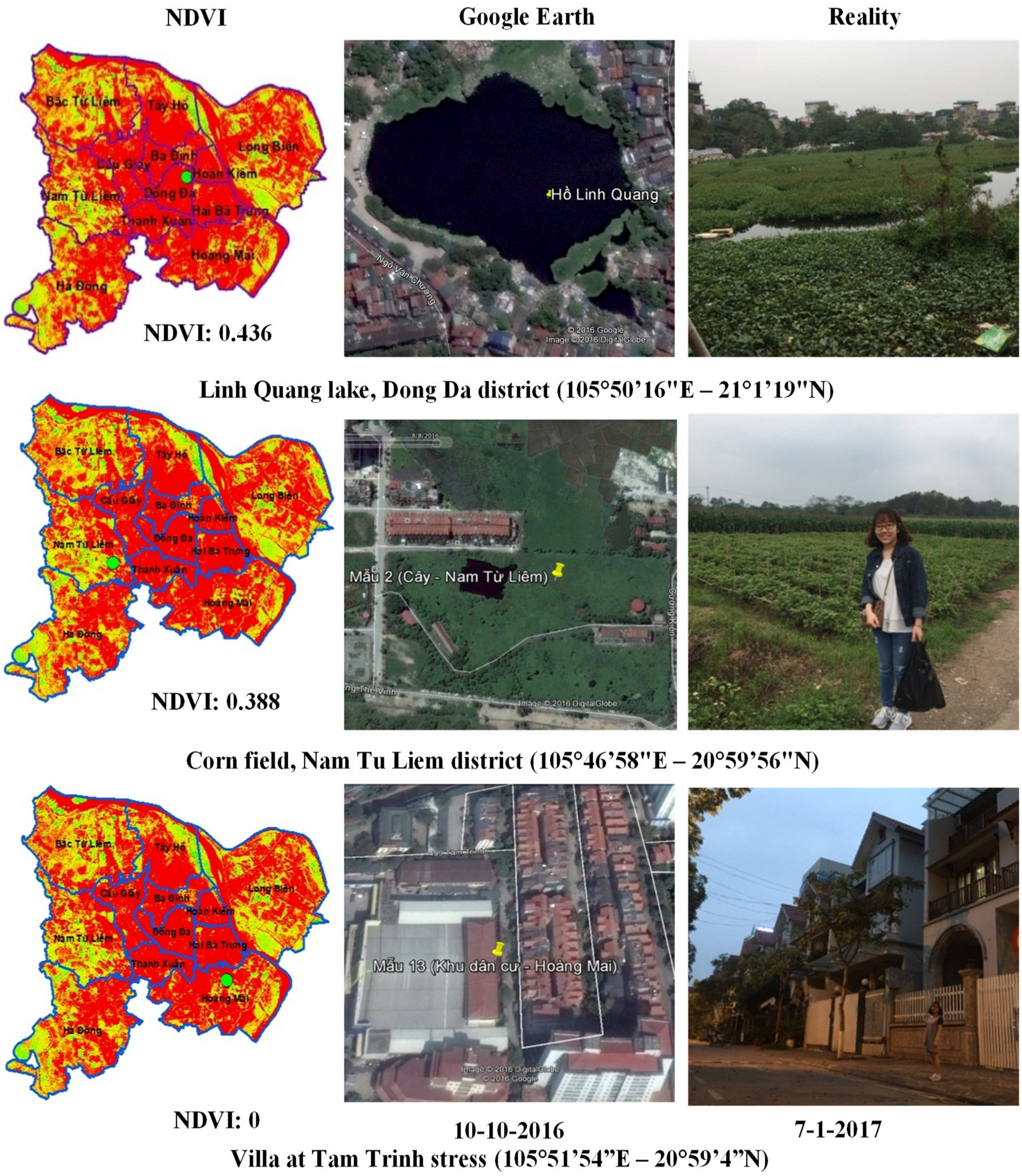

Figure 5. Results of vegetation classification at some survey sites.

To exmamine the accuracy of vegetation classification, 15 independent survey sites were used to re–define the NDVI index including 8 sites vegetation class, 1 sites water, 4 sites traffic and 2 sites in the residential areas. The results shown that NDVI values at all sites are highly reliable. Especially, at Linh Quang Lake (Dong Da District), the NDVI was approximately 0.44 although under the plan, this is the water surface. In fact, the surface of Linh Quang Lake has been covered by duckweed and thick moss so the vegetation index calculated from high index satellite images is reasonable (Figure 5).

The calibrated and validated NDVI indexes are used to establish the vegetation distribution map in the inner city of Ha Noi from 12 satellite images for 12 different periods from 2013 to 2016. The results show that the green trees’ areas in the inner of Ha Noi ranges from 148.8 to 160.7 km^2. On December 2013, there is the lowest green areas, on June 2016, there is the largest green area (**Error! Not a valid bookmark self-reference.**). High green areas are concentrated in the summer months, from May to September, while the green areas are lower in the winter months (from October to January).

Table 2. Green trees area (km^2) in the inner city according to satellite image interpretation.

Satellite images	Time											
	June 2013	Dec 2013	Jan 2014	Jan 2015	May 2015	July 2015	Aug 2015	May 2016	June 2016	Sep 2016	Oct 2016	Dec 2016
Green plant area (km^2)	151.8	148.8	149.4	152.2	157.3	155.1	156	160.7	160.3	157	156.2	151.3

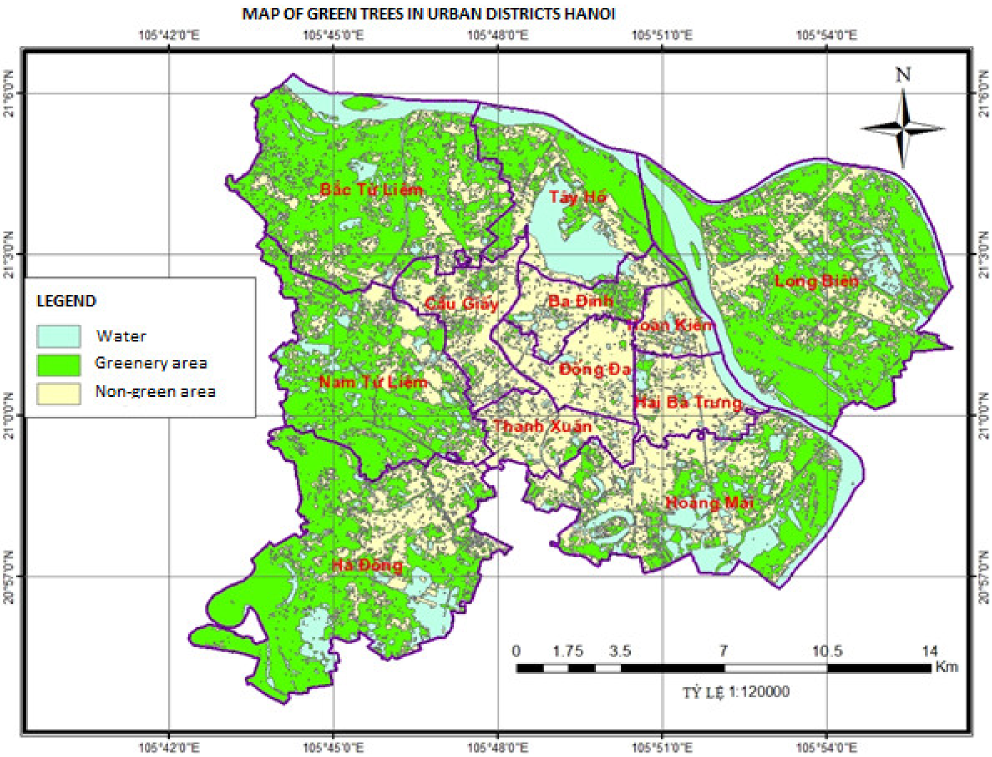

Figure 6. Vegetation distribution map in the inner of Ha Noi, on December 2016.

Because of the small number of satellite images, it does not reflect the changes of trees in time in Ha Noi. In order to restore the green area of the missing months, the multiple correlation function was constructed based on green plants area data that interpreted from satellite images and climatic factors such as monthly average temperature, average monthly humidity, total rainfall of studied area (Ha Dong station) at corresponding times (Table 3).

Table 3. Data were used to construct the linear regression equation for the correlation between green building area and climatic factors.

Time	**Green plant area interpreted from satellite imagaes**	**Monthly average temperature (^oC)**	**Average monthly humidity (%)**	**Total rainfall (mm)**
6/2013	151.8	29.4	78	237
12/2013	148.8	15.5	75	28
1/2014	149.4	17.0	77	3
1/2015	152.2	17.7	81	30
5/2015	157.3	30.0	80	95
7/2015	155.1	29.7	77	132
8/2015	156.0	29.5	81	287
5/2016	160.7	28.4	80	412
6/2016	160.3	30.9	75	74

Time	Green plant area interpreted from satellite imagaes	Monthly average temperature (°C)	Average monthly humidity (%)	Total rainfall (mm)
9/2016	157.0	28.7	79	119
10/2016	156.2	27.5	74	40
12/2016	151.3	20.8	72	7

The multiple correlation represents the relationship between the area of green tree and the average monthly rainfall, monthly humidity and total monthly rainfall in Ha Noi:

$$GA = 135.09 + 0.5T + 0.085H + 0.002R \quad (3)$$

3.1. Restoration green tree area in the inner of Ha Noi

Using multiple correlation, the total area of green trees in the inner city from 2013 to 2016 has been restored. Research results show that green areas increase in rainy months and decrease in autumn and winter months. In addition, green areas in the inner city from 2013 to 2016 are quite stable and tend to increase slightly from 153.90 to 155.15 (Table 4, Figure 7).

Table 4. Green tree area in the inner of Ha Noi by the time.

Time	2013	2014	2015	2016
Tree area (km^2)	153.9	154.39	154.61	155.15

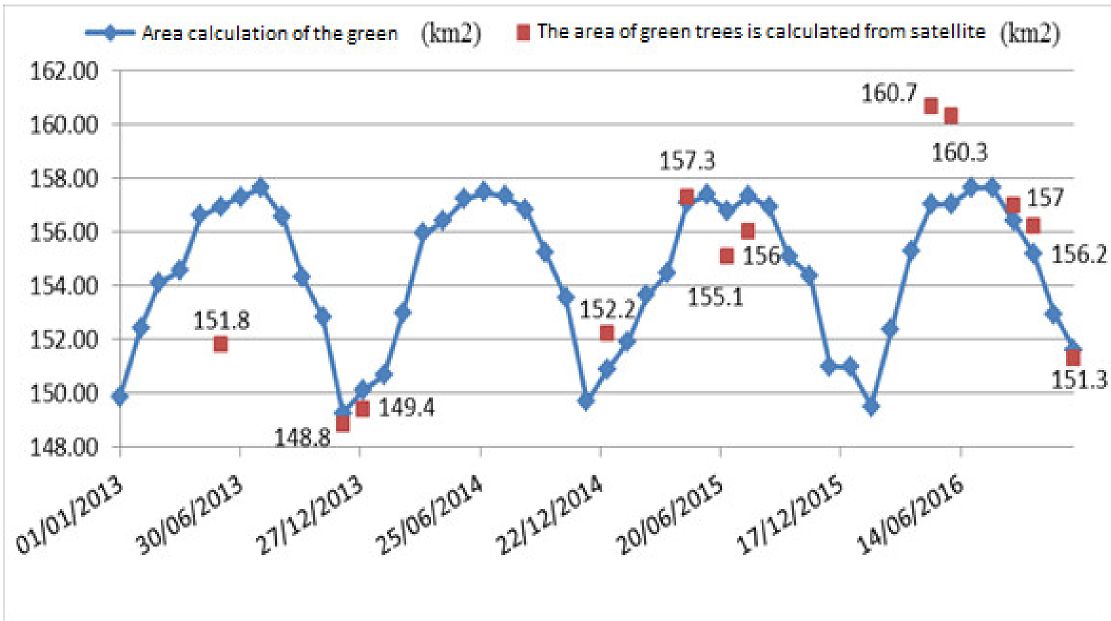

Figure 7. Green trees area in the inner city of Ha Noi in the period between 2013 and 2016.

Use the population data from the general statistics office to estimate the annual average of green trees in the inner city according to TCVN 9257: 2012. The results show that the inner city has a high density of trees per capita though it tends to decrease from 2013 to 2016 but compared with TCVN 9257: 2012 still exceeds 3 times. Although the green trees area in this period tends to increase slightly, however, given the urban population of Ha Noi increases rapidly (5.5% from 2013 to 2016), the density of trees per capita tends to decrease (Table 5).

Table 5. The green trees dessity in the inner of Ha Noi.

Time	Green tree area (km^2)	Population (million people)	The density of trees (m^2/person)	TCVN 9257:2012
2013	153.90	3089.20	49.80	12–15

Time	Green tree area (km^2)	Population (million people)	The density of trees (m^2/person)	TCVN 9257:2012 (m^2/person)
2014	154.39	3156.00	48.90	
2015	154.61	3241.50	47.70	
2016	155.15	3259.90	47.60	

3.2. Restoration of green tree areas in the inner of Ha Noi

Restoration of green tree areas in each district is carried out similarly to the inner city. Table 6 shows the reliability of the relationships between green plant areas each district and climatic factors.

Table 6. Evaluation the correlation between variables.

District	The correlation coefficient (R)	Evalution
Hoang Mai	0.81	Close correlation
Tay Ho	0.79	
Hoan Kiem	0.77	
Hai Ba Trung	0.74	
Dong Da	0.72	
Ba Dinh	0,71	
Thanh Xuan	0.68	Quite close correlation
Cau Giay	0.67	
Nam Tu Liem	0.65	
Bac Tu Liem	0.55	
Long Bien	0.31	Avarage correlation
Ha Dong	0.30	

The linear regression equation was divided 12 districts in Ha Noi based on the correlation coefficient: the close correlation, the quite close correlation coefficient and the average correlation. Consequently, given the close correlation and quite close correlation, it is possible to use green tree area data in combination with interpreted area data to calculate the average green tree area in the period between 2013 and 2016. The pronvinces in the average correlation will use the green tree area interpreted from Landsat 8 to calculate the average green tree area in the period from 2013 to 2016.

Table 7. Green tree area in each district over the years.

Time / District	Green tree area (km^2)				
	2013	2014	2015	2016	2013 – 2016
Hoang Mai	16.97	16.87	16.9	16.96	16.93
Tay Ho	9.17	9.16	9.35	9.5	9.29
Hoan Kiem	0.83	0.79	0.83	0.94	0.85
Hai Ba Trung	0.97	0.95	0.92	1.18	1.00
Dong Da	0.94	0.88	0.9	1.02	0.94
Ba Dinh	2.5	2.49	2.58	2.66	2.56
Thanh Xuan	1.56	1.48	1.47	1.42	1.48
Cau Giay	2.6	2.54	2.65	2.58	2.59
Nam Tu Liem	22.62	22.8	22.75	21.89	22.52
Bac Tu Liem	29.73	29.74	29.69	29.67	29.71
Long Bien	33	34.58	33.65	36.28	34.38

Ha Dong	30.6	31.3	32.43	31.54	31.46

3.3. Assessment of green tree density according to TCVN 9257:2012

The article assesses the green trees destiny in the inner city in 2016 based on the general statistics in 2016.

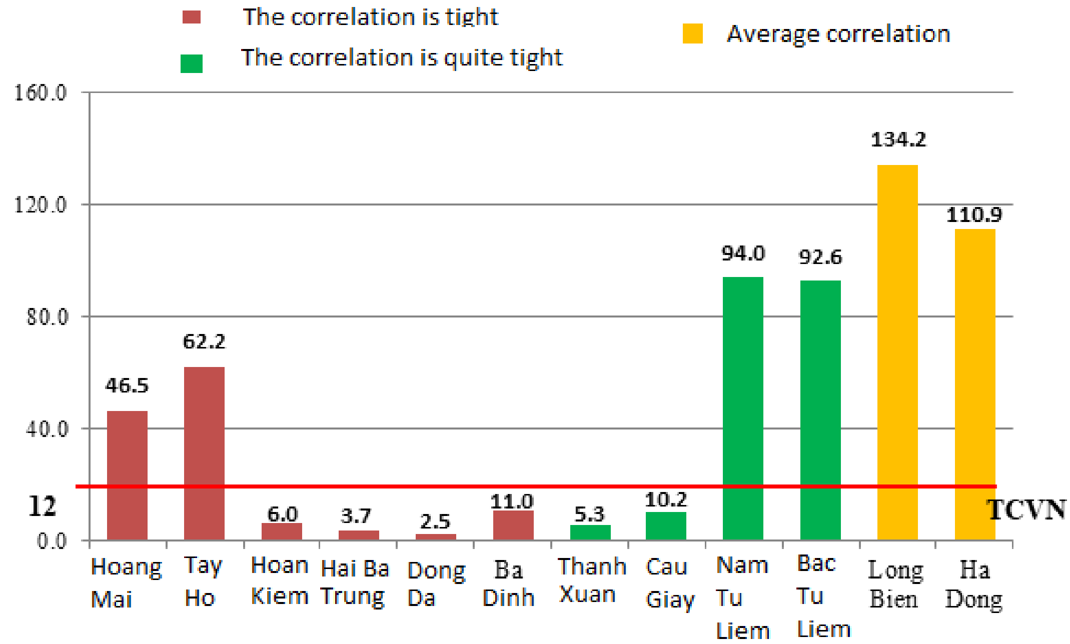

Figure 8. The green tree density in the inner of Ha Noi.

According to Table 7, the green tree density in the inner city are quite different between the central districts and suburbs. In the suburb such as Long Bien, Ha Dong, Nam Tu Liem, North Tu Liem, Tay Ho, Hoang Mai the green tree density in the people is quite high, exceeding TCVN 9257:2012. To be specific, Long Bien district has the highest the green tree density, with 134.2 m^2/person up to 11 times, followed by Ha Dong (110.9 m2/person), Nam Tu Liem (94 m^2/person), Bac Tu Liem (92.6 m^2/person), Tay Ho (62.2 m^2/person) and Hoang Mai (46.5 m^2/person).

Meanwhile, central districts such as Dong Da, Hai Ba Trung, Ba Dinh, Hoan Kiem, Thanh Xuan have very low the green tree density, lower than the minimum standard of TCVN 9257: 2012. To be specific, Dong Da is the lowest green tree density with 2.5 m^2/person, lower than the TCVN 9257:2012 (> 12 m^2/person) to 4.8 times. Followed by Hai Ba Trung district, the green tree destiny is 3.7 m^2/person, lower than the standard allowed more than 3 times. Hoan Kiem and Thanh Xuan have the green tree density at 5.3–6 m^2/person, lower than the permitted standard 2 times. Cau Giay and Ba Dinh have a density of 10.2 m^2/person and 11 m^2/person, respectively, reaching the minimum level of TCVN 9257:2012.

The explanation for the high green tree density in the suburbs that the population is not as crowded as in the central districts, the vacant land area is relatively large. Morever, the stuburbs concentrate many parks and large gardens of the city. For instance, Yen So park (Hoang Mai) is the largest urban park in Viet Nam – the largest green park of Ha Noi with total area 323 ha There are several parks and flower gardens, such as Yen So Park (Hoang Mai District), Viet Nam's largest urban park, the largest green park in Ha Noi with a total area of 323 hectares. In which, the park and lake area is 280 ha. Hoa Binh Park (BacTu Liem district) is the most modern park in the capital with an area of 20 ha; Ho Tay Flower Valley (Tay Ho provice) has an area of about 7,000 m^2, and includes many different types of flowers; Nhat Tan flower garden, Hong river rocks (Tay Ho district), etc.

In the contract, the central districts where the population lives and are crowded. Especially, Dong Da district is the region with the largest population with 401,700 people (the population density of Dong Da is 40.331 person/km2). Notably in the central district, 100% of the total area in natural land is non–agricultural land. Moreover, these are place which develop rapidly of infrastructure, agencies, schools, hospitals, monuments, landscapes... so people tend to live these areas. The empty lands are converted used purpose, the house was cleared, the trees were cut to the "century" works: entertainment complex, commercial center, shopping, apartment ... Given the dizzying development of the apartment building is the rapidly shrinking of green tree area. These are the reasons for the green plant density in these districts which is much lower than TCVN 9257:2012.

4. Conclusions

Remote sensing and GIS combined with multivariate regression in the study of urban green tree changes in the inner of Ha Noi show advantages to traditional methods. The results show that the area of green trees in the inner of Ha Noi is quite stable and tends to increase slightly at 0.8% in the period from 2013 to 2016. The average greenback annual average from 2013 to 2016 is 50.8%. Plant density per capita has fallen from 49.8 m^2/person (2013) to 47.6 m^2/person (2016) compared with TCVN 9257:2012 still exceeds 3 times. The main cause of the decline is the urbanization of districts and the urban population of Ha Noi on the increase of about 5.5% from 2013 to 2016. The density of green tree per capita in the inner of Ha Noi is three times larger than Viet Nam standards.

The green tree destiny is clearly divided among urban and suburban districts such as Long Bien, Ha Dong, Nam Tu Liem, Bac Tu Liem, Tay Ho and Hoang Mai with quite high exceeding the national standard for planning public trees in urban areas many times. Particularly, Long Bien districts has the highest density of green trees in 12 districts up to 11 times, followed by Ha Dong (9 times), Nam Tu Liem (nearly 8 times), Bac Tu Liem over 7 times), Tay Ho (5 times) and Hoang Mai (nearly 4 times); meanwhile, urban centers such as Dong Da, Hai Ba Trung, Ba Dinh, Hoan Kiem and Thanh Xuan have low tree density, lower than standard. Specifically, Dong Da district has the lowest density of green trees in 12 urban districts about 4.8 times. Next to Hai Ba Trung districts more than 3 times. Hoan Kiem and Thanh Xuan are two times lower than the permitted standard. Cau Giay and Ba Dinh have the density of green trees approaching the standard level.

Acknowledgments: The authors would like to thank the People's Committee of Hanoi, Water Resources Institute for research funding and for providing key information for this study.

Author contributions: Constructing research ideas: H.K.V., T.T.H.; Select research method: H.K.V; Survey, sampling and analysis: Trang, T.H; Data processing: T.T.H; Writing–original draft preparation: H.K.V; Writing–review and editing: H.K.V.

Conflicts of Interest: The authors declare no conflict of interest.

References

1. Chang, Q.; Liu, X.W.; Wu J.S.; He, P. MSPA–based urban green infrastructure planning and management approach for urban sustainability: Case study of Longgang in China. *J. Urban Plan. Dev.* **2015**, 141, *3.*
2. Ossola, A.; Hopton, M.E. Measuring urban tree loss dynamics across residential landscapes. *Sci. Total Environ*. **2018**, *612*, 940–949, doi: 10.1016/j.scitotenv.2017.08.103.
3. Pu, R.L.; Landry, S. A Comparative analysis of high spatial resolution IKONOS and WorldView–2 imagery for mapping urban tree species. *Remote Sens. Environ*. **2012**, *124*, 516–533.
4. Parmehr, E.G.; Amati, M. Estimation of urban tree canopy cover using random point sampling and remote sensing methods. *Urban For. Urban Green*. **2016**, *20*, 160–171.
5. Shojanoori, R.; Ismail, M.H.; Mansor, S.; Shafri, H. Generic rule–sets for automated detection of urban tree species from very high–resolution satellite data. *Geocarto Int.* **2018**, *33*, 1–36.

6. Chance, C.M.; Coops, N.C.; Plowright, A.A.; Tooke, T.R.; Christen, A.; Aven, N. Invasive shrub mapping in an urban environment from hyperspectral and LiDAR–Derived attributes. *Front. Plant Sci*. **2016**, 1–19. https://doi.org/10.3389/fpls.2016.01528
7. Nasi, R.; Eija, H.; Minna, B.; Paivi, L.S. Remote sensing of bark beetle damage in urban forests at individual tree level using a novel hyperspectral camera from UAV and aircraft. *Urban For. Urban Green* **2018**, *30*, 72–83. https://doi.org/10.1016/j.ufug.2018.01.010.
8. Harris, R.; Baumann, I. Open data policies and satellite Earth observation. *Space Policy* **2015**, *32*, 44–53. https://doi.org/1010.1016/j.spacepol.2015.01.001.
9. Zhu, Z.; Michael, A.W.; David, P.R.; Curtis, E.W.; Matthew, C.H.; Volker, C.R.; Sean P.H.; Crystal, S.; Patrick, H.; Peter, S.; Jean–Francois, P.; Leo, L.; Nima, P.; Ted, A.S. Benefits of the free and open Landsat data policy. *Remote Sens. Environ.* **2019**, *224*, 382–385.
10. https://hanoi.gov.vn/home
11. http://www.tnmtnd.hanoi.gov.vn/
12. https://Landsat.usgs.gov/Landsat8.php
13. https://www.usgs.gov
14. http://vietgis.com.vn/
15. Chi, P.K. New satellite generation – LDCM or Landsat 8, GeoViet. 2013.
16. Esau, I.; Miles, V.V.; Davy, R.; Miles, M.W.; Kurchatova, A. Victoria, V.M. Trends in normalize difference vegetation index (NDVI) associated with urban development in northern West Siberia. *Atmos. Chem. Phys*. **2016**, *16*, 9563–9577. https://doi.org/10.5194/acp–16–9563–2016.
17. Rumiana, V.; Monika, K. Mapping urban green spaces based on remote sensing data: Case studies in Bulgaria and Slovakia. Proceeding of the 6th International Conference on Cartography and GIS. 2015.
18. Hanoi People's Committee. Land use planning up to 2020 and 5–year land use plan (2011–2015) for Hanoi districts.
19. Kham, D.V. et al. Building a model for forecasting rice yield and yield in the Red River Delta using Modis image data. 2011.
20. http://climatechangegis.blogspot.com/2012/03/cac–chi–so–thuc–vat–trong–vien–tham_4603.html
21. Hung, T.H.; Chi, P.K. Pilot study on application of remote sensing and GIS to manage urban green spaces and trees in Ha Tinh and Tra Vinh cities, 2011.

VIETNAM JOURNAL OF HYDROMETEOROLOGY

Study on assessing the impact of climate change (temperature and rainfall) on rice yield in the Long Xuyen Quadrangle region (LXQR) – Vietnam

Can Thu Van[1*], Phan Thi Thuy Duong[1], Dinh Thi Nga[1], Luu Van Ninh[2]

[1] Ho Chi Minh City University of Natural Resources and Environment, 236B Le Van Sy, ward 1, Ta Binh, Ho Chi Minh City; ctvan@hcmunre.edu.vn; pttduong@hcmunre.edu.vn; dtnga@hcmunre.edu.vn;
[2] Hydro–Meteorology Center of An Giang Province, 64 Ton Duc Thang, My Binh ward, Long Xuyen City, An Giang; luuninhtv@gmail.com;
*Correspondence: ctvan@hcmunre.edu.vn; Tel.: +84–983738347
Received: 25 December 2020; Accepted: 16 April 2021; Published: 25 April 2021

Abstract: The impacts of climate change such as sea level rise, floods, droughts, saltwater intrusion, extreme weather ... are more and more evident. It causes significant damage to the socio–economy of Vietnam, especially the rice farming industry. In Vietnam, over the past 50 years, the average temperature has risen by about 2–3 degrees Celsius and the sea level has risen by about 20 cm. According to the simulation scenarios, it is estimated that by the end of the twenty–first century, compared to the average in the period 1980–2005, the average temperature in Vietnam could increase by 2.3 degrees Celsius, the annual rainfall would increase by about 5%. and the sea level could rise by 75 cm. There are many influencing factors affecting rice yield such as: meteorological factors, hydrology, saline intrusion, farming, pests,... This study, only the change in yield is assessed rice due to the impact of changes in temperature and precipitation in the context of climate change in the LXQR). By using the CROPWAT model to calculate rice yields with temperature changes and rainfall over periods according to climate change scenarios, the results show that under the RCP4.5 scenario when heat If the degree and rainfall increase, the rice yield decreases by 25.4% on average; RCP8.5 rice yield decreased by 25.3% on average.

Keywords: LXQR; Climate change; Cropwat; Rice yield; Assessment of the damage.

1. Introduction

Climate change has been one of the biggest challenges facing people, the negative impacts of climate change on human life are becoming more and more obvious [1–2]. The direct effects of climate change on water resources are abnormal rainfall changes, rising temperatures and extreme weather events such as long–term droughts and mid–to–saturated floods. Climate change will affect water resources and reduce water resources in many places, leading to water scarcity [3]. Water scarcity is a major problem for many developing countries, including Vietnam, especially in relation to agricultural irrigation in the Mekong River Delta (MRD) and the LXQR. where there is a serious shortage of fresh water in the dry season for many different reasons. For rice, the variation of yield and yield has a great participation of hydro–meteorological factors [4]. To estimate and evaluate the impact of hydro–meteorological factors on crop yields in general and rice in particular, the Food and Agriculture Organization (FAO) developed a CropWat model in 1990, based on temperature conditions, precipitation, sunny hours, humidity, wind speed [5–6].

LXQR is a quadrilateral–shaped land in the MRD, located in three provinces of Kien Giang, An Giang and Can Tho. The four sides of the LXQR are the Vietnam–Cambodia border, the Gulf of Thailand, the Cai San canal and the Bassac River (Hau River). The four corner vertices of this quadrilateral correspond to four cities: Chau Doc, Long Xuyen, Rach Gia and Ha Tien (Figure 1). The LXQR is one of the major food production and processing centers in the MRD. Formerly An Giang, and now Kien Giang is the locality with the largest rice production in the region. This is the area that has positively contributed to the overall achievement of the MRD region.

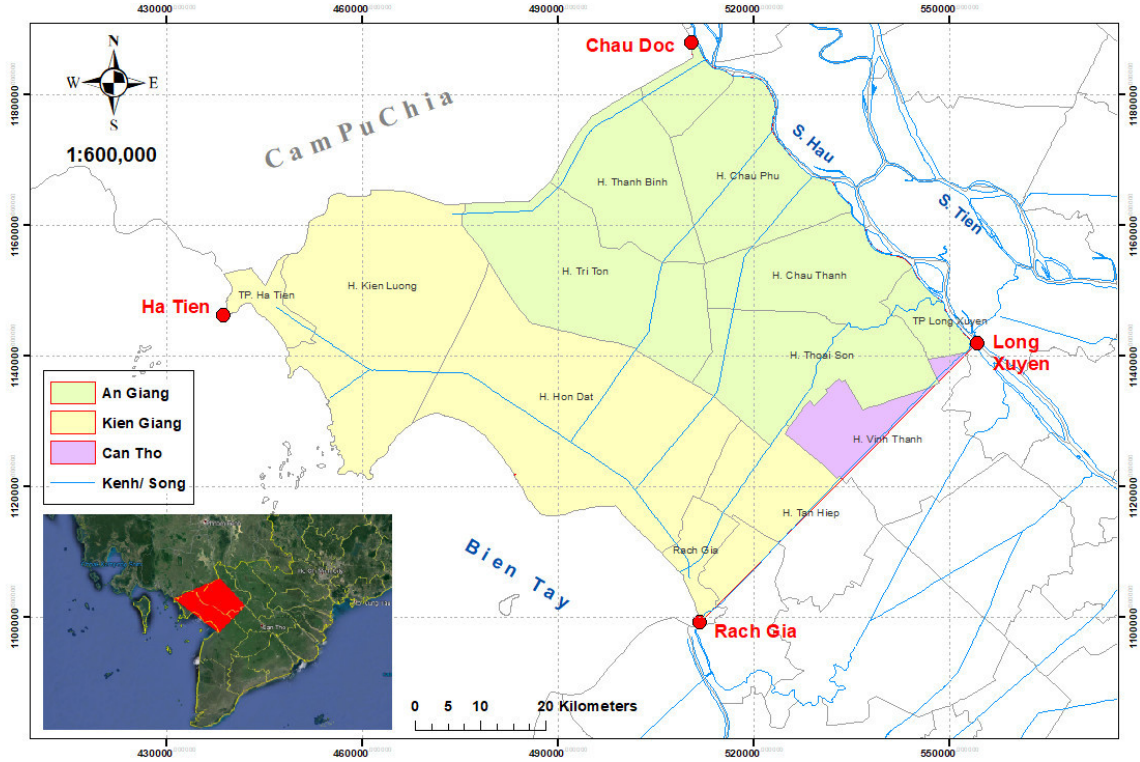

Figure 1. Study area of LXQR.

In the next period, it is forecasted that the LXQR region will face many challenges, in which the issue of climate change and the possibility of droughts, increased saltwater intrusion due to sea level rise. Rice is playing a very important role in the agricultural sector. industry of the region. In Vietnam, over the past 50 years, the average temperature has risen by about 2–3 degrees Celsius and the sea level has risen by about 20 cm [7]. According to the simulation scenarios, it is estimated that by the end of the twenty–first century, compared to the average in the period 1980–2005, the average temperature in Vietnam could increase by 2.3 degrees Celsius, the annual rainfall would increase by about 5%. and the sea level could rise by 75 cm. The change of hydro–meteorological factors in the region can affect crop yield in general and rice yield in particular [8]. The study is conducted to evaluate the impact of hydro–meteorological factors on rice productivity in the study area through future climate change scenarios and thereby calculate the amount of damage caused by the impacts of Climate change through temperature and precipitation factors. The results of this study help to provide useful information for managers in making policies and strategies for the development of agricultural production in the future in the context of global climate change.

2. Materials and Methods

2.1. Methodology

This paper uses CROPWAT 8.0 software, which is the most advanced irrigation regimen software released in 1992, developed and recommended by the FAO for worldwide use. Plant water requirements and irrigation planning based on the data provided by the user [9] (Figure 2).

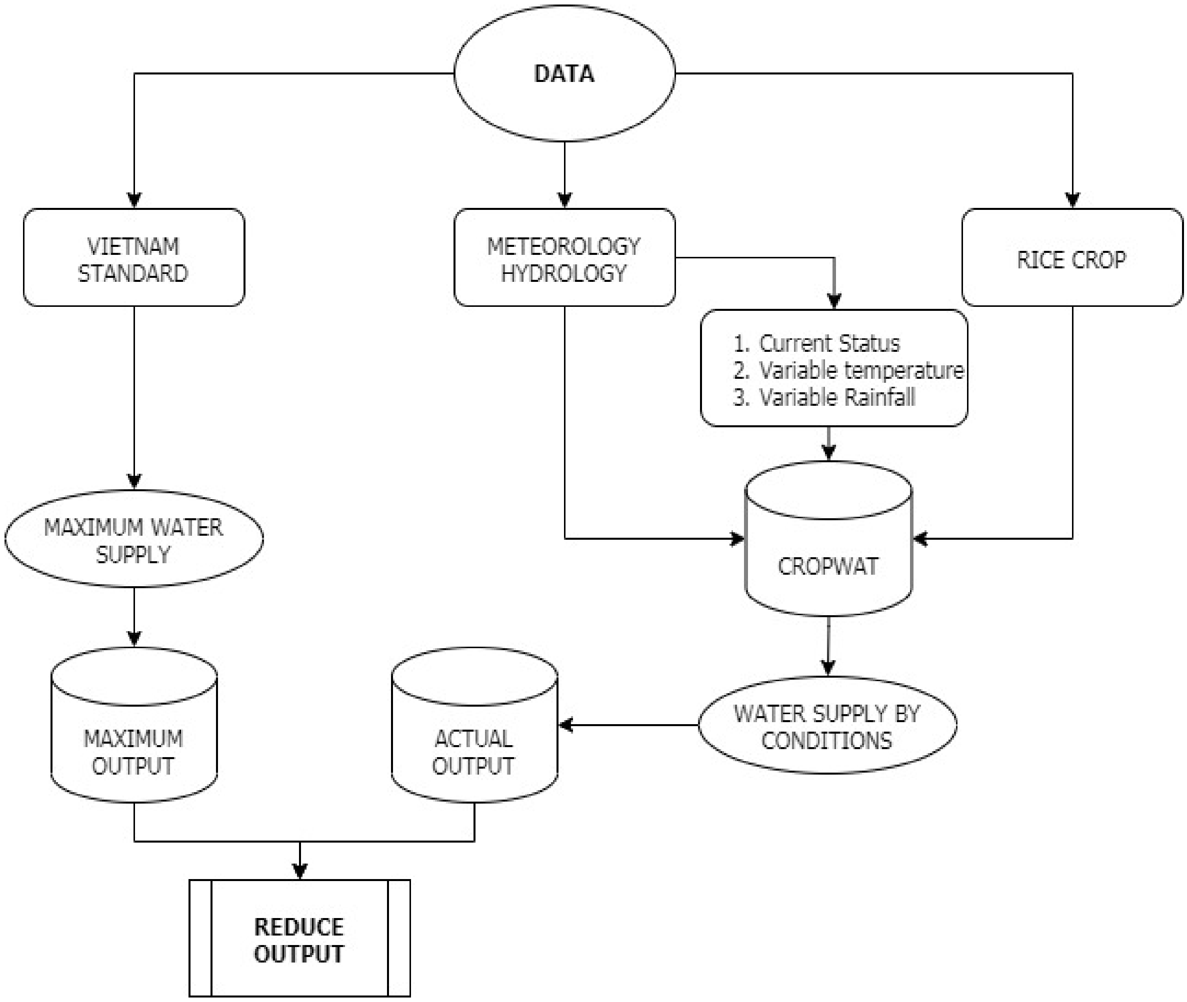

Figure 2. Diagram of implementation steps.

According to [9], the response of crop yield to irrigation water was quantified by a crop yield reduction factor (KY), related to a relative yield decrease (1–Ya/Ym) for a Relative water demand deficit (1–ETa/ETc). Therefore, the Ky values for most crops are based on the assumption that the relationship between relative yield (Ya/Ym) and relative water demand (ETa/ETc) is linear and has a value for water deficit amounts to about 50% or 1–ETa/ETc = 0.5.

According to [3], the yield reduction coefficient is of experimental origin (K_y) for the individual growth stages (i.e., establishment, vegetation, flowering, yield formation, or period). segment nine) as well as during total growth.

$$\left(1-\frac{Y_a}{Y_m}\right) = K_y\left(1-\frac{ET_a}{ET_c}\right) \quad (1)$$

where Ya is the real yield (corresponding to ETa) (kg/ha); Ym is the maximum theoretical yield (corresponding to ETc) (kg/ha); Eta is the actual water demand (mm/day) for each crop; Etc–potential water demand for each crop; K_Y is the yield response coefficient to water stress.

To get the actual yield, multiply the relative seasonal yield by the maximum theoretical yield:

$$Y_a = Y_m\left(1- K_y\left(1-\frac{ET_a}{ET_c}\right)\right) \quad (2)$$

Then, the yield price of crops and fisheries is calculated by the formula [9]:

$$\text{Market Value} = \text{Ya} * \text{Area} * \text{Price} \quad (3)$$

where Market Value is the quantity of output of crops/aquatic products ($); Ya is an actual yield (kg/ha); Area is the cultivated area (ha); Price is the market price of crop/seafood per unit area ($/kg) [10–12].

2.2. Data collection

2.2.1. Hydro–Meteorology Data

Meteorological and hydrological data collected up to 2018 provided by the Hydrometeorology Center of An Giang province (Chau Doc station) and the hydrometeorological center of Kien Giang province (Rach Gia station) have been revised, reliable enough, is the basis in calculating the price of agricultural productivity and climate change scenarios in terms of rainfall, temperature, average number of hours of sunshine, humidity, wind speed and other characteristics for this study [13–16].

2.2.2. Socio–economic data

Data on natural conditions, socioeconomic, and agricultural production in the MRD in 2018 are released by the General Statistics Office, the Ministry of Planning and Investment [17–19].

2.2.3. Documents related to rice plants

Rice seasons in the region according to the development stages and Kc coefficients of each growing period of rice are shown in Table 1 and Table 2 below.

Table 1. Rice seasons in the study area [10].

No.	**Rice crops**	**Prepare the land (I)**	**Initial stage (II)**	**Development stage (III)**	**Harvesting stage (IV)**	**Planting time**	**Harvest time**	**Number of days**
1	Winter spring Crop	10	10	60	25	15/12	30/3	105
2	Summer–autumn Crop	10	10	65	31	15/4	06/8	111
3	October Crop	10	10	60	20	20/8	30/11	100

Table 2. Kc coefficients of rice plants in the study area [11–12].

Rice crops	**Prepare the land (I)**	**Initial stage (II)**	**Development stage (III)**	**Harvesting stage (IV)**
Winter spring Crop	0,30	0,54	1,05	0,81
Summer–autumn Crop	1,03	1,19	1,74	1,12
October Crop	1,04	1,17	1,68	1,14

2.2.4. Climate change scenarios

According to the climate change scenarios of the Ministry of Natural Resources and Environment [5], the beginning of the century (2016–2035) between the century (2045–2065) and the end of the century (2080–2099) with 2 scenarios of the emission concentration medium low (RCP4.5) and high (RCP8.5) [20–21].

This study is limited to the study period from the beginning of 2016–2035 and according to that result, the temperature of the period is expected to change (increase) compared to the standard period (1992–2018) at the An Giang meteorological station. And Kien Giang in two scenarios as shown in Table 3 below.

Table 3. Scenario of change in temperature and average rainfall in the period 2016–2035 [6].

	RCP4.5		RCP8.5	
	An Giang	**Kien Giang**	**An Giang**	**Kien Giang**
Temperature (°C)	+0.7	+0.7	+0.9	+0.8
Amount of rain (%)	+4.7	+4.9	+8.2	+6.5

3. Results and discusion

3.1. Effect of temperature on rice yield

The average temperature increase under the RCP 4.5 and RCP 8.5 scenarios is 0.7°C and 0.9°C respectively, generally making the rice yields of the rice growing districts in the LXQR decrease.

Specifically:

In winter–spring crop (WSC), ETc evaporation according to RCP 4.5 scenario is 689.8 mm/day and according to RCP 8.5 is 693.7 mm/day (data extracted from the results simulating the Cropwat model), while the actual water demand is 770 mm/day (TCVN), the water demand is not enough according to reality, thus reducing rice yield. Compared to the maximum yield of the WSC crop (8.00 tons/ha), when the temperature increases by 0.7°C under the RCP 4.5 scenario, the productivity of the WSC 4.5 crop decreases by 10.5% (equivalent to 0.84 tons/ha). When the temperature increased by 0.9°C under the RCP 8.5 scenario, the rice yield decreased 10.0% (equivalent to 0.80 tons/ha. In addition, the WSC coincides with the dry season, the evaporation of water evaporation increases, the water demand for plants is less, rainfall and other factors do not change, so rice yield decreases (Figure 3).

In the summer–autumn crop (SAC), rice yields decreased by 43.3% (equivalent to 2.59 tons/ha) and 43.7% (equivalent to 2.62 tons/ha), respectively. The evaporation of ETc of SAC crop under RCP 4.5 scenario is 956.7 mm/day and under RCP 8.5 scenario is 962.3 mm/day (data extracted from the modeling results of Cropwat), meanwhile Actual water demand is 580 mm/day (TCVN).

In the October crop (OC), rice yield decreased by 24.5% and 25.1%, respectively (decreasing by 1.71 tons/ha and 1.76 tons/ha). The evaporation of ETc of the OC under the RCP 4.5 scenario is 652 mm/day and under the RCP 8.5 scenario is 657 mm/day (data extracted from the modeling results of the Cropwat model), the actual water demand is 500. mm/day (TCVN). The OC also coincides with the rainy season, with a lot of rainfall, the amount of water needed for plants is greater than the actual demand, thus affecting yield. (Figure 3).

In general, when temperature increases, rainfall, humidity, sunny hours, and wind speed do not change, the amount of water evaporation increases, but the amount of water needed for plants is limited, affecting yield rice in crops.

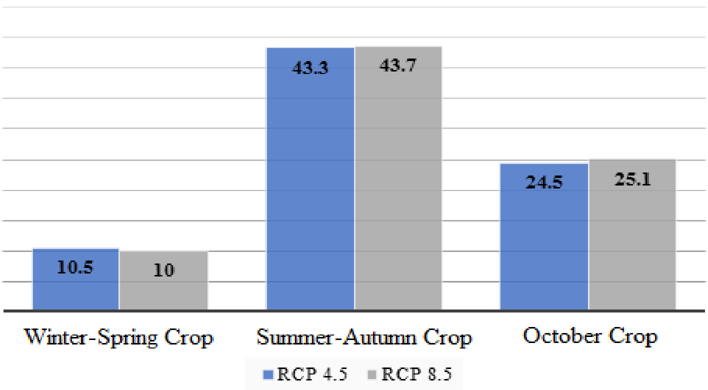

Figure 3. Rate of decrease in rice yield due to the effect of temperature under climate change scenarios (%).

3.2. Effects of changes in rainfall caused by climate change on rice yield

The average rainfall under the RCP 4.5 scenario increased by 4.7% and the RCP 8.5 by 8.2%, in general, both resulted in a decrease in rice yields of the crops.

Specifically:

In Winter–Spring crop, rice yield decreased by 12.2% and 12.5%, respectively (down 0.98 tons/ha and 1.00 tons/ha) compared to the maximum yield of the crop when it rains. increased by 4.7% and 8.2%, respectively. According to simulation results from CROPWAT model, the evaporation of ETc in the DXP 4.5 scenario is 676.9 mm/day and according to the RCP 8.5 scenario is 674.8 mm/day. The time of the winter season coincides with the dry season, temperature and other meteorological factors do not change, but the future rainfall will increase to exceed the potential water demand of the rice crop, thus affecting the rice yield but not much (Figure 4).

The productivity of Summer–Autumn rice crop also decreased, according to simulation results from CROPWAT model, ETc evaporation of HT crop under RCP 4.5 scenario was 923.8 mm/day and under RCP 8.5 scenario 915.0 mm/day, while the actual water demand is only 580 mm/day (TCVN). According to the scenarios with increased rainfall, the yield of HT crop rice decreases sharply. Rice yield decreased by 40.9% and 40.3%, respectively (decreasing equivalent to 2.46 tons/ha and 2.42 tons/ha). In general, when temperature and other factors do not change, rainfall greatly affects the yield of SAC (Figure 4).

In the October crop, rice yield decreased by 20.7% and 19.9% respectively (decreasing equivalent to 1.45 tons/ha and 1.39 tons/ha). According to simulation results from CROPWAT model, the evaporation of ETc of Seasonal crop under RCP 4.5 scenario is 622.8 mm/day and under RCP 8.5 scenario is 616.8 mm/day, meanwhile Actual water demand is 500 mm/day (TCVN) so rice yield is affected (Figure 4).

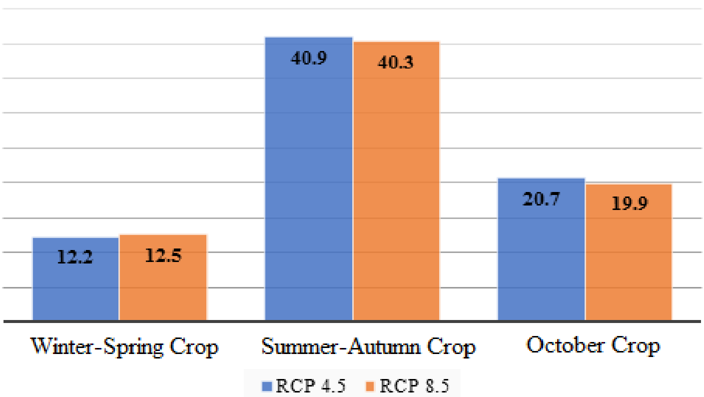

Figure 4. Rate of decrease in rice yield due to the effect of rainfall under climate change scenarios (%).

In summary, when the rainfall increases, the factors of temperature, humidity, sunshine hours, and wind speed do not change, the amount of evaporation will decrease compared to the baseline period, the water demand needed for plants is met. Excess compared to the potential water demand, thus affecting the rice yield in the crops.

4. Conclusions

When the temperature increases, the rainfall, humidity, sunny hours, and wind speed do not change, the amount of water evaporation increases, but the amount of water needed for plants is limited, thus reducing the rice yield. in cases.

When the rainfall increases, the factors of temperature, humidity, number of hours of sunshine, and wind speed do not change, the amount of evaporation will decrease compared to the baseline period, the water demand needed for tall trees is met. With the potential water demand, the rice yield in the crops is also reduced.

In addition to temperature and precipitation, other meteorological factors such as wind, humidity, hours of sunshine,... also affect rice yield and will be considered in later studies. In fact, climatic factors have a mutual relationship: the change of one factor leads to the change of another factor. Therefore, there should be more in–depth studies on the effects of these factors on rice yields in particular and crops in general.

Calculation results in the study have shown the impact of climate change, namely the increase in temperature and rainfall in the Mekong Delta on the rice yield here.

As mentioned from the beginning, the study just stopped at assessing the impact of two independent factors, temperature and precipitation, so the results have not been fully and accurately reflected. These factors will be calculated and included in the evaluation in the next studies.

Author contribution statement: Research ideas, build scientific bases and methods to calculate yield losses of rice crops due to changes in temperature and rainfall due to climate change: C.T.V.; Orientation for data collection and use to calculate water demand for rice plants; Write the manuscript and correct the article; Applying SWAT model to calculate water demand for rice and calculate rice yield according to scenarios: P.T.T.D.; Build a scientific basis to determine the maximum yield of rice and Analyze the calculation results: D.T.N.; Collect, edit, process survey data, survey on the hydro–meteorological situation, economy, society and rice in the TGDXX: L.V.N.; Analysis of local climate change conditions as an input to the calculation model: C.T.V.

Acknowledgments: The article is made and completed on the database from products under the subject of the Ministry of Natural Resources and Environment, "Establishing the scientific basis of economic evaluation of water resources vulnerability under the impact of climate change; trials for rice, seafood and fruit trees in LXQR" MS: TNMT.2018.02.12. The authors sincerely thank you.

Competing interest statement: The authors declare no conflict of interest.

References

1. Duong, V.N.; Thai, M.T.; Do, H.T. Assessment of water resource demand and reserves for agricultural production in LXQR, Kien Giang province, 2015–2016. *J. Agric. Rural Dev.* **2019**, *1*, 70–79.
2. McGuire, S. FAO, IFAD, and WFP. The state of food insecurity in the world 2015: meeting the 2015 international hunger targets: taking stock of uneven progress. Rome: FAO, ed: Oxford University Press, 2015.
3. McGuire, S. WHO, World Food Programme, and International Fund for Agricultural Development. The State of Food Insecurity in the World 2012. Economic growth is

necessary but not sufficient to accelerate reduction of hunger and malnutrition. Rome, FAO. (Eds). Oxford University Press. 2013.

4. Nguyen, V.V.; Nguyen, V.L.; Ngo, T.G.; Nguyen, H.S. Impacts of climate changes on yield of Dong Xuan rice in Son La province and coping measures. *Sci. Tech. Hydrometeorol. J.* **2002**, *504*, 1–9.
5. Lee, S.K.; Dang, T.A. Predicting the water use–demand as a climate change adaptation strategy for rice planting crops in the Long Xuyen Quadrangle Delta. *Paddy Water Environ.* **2019**, *17*, 561–570.
6. Nguyen, T.T.; Van, P.D.T.; Nguyen, H.T. Flow dynamics in the Tu Giac Long Xuyen area under the impact of a dyke to prevent floods. *J. Sci. Can Tho University* **2013**, *25A*, 85–93.
7. Nguyen, T.M.H.; Tran, V.T.; Huynh, V.T.M.; Van, P.D.T. Evaluate the effects of hydro–meteorological factors and agricultural production on rice productivity in the mezzanine area in An Giang province. *J. Sci. Can Tho University* **2012**, *23A*, 165–173.
8. Luu, V.N. Research on building hydro–meteorological database of An Giang province in the context of climate change. General report on scientific research projects at An Giang province, 2018.
9. MONRE. Climate change and sea level rise scenarios for Vietnam. Vietnam Map and Environmental Resources Publishing House, 2016.
10. Doorenbos, J.; Kassam, A. Yield response to water. *Irrigation Drainage Paper* **1979**, *33*, pp. 257.
11. Allen, R.G.; Pereira, L.S.; Raes, D.; Smith, M. Crop Evapotranspiration–Guidelines for computing crop water requirements–FAO Irrigation and drainage paper 56. *Fao. Rome.* **1998**, *300*, D05109.
12. Hydraulic structure–Irrigation and drainage system – Method of irrigation coefficient determination for rice crop, 2012.
13. Tuan, N.D.; Van, C.T. Impact Assessment of Climate Change on Surface Water Resources in An Giang Province. *J. Sci. VNU Sci. Technolo.* **2015**, *31(3S)*, 261–268.
14. Tuan, N.D.; Van, C.T.; Truong, C.D.; Khanh, N.T.; Anh, V.T.V.; Hong, N.V. Design of Decision Support Systems for Management of Land and Water Resources in Mekong Delta Responding to Climate Change. *Sci. Tech. Hydrometeorol. J.* **2015**, 659, 34–41.
15. Tuan, N.D.; Can, T.V.; Truong, C.D.; Huong, L.T.V. Building and Integrating Information for Building Decision Support System (DSS) in Land and Water Management in the Mekong Delta for Climate Change Response. *Sci. Tech. Hydrometeorol. J.* **2015**, *660*, 32–37.
16. Hai, T.X.; Nghi, V.V.; Hung, V.H.; Tuan, D.N.; Lam, D.T.; Van, C.T. Assessing and Forecasting Saline Intrusion in the Vietnamese Mekong Delta under the Impact of Upstream Flow and Sea Level Rise. *J. Environ. Sci. Eng. B* **2019**, *8*, 174–185. https://doi.org/10.17265/2162–5263/2019.05.005
17. Van, C.T.; Son, N.T. Study on hydrological and hydraulic simulation in the Mekong Delta to evaluate the impact of the ring dike system on the surface flow change in Dong Thap Muoi area. *Sci. Earth Environ.* **2016**, *32(3S)*, 256–263.
18. Tuan, N.D.; Van, C.T.; Phuong, P.V.H.; Huong, L.T.V. Building the knowledge base serves establishing decision support system (DSS) for land and water resources management in The Mekong River Delta response to climate change. Procceding ICENR ILTER–EAP Ecological insights and environmental protection for sustainable development under climate changes in East–Asia and Pacific regions 10/2016.

19. Van, C.T.; Tri, D.Q.; Son, N.T.; Thao, T.T.T.; Hoa, D.T.H. Determining the vulnerability index in the context of high floods in An Giang province. *IOP Conf. Ser. Earth Environ. Sci.* **2019**, *307*, 012015, https://doi.org/10.1088/1755–1315/307/1/012015.
20. Vo, T.D.; Le, T.S.; Vo, D.M.L. Analysis of factors affecting yield of winter–spring paddy in agro–ecological zones along the west coast of Mekong Delta. *J. Sci. Can Tho University* **2019**, *55(5D)*, 99–108.
21. Bao, T.; Nguyen, T.P.; Bui, C.N.; Tran T.H. Study to evaluate the effects of climate change on rice yield in the Mekong Delta. *Sci. Tech. Hydrometeorol. J.* **2011**, *611*, 1–5.

VIETNAM JOURNAL OF
HYDROMETEOROLOGY

Research Article

Research on assessment of suface water environment and sediment in seawater shallow area in Bac Lieu Province and proposing solutions for protection

Phu Huynh[1*], Han Huynh Thi Ngoc[2]

[1] Hochiminh City University of Technology (Hutech); h.phu@hutech.edu.vn
[2] Hochiminh City University of Nature Resources & Environment; htnhan_ctn@hcmunre.edu.vn
*Correspondence: h.phu@hutech.edu.vn; Tel: +84–966687548

Received: 22 February 2021; Accepted: 20 April 2021; Published: 25 April 2021

Abstract: The quality of coastal water and sediment environment in Bac Lieu province tend to deteriorate due to waste (solid, liquid, gas) from the mainland into the river basins before being discharged into the sea. The paper presents the results of research on water quality in river basins dumping into the sea and coastal sediments. By methods of research, survey, observation, analysis of water quality, coastal sediment and calculation of WQI index, compared with QCVN 08–MT:2015/BTNMT, QCVN 43:2017/BTNMT *(column sediments of salt water, brackish water).* The results of physical and chemical parameters according to the dry season and the rainy season exceed the permitted threshold; pH: 6,69–9,20; TSS: 8–1,928 mg/l (exceeding 38.5 times). BOD_5: 7–325 mg/l, COD: 13.8–602.6 mg/l, Ammonium (NH_4^+): 0.1–28.5 mg/l. WQI Nha Mat estuary: 37–73 and Ganh Hao seaport WQI: 52–68. Thus, the water environment in the continental river basins and coastal water quality shows signs of pollution from 2016 to 2020. Sediments in the coastal area in 2018, there are 6/12 samples with high Arsenic concentration, in 2019–2020 there are 10/12 areas with Cd, Pb (0.57–0.83 mg/l). This result will serve the planning, planning, management and control of water quality, coastal sediments and river basins to the coast of Bac Lieu Province in the direction of sustainable development.

Keyword: Bac lieu Province; The shallow seawater areas; Sediment; Water quality; WQI.

1. Introduction

In recent years (2016–2020), the environmental quatily of coast in Bac Lieu province tended to be worsened by the population growth and development of socio–economic activities. In which, the directly affecting the quality of the coastal environment in Bac Lieu province was wastewater from residential aseas, manufacturing facilities and introductrial zones, aquaculture, tourism activities, ect. flowing into the basin of rivers before to the sea.

Therefore, assessment of the effects of wastewater on the water quality of the rivers and canals from 2016 to 2020 is a necessary research. This study investigated and assessed the quality of water based on physical and chemical parameters, identified the main causes of pollution for the river basins that flow to the sea.

Domestic researches on marine pollution, proposing development models for some key areas, presented in detail the role of the sea and coastal in the industrialization and modernization of the country [1–4]. Some persistent organic pollutants in the coastal marine environment in the North of Vietnam" in the Monograph Series on the Sea, Vietnam Island, addressing problems in large coastal cities, this region has the potential to accumulate [5–6]. Persistent organic substances have the potential to adversely affect the environment, ecology and public health. One of the causes of marine environmental pollution is that wastewater from the IZs and EPZs pour directly into rivers, streams, canals, and canals and continue to flow into the sea.

Studies of marine environment in Asia–Pacific; The ASEAN–Canada project on marine pollution aims to define the criteria for marine resource protection and pollution management; The ASEAN–US project on coastal resource management aimed at developing an integrated coastal management plan; Project on the management of the marine and coastal environment in the East Sea by the Asian Development Bank (ADB5712–REG); Agreement on Environmental Protection of the East Sea and Gulf of Thailand dated March 28, 2001; International Law and Marine Environmental Protection, New York University, USA [7]. The book introduces a number of key contents such as the United Nations Environment Program (UNEP) and a joint statement "Stockholm Declaration" An introduction to the negotiation process and the basic contents of the United Nations Convention on the Law of the Sea 1982 (UNCLOS). UNCLOS is sometimes referred to as a "constitution of the oceans" because of its comprehensiveness and scope, in particular Part XII of UNCLOS deals with the protection and preservation of the Marine Environment with the obligation to general and state parties' specific obligations to prevent, reduce, and control pollution [6–13]. State policy on marine environment: 1972–2002, seas and coastal areas, Japan, Tokyo. Accordingly, the book mentions some basic contents such as: Increasing coastal and marine environmental degradation, the main threats to the oceans such as marine pollution, overexploitation, and environmental.

There have been many papers written on the issue of marine environmental pollution, marine economic activities in Vietnam as well as the impact of marine economic activities on the socio–economy. However, there is no specific topic mentioning the impact of marine environmental pollution on the socio–economic activities of Bac Lieu province today [14–24]. Research on assessment of coastal pollution and coastal sediments in Bac Lieu Province will clarify the current environmental situation of coastal areas. coastal areas in Bac Lieu Province.

2. Materials and methods

2.1. Description of study area

Bac Lieu is a provancial city in the Mekong Delta region, covers an area of 266,900,08 hectares with coordinates from 9°0'0" to 9°38'9" North latitude and from 105°14'15" to 105°51'54" East longitude. Bordering with Hau Giang and Kien Giang provinces in the North and Northwest; Bordering with Soc Trang province in the East and Northeast. Bordering with Ca Mau province in the West and Southwest; Bordering with the East Sea in the East and Southeast. Provincial administrative units: Bac Lieu city, Gia Lai town and 05 districts: Hong Dan, Phuoc Long, Vinh Loi, Dong Hai, Hoa Binh and a total of 64 comunes, wards, towns (Figure 1) [1–2].

2.2. Methods

2.2.1. Methods of document collection, analysis and synthesis

+ Collect references on natural conditions, socio–economic conditions, environmental and hydrological document of major rivers, main canals in Bac Lieu province;

+ Collect, statistic and update the characteristics of wastewater sources, characteristics of sources received from the field investigation, from related research projects and topics already in the region, from research institutions. rescue, production, business and service establishments;

+ Collect documents on the theoretical basis to calculate the pollution of the different waste sources of the receiving source.

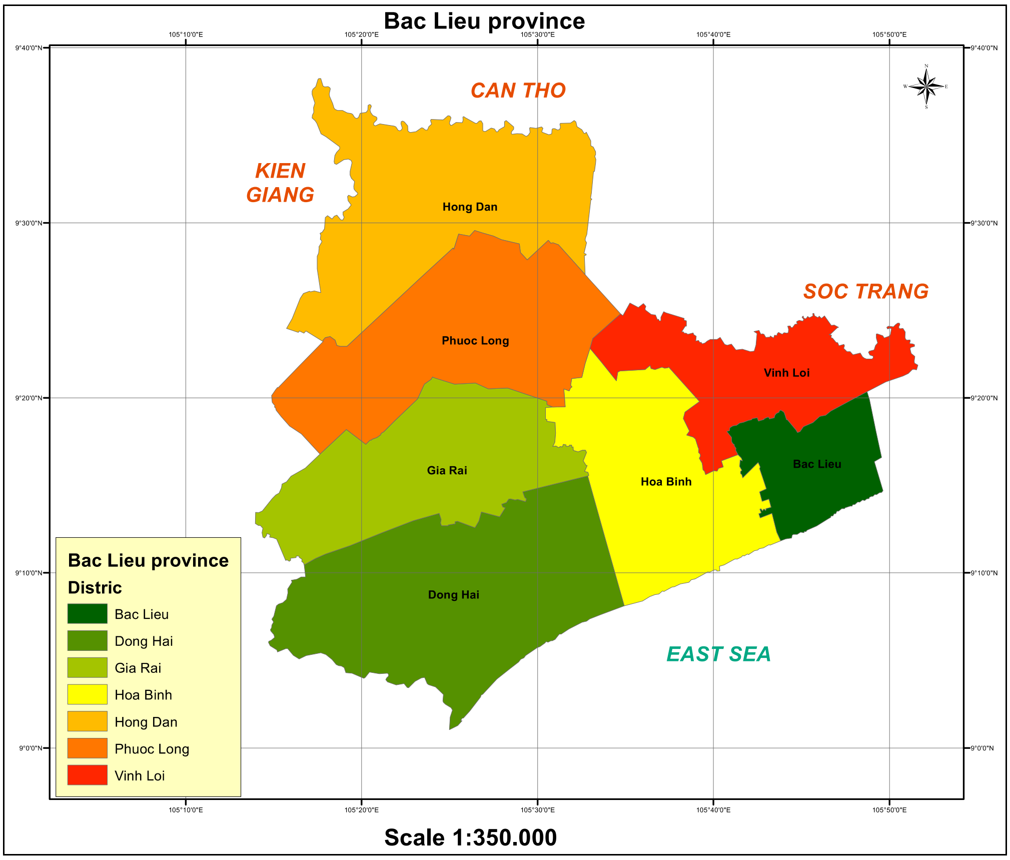

Figure 1. Administrative map of Bac Lieu province.

2.2.2. Methods of field survey, hydrological measurement, additional sampling and analysis

Field survey, hydrological measurement, sampling and analysis of wastewater, river water samples, sediment sampling to WQI calculation for water quality assessment. Compared with Vietnamese Standard QCVN 08–MT 2015/BTNMT.

2.2.3. Methods of analyzing, analyzing statistics and processing data

Synthesis, statistics, meteorological processing, hydrological and socio–economic data, dissecting the data of different waste sources have been investigated to calculate WQI for accurate assessment of surface water quality.

2.2.4. Research data collection

The data collection in this study are presented in Table 1 and Table 2.

Table 1. Sampling locations of coastal seawater in Bac Lieu Province.

Numerical order	Symbol	Sampling locations	Note
1	NBVB1	5km from Nha Mat estuary	
2	NBVB2	5km from Nuoc Ngot canal (Vinh Trach Dong commune)	
3	NBVB3	5km from Cai Cung estuary	
4	NBVB4	5km from Ganh Hao estuary (Ganh Hao town)	
5	NBVB5	5km from the estuary of Huyen Ke canal (Dien Hai commune)	

Table 2. Sampling location for surface water environment monitoring in BacLieu province.

Numerical order	Symbol	Sampling locations	Note
1	NM1	Cai Day canal, Chau Hung town, Vinh Loi district	
2	NM2	Bac Lieu–Ca Mau canal, Hoa Binh town, Hoa Binh district	Bac Lieu–Ca Mau canal (Hoa Binh bridge)
3	NM3	30/4 canal, Vinh Hau commune, Hoa Binhdistrict	
4	NM4	Quan Lo Phung Hiep Canal, town Phuoc Long, Phuoc Long district	
5	NM5	Pho Sinh canal, Phuoc Long commune, Phuoc Long district	
6	NM6	Xom Lung canal, Lang Tron ward, Gia Rai town	
7	NM7	Outside Gia Rai sluice, Ward 1, Gia Rai town	
8	NM8	Buu 2 canal, Kenh Tu, Dien Hai Commune, Dong Hai district	
9	NM9	Cau No.4 canal, Long Dien Dong Commune, Dong Hai district	In 2017 and 2018, no monitoring was conducted
10	NM10	Tac Van canal, Lung Sinh hamlet, Dinh Thanh commune, Dong Hai district	No monitoring was conducted in 2017
11	NM11	Cua Mat estuary, Bac Lieu City	
12	NM12	Hung Thanh sluice gate, Vinh Loi district	
13	NM13	Dau Bang sluice gate, Gia Rai town	
14	NM14	Chu Chi intersection, Phuoc Long district	
15	NM15	Cai Cung sluice gate, Long Dien Dong commune, Dong Hai	
16	NM16	Ganh Hao estuary, Dong Hai district	
17	NM17	Ninh Quoi crossroads, Hong Dan district	
18	NM18	Vinh Loc–Ba Dinh, Hong Dan district	

3. Results and Discussion

3.1. Evolution of water quality according to physical and chemical criteria from river channels to the sea in Bac Lieu province

Surface water quality have been based on physical and chemical indicators, such as pH, DO, BOD_5, COD, TSS (Total suspended solids), $N–NH_4$, $P–PO_4$, Turbidity, Coliforms. The pH of period from 2016 to 2020 ranged from 6.69 to 9.20; the pH of the Cau No. 4 canal (NM9) was higher than the maximum allowed value in 2019 and pH was in the allowable value range (B1) at the remaining locations.

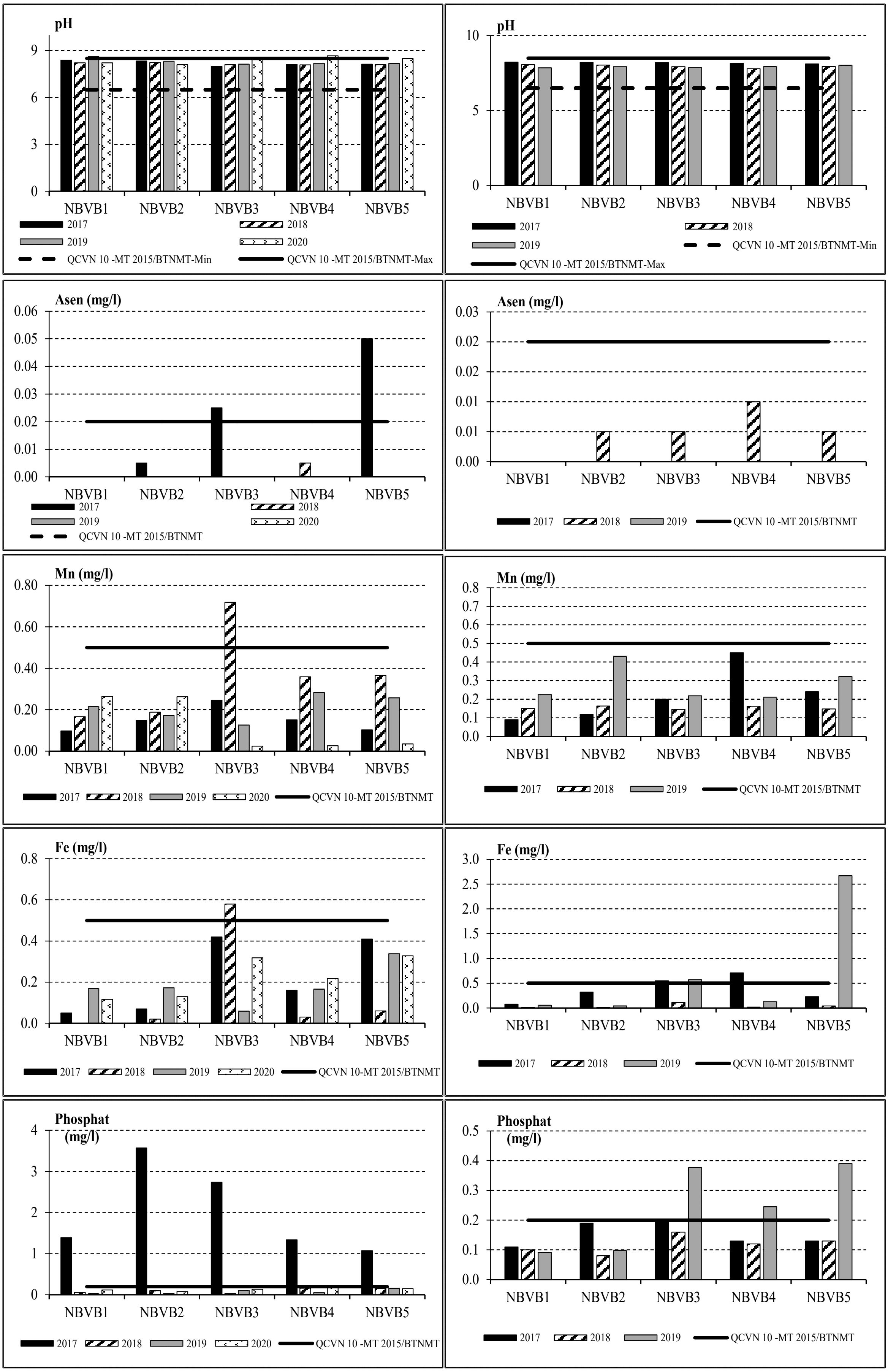

Figure 2. The variability charts of the water quality has been based on the physical and chemical indicator.

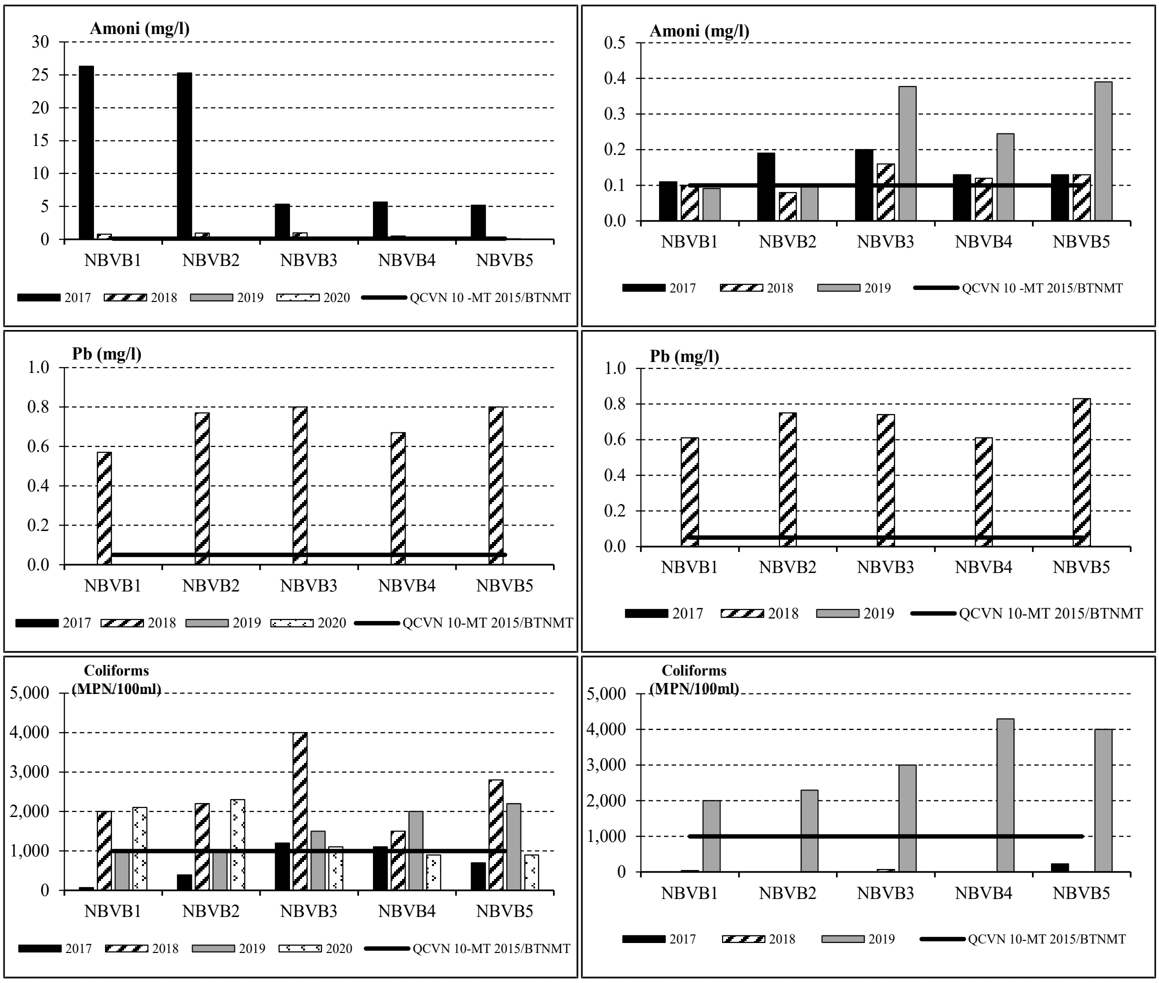

Figure 2. The variability charts of the water quality has been based on the physical and chemical indicator (continute).

In 2016, the BOD_5 was lower than the allowable value and this indicator has increased higher and higher than the maximum allowed value over the 2017–2020 period. In the rainy season, BOD_5 parameter fluctuated from 8 to 410 mg/l. The highest parameter of BOD_5 was at 30/4 canal, Hoa Binh district (NM3) in 2020 and the lowest value was at Cai Day canal, Chau Hung town, Vinh Loi district (NM1) in 2016. In the dry season, the BOD_5 fluctuated from 7 to 325 mg/l. The highest value of BOD_5 was at Cai Cung sluice gate, Dong Hai district (NM15) in 2017 and the lowest value was at 30/4 canal (NM3) in 2016. In 2017, this indicator has increased dramatically at the locations that were observed near the estuary such as Buu 2 canal (NM8), Nha Mat estuary (NM11), and Cai Cung sluice gate (NM15).

TSS indicator of surface water had a significant difference between the two seasons of the year during the period from 2016 to 2020. In the rainy season, TSS was higher than the maximum allowable limit, made up from 8 to 1,928 mg/l. In which, TSS was many times larger than the the allowed limit at 30/4 canal (NM3), Buu 2 (NM8) canal, Cai Cung sluice gate (NM15) and Ganh Hao gate (NM16). The highest parameter of TSS was at Buu 2 canal, Dong Hai district (1,928 mg/l, exceeded 38.5 times) in 2019. In the dry season, TSS was nearly equality or exceeded the maximum allowed value (21.43–1,011 mg/l). The highest parameter of TSS was at Buu 2 canal (NM8), which accounted for 986 mg/l (exceeded 32.8 times) in 2019.

In 2016, COD was lower than the maximum permitted standard. COD increased highly from 2017 to 2020, stood at 13.8–602.6 mg/l in dry season. The COD was highest at 30/4 canal, Hoa Binh district (NM3) in 2020 and lowest at Cai Day canal, Chau Hung town, Vinh Loi district (NM1) in 2016. In the rainy season, COD ranged 11–487 mg/l, COD was highest at Buu 2 canal (NM8) in 2017 and lowest at 30/4 canal (NM3) in 2016. In 2017, coastal monitoring locations: Buu 2 canal, Nha Mat, Cong Cai estuary, COD climed dramatically. In rainy season, COD decreased compared to dry season. DO indicator in surface water ranged from 4.0 to 7.9 mg/l in the 2016–2020 period. The monitoring positions reached the limit QCVN 08–MT:2015/BTNMT, level B1. In the rainy season, DO at the locations of Cai Day (NM1), Bac Lieu–Ca Mau (NM2), 30/4 canal (NM3), Pho Sinh (NM5) and Xong Lung canal (NM6) was high, ranging from 7.01 to 7.92 mg/l in 2017.

Ammonium met the permitted standards in 2016. Ammonium changed significantly over the 2017–2020 period. In the dry season, Ammonium fluctuated from 0,1 to 28,5 mg/l. In general, Ammonium at monitoring positions met the permitted standards in 2016, 2019 and 2020. In the rainy season, Ammonium fluctuated greatly but lower than the dry season, ranging from 0.06–2.46 mg/l. In 2016, Nitrite indicator met the permitted standards, but this figure changed significant in the 2017–2020 period. In 2019, the parameter of Nitrite increased very high, many times higher than the permitted value. In the dry season, there were 16/18 monitoring positions where the Nitrite indicator was higher than the maximum allowable value. In the rainy season, the parameter of Nitrite rised higher than in the dry season, ranging from 0.002 to 1.123 mg/l. 30/4 canal (NM3), 1.123 mg/l, Cai Day Canal (NM1), 0.683 mg/l and Bua 2 canal (NM8), 0.583 mg/l. In the rainy season, Nitrite fluctuated from 0.002 to 0.558 mg/l, all monitoring positions had nitrite parameter higher than the permitted maximum level. In which, the location with the highest Nitrite was Hung Thanh (NM12) and the location with the lowest Nitrite was Cai Day canal (NM1).

In the dry season, the phosphate was higher than the maximum allowable value in 2016 and 2017. Especially, Photphate parameter at 4 locations, Nha Mat (NM11), Cai Cung sluice gate (NM15), Ganh Hao (NM16), Ninh Quoi intersection (NM17) and Vinh Loc–Ba Dinh (NM18) was many times higher than the permitted standard in 2017. Phosphate tended to decrease much compared to previous years and its value was lower than the maximum permitted limit. The phosphate in the rainy season was much lower than one in the dry season (0.0–0.97 mg/l). In 2017, the phosphate was the highest in all years, such as Cai Day canal (NM1), Bac Lieu canal–Ca Mau (NM2), Cua Ganh Hao (NM16).

Chloride in surface water was higher than the maximum value, column B1 in 2016, 2018, 2019 and 2020. In the dry season, chloride fluctuated signifincantly, 2.2–22.759 mg/l. the location had high chloride, Dau Bang (NM13), made up 22.759 mg/l in 2020, chloride parameter of Xom Lung canal (NM6) was 21.128 mg/l in 2020. In the rainy season, chloride was about 42.00–19.143 mg/l. Some monitoring locations had high chloride, such as chloride parameter of Nha Mat (NM11) was 19.143 mg/l in 2018 and Tac Van Canal (NM10) had a chloride parameter o 17.069 mg/l in 2016. The indicator of total iron in surface water ranged from 0.03 to 2.97 mg/l in the 2016–2019 period. In the dry season, total iron ranged from 0.03 to 2.37 mg/l. There were 5/18 monitoring locations with total iron higher than allowed maximum, 30/4 canal (NM3) in 2019, Gia Rai sluice (NM7) in 2016, Buu 2 canal (NM8) in 2016, Cau No.4 canal (NM9) in 2020 and Tac Van canal (NM10) in 2020, the remaining locations were lower than the permitted limit. In the rainy season, the parameter of total iron was from 0,1 to 4,84 mg/l. There were 9/18 monitoring positions with the parameter of total iron was higher than the maximum allowed value. The location with the highest parameter of total iron was Buu 2 canal (NM8) in 2020, the location with the lowest total iron value was Dau Bang (NM13).

The indicator of total Coliforms in surface water was lower than the maximum allowed limit in the 2016–2020 period. In the dry season, parameter of total Coliforms was 75–9.500 MPN/100 ml, there were 02/18 monitoring positions in 2020, which were at Cai Day canal (NM1) and Quan Lo Phung Hiep canal (NM4) with parameter of total Coliforms was higher than the allowed limit. In the rainy season, the parameter of total Coliforms was 230–10.200 MPN/100 ml, with 6/18 monitoring locations were Cau No.4 canal (NM9) in 2016; Cai Day canal (NM1), Quan 3 canal and Figure 4. Phung Hiep (NM4), Cua Nha Mat (NM11), Chu Chi intersection (NM14) and Ninh Quoi crossroad (NM17), the parameter of total Coliforms was higher than the maximum allowed standard in 2019.

3.2. The variation in water quality of rivers and canals flowing into the sea according to WQI index

Calculating WQI index (2016–2020) was based on the results of physical and chemical parameters (pH, Coliforms, NO^{3-}, NO^{2-}, BOD_5, COD, NH^{4+}, PO_4^{3-}, DO) of water quality at monitoring locations (Table 2). Calculation results are shown in Figures 3 and 4.

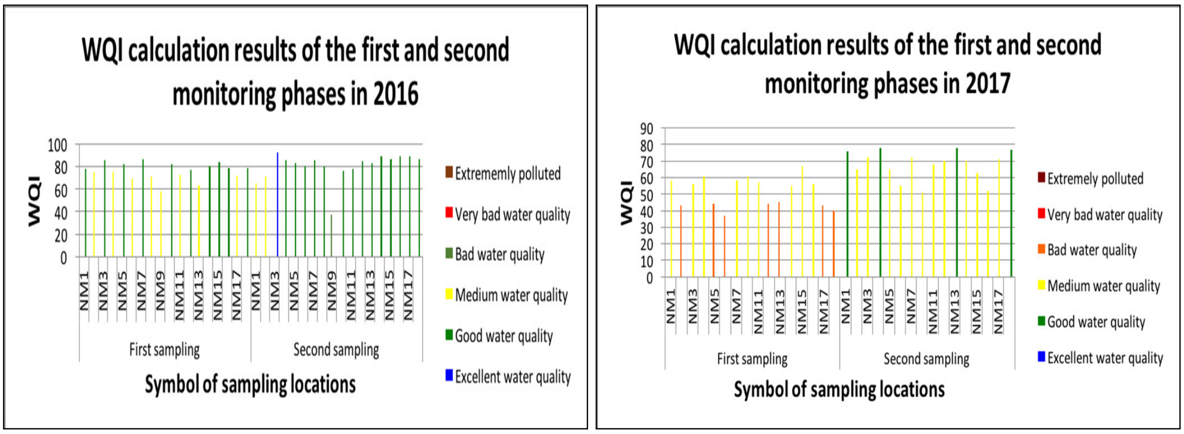

Figure 3. WQI indicators of the first observation in 2016 and 2017.

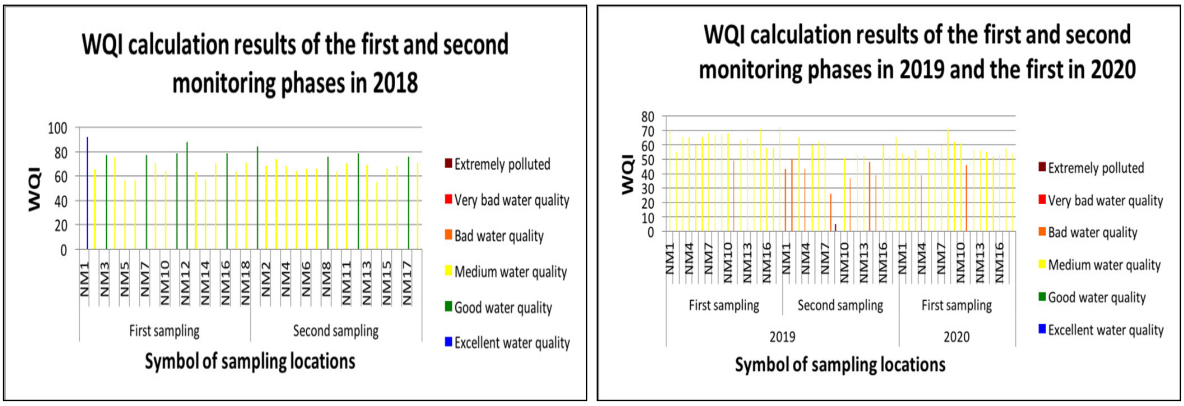

Figure 4. WQI indicators of observation in rainy and dry seasons in 2018, 2019 and 2020.

3.3. The variation of the quality in coastal sediments in Bac Lieu province

The variation of pollution parameters in coastal sediments of Bac Lieu province during the period from 2016 to 2020, the results of two monitoring periods, corresponding to dry and rainy seasons, compared with QCVN 43:2017/BTNMT–National technical regulation on sediment quality (sediment column of salt water, brackish water).

Heavy metals in marine sediments, such as Arsenic, Cadmium, Cu, and Chromium at all positions were lower than the permitted limit (2016–2020). The value of analyzed parameters had a significant variation between years (Figures 4a–4d) but there was no pollution manifest.

In 2018, there were 6/12 soil samples with arsenic > 8 mg/l in the coastal area of Chau Thoi commune. Also in those locations, it was Zn > 10 mg/l in 2019. In 2020, there were 10/12 soil samples with Cd > 9 mg/l, higher than the standard.

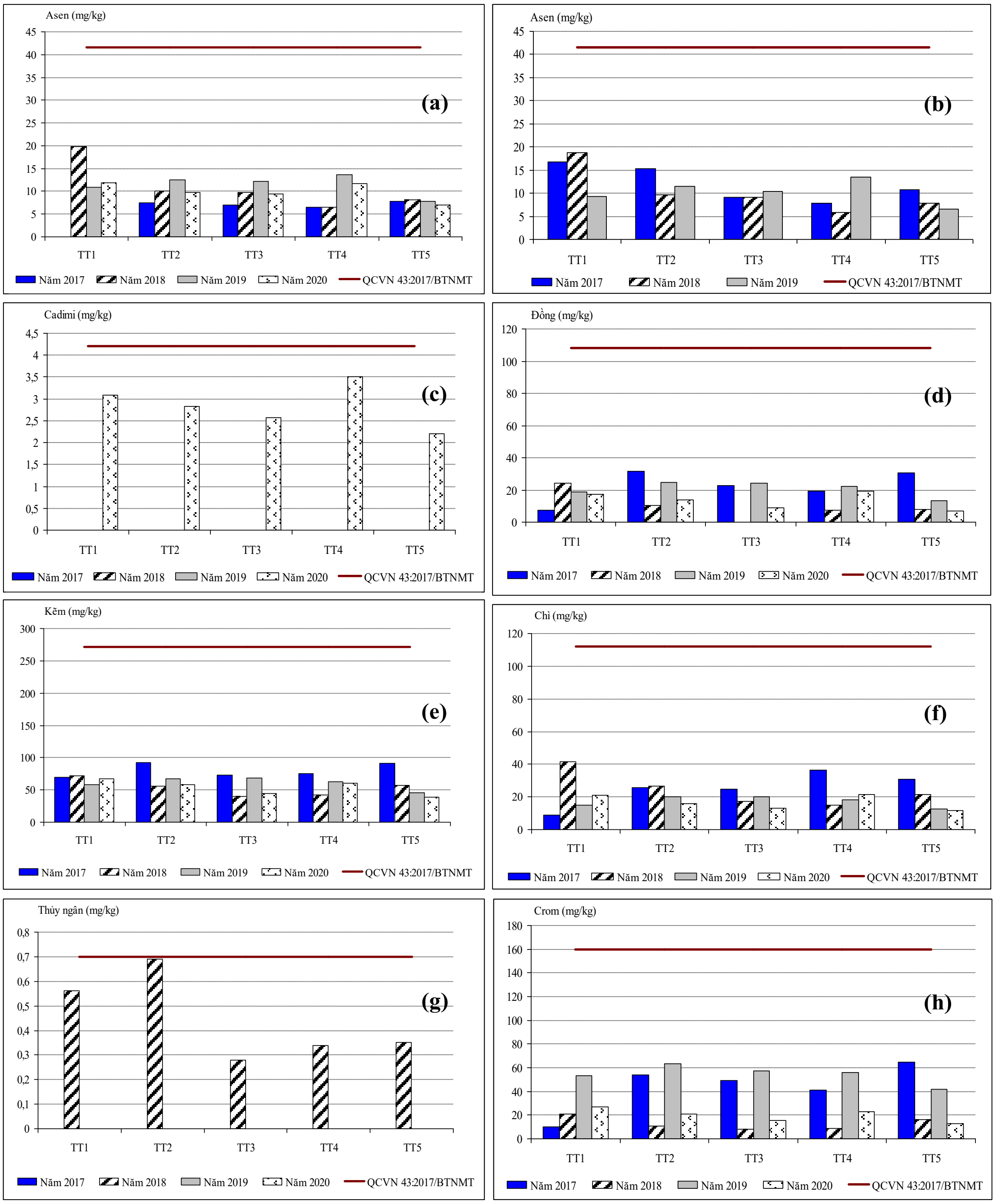

Figure 5. The charts show the variation of heavy metals in sediments: (a) The variation of As in the dry season; b) The variation of the As in the rainy season; c) The variation of the Cd in the dry season; d) The variation of the Cu in the dry season; e) The variation of the Zn in the dry season; f) The variation of the Pb in the dry season; g) The variation of the Hg in the dry season; h) The variation of the Cr in the dry season.

3.4. Proposing solutions for protection

Perfecting waste source management mechanisms and policies, economic tools are used to influence costs and benefits in the operation of economic organizations to create impacts on the behavior of economic organizations that was beneficial for the environment. Managing different sources of waste accords to directive No. 25/CT–TTg dated 31/8/2016 of the Prime Minister of Vietnam on a number of urgent tasks and solutions to environmental protection, assigning the provincial People's Committee to force factories with large–scale of wastewater discharge to install monitoring equipment to control and monitor their discharge in accordance with the provisions of Vietnamese law and report directly to the Department of Natural Resources and Environment to perform waste source management. Conducting propaganda to raise awareness of the community and businesses was through the media or practical operation models. Building a network of automatic water environmental monitoring stations, enhancing environmental supervision–monitoring at factories in the area and setting up a mobile monitoring–monitoring unit are very necessary.

4. Conclusion

The article analyzed and evaluated the water quality through physical and chemical parameters, the results of monitoring the quality of surface water environment during the period from 2016 to 2020 showed that the physical and chemical parameters, such as TSS, BOD_5, COD, Ammonium, Nitrite, Phosphate, Total Iron, Chloride, and Colifoms exceeded the permitted standards (QCVN 08–MT:2015/BTNMT–level B1). In which the parameters: TSS, BOD5, COD, Ammonium, Phosphate, Chloride were many times higher than the standard. The WQI indicator fluctuates significantly in the 2016–2020 period, WQI tended to decrease gradually, showing the green color from 2016 to 2020, most of the sampling indicators was yellow color WQI < 70, showing slightly polluted water to polluted; variation in surface water quality in Bac Lieu province were changing towards more and more pollution in the 2016–2020 period. The average water quality indicator on 18 monitoring locations in the first observation in 2016 on the VN–WQI was 76 (good level), by the first observation in 2020, the average water quality indicator on the VN–WQI was only 55 (average). The parameters of coastal sediments were below the allowed threshold according to QCVN 43:2017/BTNMT– saline and brackish sedimentary column. Proposing solutions to prevent environmental pollution and towards the sustainable development of water environment in coastal areas of Bac Lieu province.

Acknowledgments: The article is completed from the results of the implementation of the study "Assessment of environmental pollution impacts in coastal areas originating from socio–economic activities in Bac Lieu province and proposing mitigation measures". (2019–2020). Phu My Institute for Environmental Technology Promotion and Water Resources.

Authors contribution: Contructing research idea: P.H.; H.H.T.N.; Select research methods: P.H; H.HTN; Survey sampling and analysis: P.H; H.HTN; Data processing: P.H.; H.H.T.N.; Writing original draft preparation: P.H.; H.H.T.N.; Writing–review and editing: P.H.; H.H.T.N.

Conflicts of interest: The authors declare no conflict of interest.

References

1. Guidelines for the formulation of integrated coastal management strategy for coastal provinces of Vietnam. Department of Environmental Protection. Ministry of Natural Resources and Environment, 2007.
2. Assessment of environmental pollution impacts in coastal areas originating from socio–economic activities in Bac Lieu province and proposing mitigation measures. Phu My Institute for Environmental Technology Promotion and Water Resources, 2019.
3. Report on environmental status of Bac Lieu province for the period 2016–2020, Center for environmental monitoring, 2020.
4. Abdullah, A.; Hutomo, M. Marintinge Protected Area–matter and Development, Jakarta, Indonesia**,** 1995.

5. Abrahamsson, J.B. Marine Environment and shipping, The IO Foundation, 1977.
6. Assessment of environmental pollution impacts in coastal areas originating from socio–economic activities in Bac Lieu province and proposing mitigation measures, 2020.
7. Schiffman, H.S. International law and the protection of the Marine environment. International Law And Institutions, Encyclopedia of Life Support Systems (EOLSS), 2003.
8. Bac Lieu Statistical Office, Bac Lieu Statistical Year book. 2017, 2018, 2019.
9. Biliana, C.S.; Robert, W.K. Integrated management of coastal and marine, University of Delaware, Newark, USA, 1998.
10. Ca, V.T. Marine environment concept and issues of marine environment. Publisher of Research on Marine and Island Management, Vietnam Administration of Sea and Islands, 2009.
11. Central Science and Education Department, Ministry of Science and Technology and Environment, Towards consolidating the system of state management agencies on environmental protection in Vietnam, 2001.
12. Chanyut, S.; Edward L. W. Results of State management over mangrove community based in Southern Thailand, Bangkok. *Ecol. Soc.* **2008**, *13*, 2.
13. Charles, N.E. Toward a common framework for integrated coastal zone management, the National Oceanic Bureau (NOS), Oceanic Administration and the U.S. National Atmospheric Administration (NOAA), Proceedings of the workshop, 2002
14. Decree No. 80/2014 / ND–CP dated August 6, 2014, Decree on drainage and wastewater treatment, 2014.
15. Circular No. 02/2009/TT–BTNMT dated 19/03/2009 regulating the assessment of the sources to rest wastewater. Ministry of Natural Resources and Environment, 2017.
16. Decision No. 341/QD–BTNMT dated 23/03/2012 promulgating the list of rivers within the province, Ministry of Natural Resources and Environment, 2012.
17. National overall environmental status report in 2006–2010. Ministry of Natural Resources and Environment, 2010.
18. QCVN 08–MT:2015/BTNMT, National technical regulation on surface water quality. Ministry of Natural Resources and Environment, 2015.
19. QCVN11–MT:2015/BTNMT, National technical regulation on industrial wastewater from seafood processing industry. Ministry of Natural Resources and Environment, 2015.
20. Decision 1327/2002 / QD–BYT dated 18/04/2002 promulgating industry standard regional polyclinics design standards. Ministry of Health, 2002.
21. Phu, H. Method of calculation & application of WQI index to assess the status water quality and proposal of management Luy river Binh thuan province. *VN J. Hydrometeorol*. **2019,** *02,* 9–15.
22. Huynh, P. Irrigation construction solution for rising Litopenaeus Vannamei in Mekong delta. The international conference on science, technology and society studies (STS), HUTECH **2020**, 92–97. ISBN 978-604-67-1574-0.
23. Phu, H. Solution for water circulation in raising Litopenaeus vannamei (Whiteleg shrimp) in Bac Lieu province. The international conference on science, technology and society studies (STS), HUTECH **2020**, 97–103. ISBN 978-604-67-1574-0.
24. Triet, L.M. Building a number of scientific bases for the unified and integrated management of water environment in Dong Nai river basin. Institute of Environment and Natural Resources, 2005.

VIETNAM JOURNAL OF HYDROMETEOROLOGY

Research Article

Impact of climate change on seasonal distribution of flows in Ca basin, Central Viet Nam

Huynh Thi Lan Huong[1*]

[1] Vietnam Institute of Meteorology, Hydrology and Climate change; huynhlanhuong@gmail.com

*Correspondence: huynhlanhuong@gmail.com; Tel: +84–912119740

Received: 04 February 2021; Accepted: 24 April 2021; Published: 25 April 2021

Abstract: Climate change has been impacting both natural and human resources greatly. Flow in river basins is subjected to strongly affect due to its direct relevance to climatic factors. Many changes in the distribution of runoff on river basins throughout the year due to the impact of climate change (CC) have been observed. In some areas, the flood season tends to shift gradually towards the end of the year, making the flood season appear later than before, but there are also areas where the flood season occurs earlier. The paper specifically analyzes changes in the distribution of flood season in a year under the impact of climate change in some areas in the Ca River basin, central Viet Nam.

Keywords: Climate change; River flow; Flow distribution; Ca River basin.

1. Introduction

At present, climate change continues to be one of the most concerning global issues, along with the coronavirus pandemic [1]. Climate warming will alter several water cycle components, such as varying the pattern and intensity of precipitation, increasing water vapor and evaporation, and changing runoff [2]. Particularly, climate change is projected to exacerbate the change of flow regimes in Vietnam significantly. River flow varies over space and time therefore knowledge about changing river flow regimes is paramount for assessing climate change risks related to freshwater. Estimation of changes in seasonality, inter-annual variability, statistical low and high flows, and floods and droughts is required to understand the impact of climate change on humans and freshwater ecosystems [3]. Climate change impact studies for river basins mostly focus on changes of river discharge and aspects of its temporal variability, in particular seasonality [4–9]. In Vietnam, research studies on impact of climate change on river flows focusing on changes of flow magnitude and occurence are prominent [10]. Studies on the impact of climate change on river flow regimes considering both spatial and temporal scales are still limited. This study looks at the changes in the timing of flood season in a year under the impact of climate change in the Ca River basin which is located in the central Vietnam and is subjected to the greatly vulnerable due to climate change. We wanted to find out how significant change of the flood flow regime in terms of spatial and temporal scales under the impact of climate change. The state-of-the-art modelling chain method was used to translate climate scenarios (as developed by Ministry of Natural Resources and Environment [11]) into scenarios of flow regime indicators including flood flow regime and of shifts between perennial and intermittent flood flow regimes.

2. Materials and Methods

2.1 Description of study site

Ca River is a transboundary river, originating from a high mountain range in Xiengkhuang in Laos with a peak of 2.000 m, flowing northwest–southeast into Vietnam, pouring into the sea at the Hoi River mouth. The Ca River is about 514 km long, of which the part flowing in the territory of Vietnam is 360 km long. Ca River basin is the largest river system in the North Central region, Ca River system is in the coordinate range $103^o14'–106^o10'$ east longitude, $17^o50'–20^o50'$ north latitude, stretching about 350 km in the northwest–southeast direction, 89 km wide; adjacent to the Ma river system to the north, the Mekong River system to the west, the Gianh river to the south and the Gulf of Tonkin to the east. The total catchment area is 27.200 km^2, of which the part of the basin lying in Vietnam has an area of 17.730 km^2, accounting for 65.2% of the entire basin area, located in the coordinates $103^o45'20''–105^o15'20''$ east longitude, $18^o15'00''–20^o10'30''$ north latitude, covers most of Nghe An Province, Ha Tinh Province and part of Nhu Xuan district, Thanh Hoa Province (Figure 1).

Ca River basin is divided into 3 separate regions including the upstream of Ca River in the west, the Hieu River basin in the north, and the La River basin in the south. Upstream of La River has 2 main river branches namely Ngan Sau and Ngan Pho. In different regions, the distribution of the flood season months in the year also varies differently. On the upstream of Ca River, there is a flood season lasting for 5 months from July to November (represented by the Dua hydrological station), the Hieu River basin has a flood season lasting for 3 months from August to October (represented by the Nghia Khanh hydrological station). Ngan Sau River basin has a flood season lasting for 3 months from September to November (represented by Hoa Duyet hydrological station), Ngan Pho River basin has a flood season lasting 4 months from August to November (represented by Son Diem hydrological station). To consider the impact of climate change on the flow regime in flood season for the Ca River basin, this study will investigate the distribution of flood season at 4 hydrological stations of Dua, Nghia Khanh, Hoa Duyet and Son Diem represented for 4 regions forming the Ca River basin.

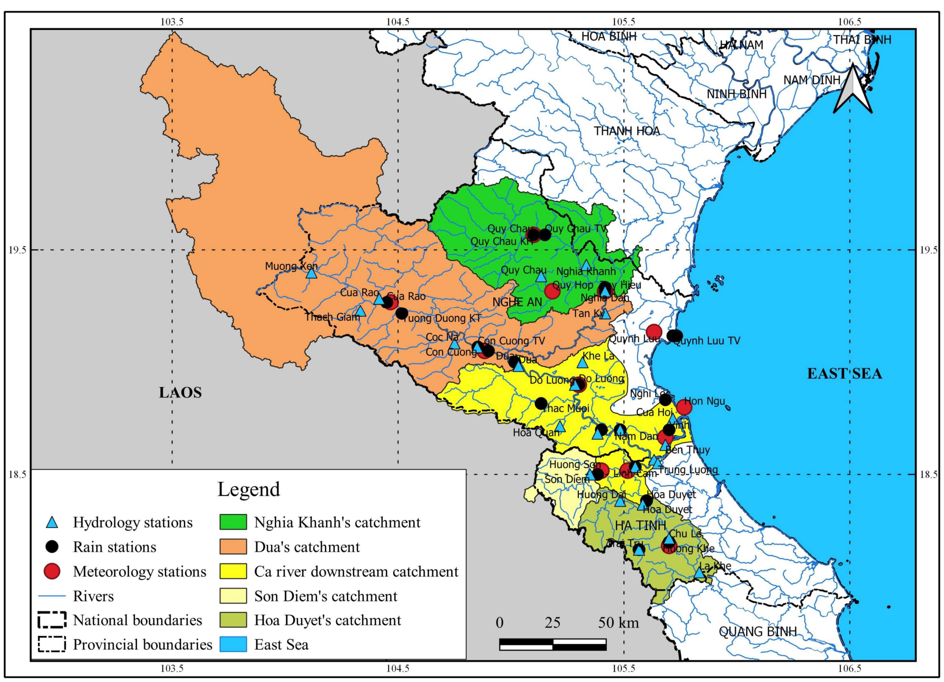

Figure 1. Ca River Basin.

2.2. Calculation Method

The hydrological model MIKE–NAM [12] is used to simulate runoff from rain. This is the method commonly used to calculate runoff for regions with tropical climatic characteristics and has been widely applied for many river basins in Vietnam. The statistical analysis method is used to analyze the impact of climate change on the change of months in the flood season in the year. The Penman–Monteith formula [13] is used to calculate the potential evaporation amount at the meteorological stations as follows:

$$ET_0 = 1 + \frac{0,408\Delta\left(R_n - G\right) + \gamma\dfrac{900}{T+273}u_2\left(e_s - e_a\right)}{\Delta + \gamma\left(1 + 0,34u_2\right)} \tag{2}$$

where ET_o is the reference crop evapotranspiration (mm/day); R_n is net radiation on plant surface (MJ/m^2/day); G is the heat flux density of the soil (MJ/m^2/day); T is the daily average temperature at an altitude of 2 m (^oC); u_2 is the wind speed at the height of 2m (m/s); e_s is the saturated steam pressure (kPa); e_a is the actual steam pressure (kPa); Δ the slope of the steam pressure curve (kPa/^oC); γ is the moisture constant (kPa/^oC).

2.3. Data used

– Daily observations of average, maximum, and minimum temperature in the 1986–2005 period at 6 meteorological stations on Ca River basin including Tuong Duong, Quy Chau, Tay Hieu, Do Luong, Vinh, and Huong Khe were used to calculate the amount of potential evapotranspiration as input to the MIKE–NAM model.

– Daily rainfall data in the 1986–2005 period at 14 hydrometeorological stations measuring rainfall on Ca River basin including Cua Rao, Tuong Duong, Quy Chau, Nghia Khanh, Con Cuong, Tay Hieu, Dua, Do Luong, Nam Dan, Son Diem, Hoa Duyet, Huong Khe, Linh Cam, Vinh were used as input to the MIKE–NAM model.

– Daily average water discharges in the 1986–2005 period at 2 hydrological stations of Dua, Nghia Khanh and the period 1997–2005 at 2 hydrological stations of Hoa Duyet, Son Diem were used to calibrate and validate parameters of the MIKE–NAM model.

– Daily data of average, maximum, minimum temperature, and rainfall at the stations in the period 2016–2035, 2046–2065, 2080–2099 derived from the scenarios RCP4.5 and RCP8.5 were used to calculate flow under climate change scenarios.

2.4. Model set up

In this study, the MIKE–NAM model was set up for 4 sub–basins including Dua, Nghia Khanh, Hoa Duyet and Son Diem. The precipitation in subbasin Dua employs data from 8 stations and the evaporation data in subbasin Dua employs from Tuong Duong station; subbasin Nghia Khanh uses precipitation data from 6 stations and evaporation data from Quy Chau station; subbasin Hoa Duyet uses rainfall data from 3 stations and evaporation data from Huong Khe station; subbasin Son Diem using rainfall data from Son Diem station and evaporation data from Vinh station (Table 1). A map of subbasins and weight of every rain gauge for 4 subbasins are shown in Figure 2 and Table 1.

Table 1. Weight of rain gauges estimated using Theissen polygon.

Rain gauge		Subbasin Dua	Subbasin Nghĩa Khanh	Subbasin Hòa Duyet	Subbasin Son Diem
Area (km²)		20,800	4,024	1,880	790
Station weight	Quy Chau	0.15	0.72		
	Cua Rao	0.48	0.03		

Rain gauge	Subbasin Dua	Subbasin Nghĩa Khanh	Subbasin Hòa Duyet	Subbasin Son Diem
Tuong Duong	0.17			
Nghia Khanh	0.03	0.15		
Tay Hieu	0.04	0.07		
Con Cuong	0.09	0.01		
Dua	0.03	0.02		
Dô Luong	0.01			
Son Diem			0.03	1
Hoa Duyet			0.29	
Huong Khe			0.68	
Meteorological gauge	Tuong Duong	Quy Chau	Huong Khe	Vinh

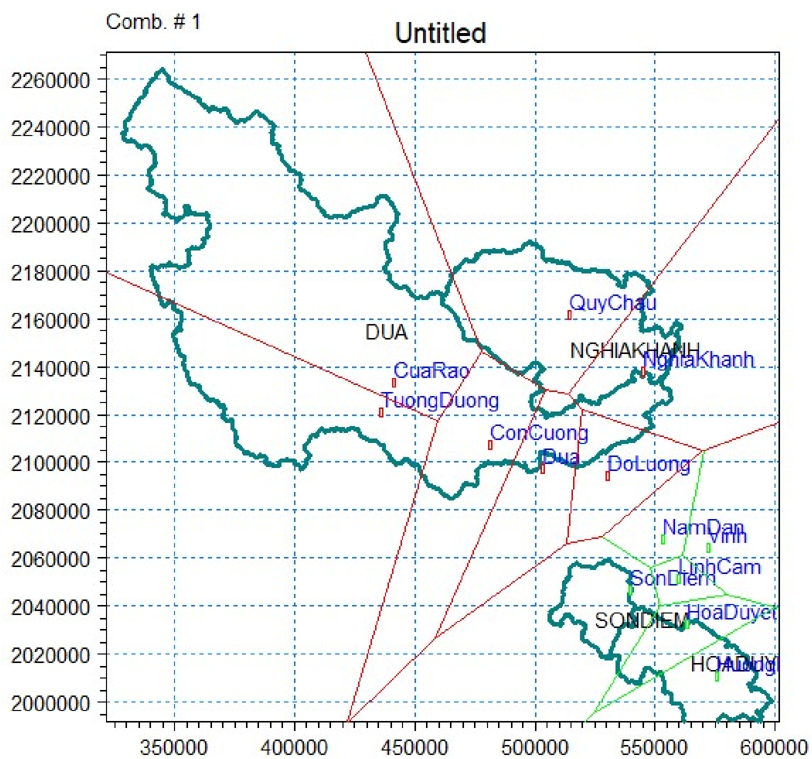

Figure 2. Map of subbasins.

3. Results and discussion

3.1. Calibration and validation of MIKE–NAM model parameter set

For the catchment of the Dua and Nghia Khanh hydrological stations, the data series from 1986–1995 was used for calibration and the data series from 1996–2005 was used for verification of the parameter set of the MIKE–NAM model. The Nash index [14] is used to test the agreement between the calculated results of runoff and actual measured data.

For the basin of Hoa Duyet and Son Diem hydrological stations, the data series from 1997–2001 was used for calibration and the data series from 2002–2005 was used for verification of the MIKE model parameters.

After calibration, the study obtained the MIKE–NAM model parameters for the basin of 4 hydrological stations of Dua, Nghia Khanh, Hoa Duyet, and Son Diem (Table 2).

Table 2. The calibrated MIKE–NAM model parameter set for the catchments of the hydrological stations in the Ca River basin.

No.	Model Parameters	Dua	Nghia Khanh	Hoa Duyet	Son Diem
1	Umax	2.3	2.37	1.4	1.8
2	Lmax	19	13.5	19.1	12.8
3	CQOF	0.328	0.7	0.679	0.967
4	CKIF	18.95	8.061	22.76	5.4
5	CK1,2	48.3	38.7	39	23
6	TOF	0.551	0.9	0.443	0.957
7	TIF	0.00003	0.000166	0.26	0.00032
8	TG	0	0.000134	0	0.000296
9	CKBF	2000	2711	2000	980.2

The MIKE–NAM model parameters for the basin of 4 hydrological stations, after being calibrated, were verified to check the reliability. The calculated and observed water discharge at the hydrological stations in the two periods of calibration and verification are shown from Figure 3 to Figure 10.

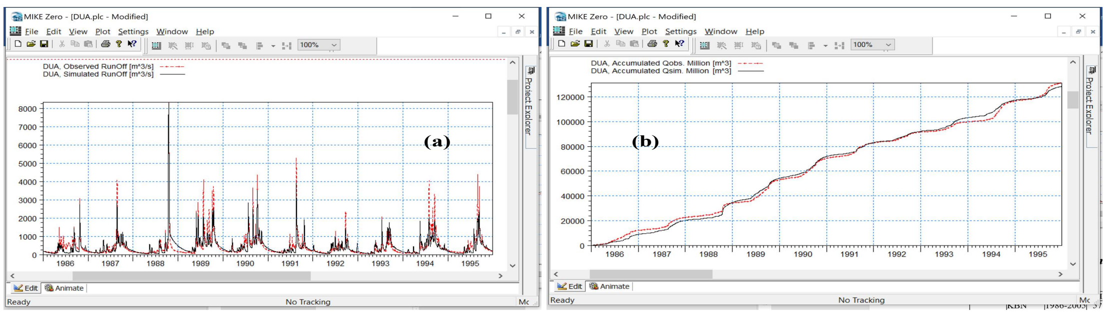

Figure 3. Process line (a) and accumulation line (b) of calculated and observed water discharge at Dua station in the period 1986–1995 (Calibration).

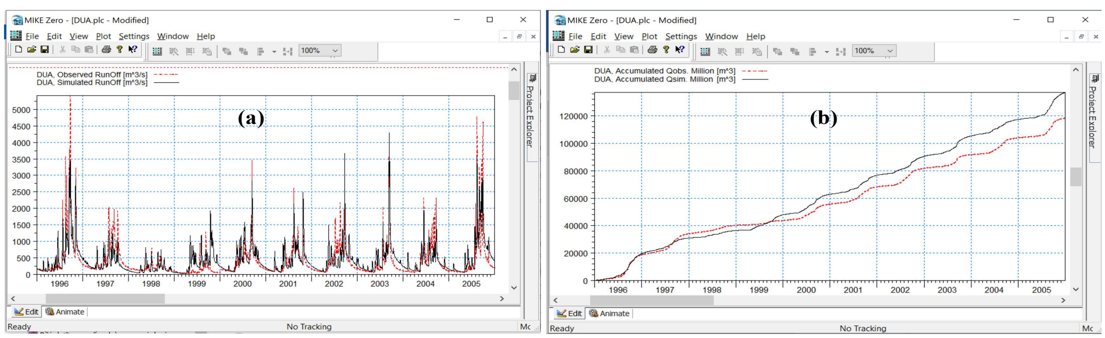

Figure 4. Process line (a) and accumulation line (b) of calculated and observed water discharge at Dua station in the period 1996–2005 (Verification).

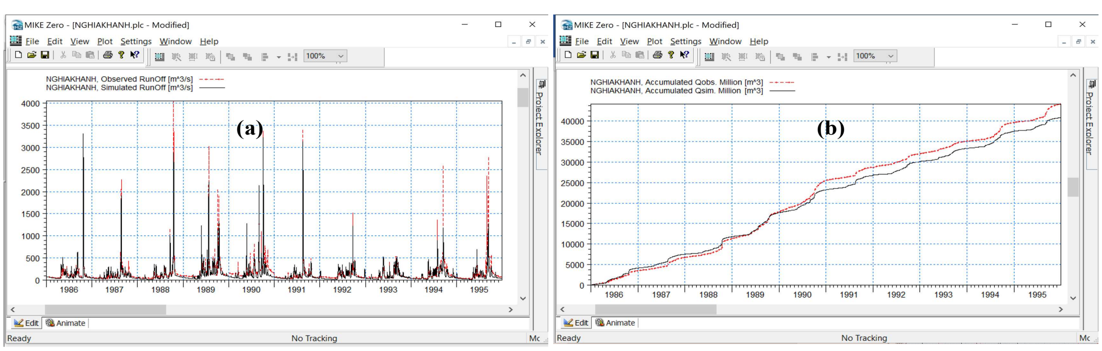

Figure 5. Process line (a) and accumulation line (b) of calculated and observed water discharge at Nghia Khanh station in the period 1986–1995 (Calibration).

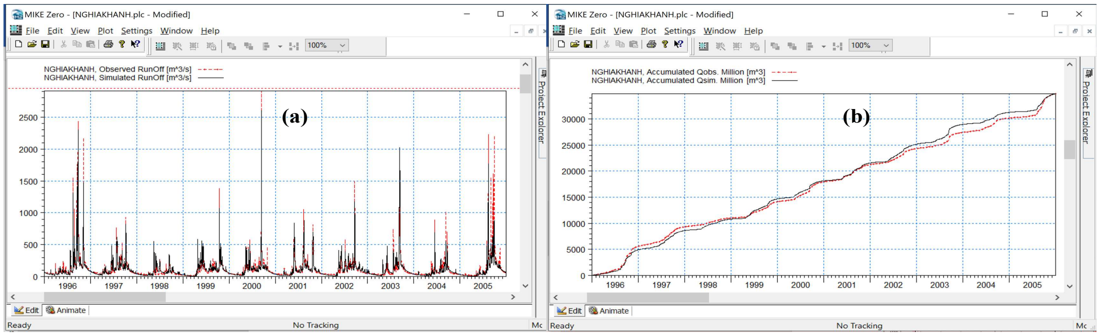

Figure 6. Process line (a) and accumulation line (b) of calculated and observed water discharge at Nghia Khanh station in the period 1996–2005 (Verification).

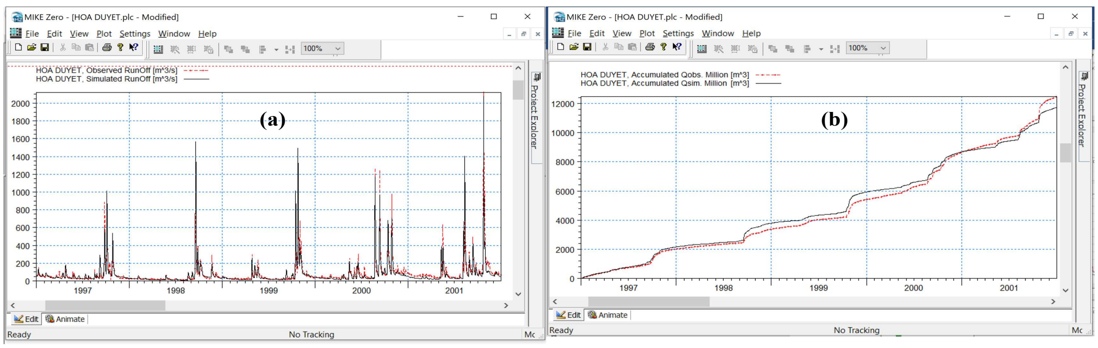

Figure 7. Process line (a) and accumulation line (b) of calculated and observed water discharge at Hoa Duyet station in the period 1997–2001 (Calibration).

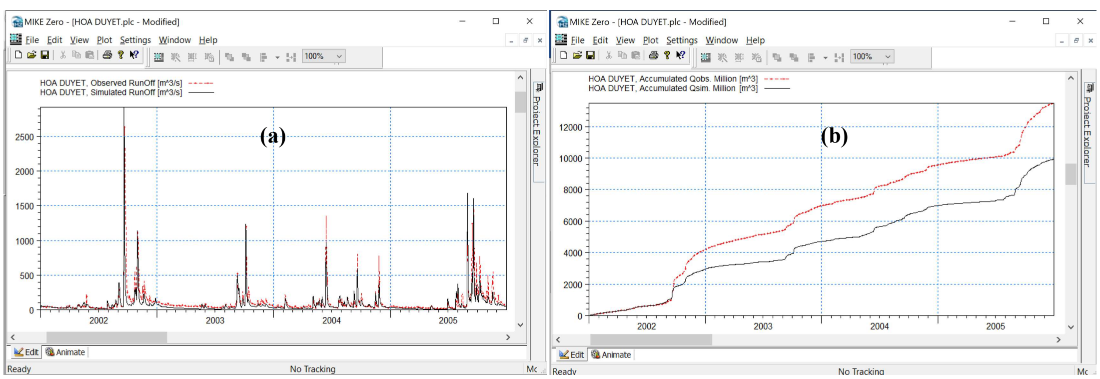

Figure 8. Process line (a) and accumulation line (b) of calculated and observed water discharge at Hoa Duyet station in the period 2002–2005 (Verification).

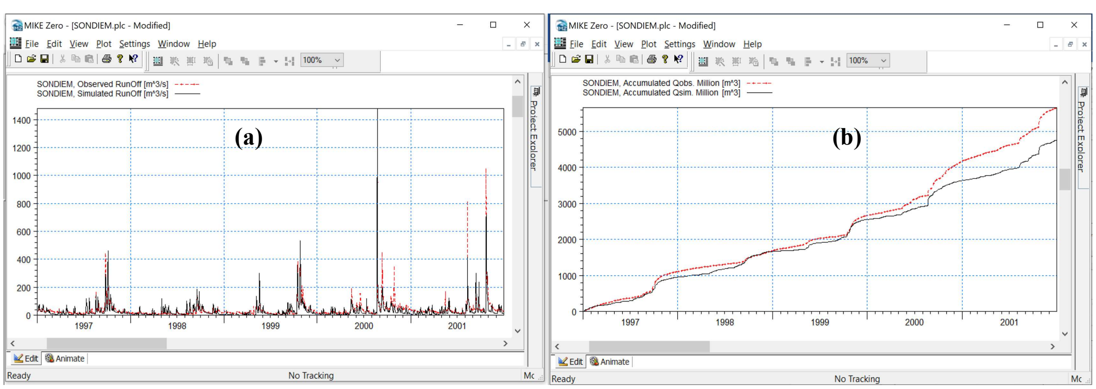

Figure 9. Process line (a) and accumulation line (b) of calculated and observed water discharge at Son Diem station in the period 1997–2001 (Calibration).

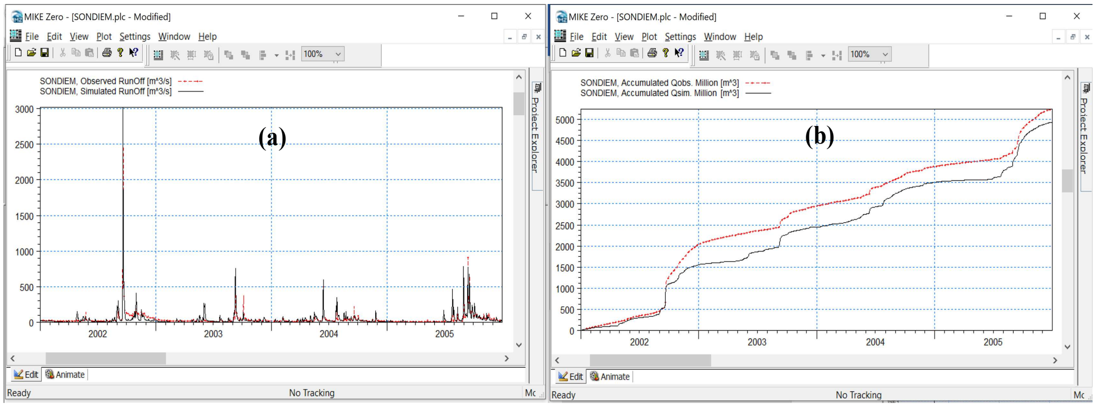

Figure 10. Simulated and observed hydrograph (a) and accumulated discharges (b) at Son Diem station in the period 2002–2005 (Verification).

The accuracy of the results of the runoff calculation to the hydrological stations on the Ca River basin is evaluated by Nash–Sutcliffe criteria. Evaluation results are presented in Table 3. It can be seen in the table 3, the results of runoff simulation to 10 hydrological stations on the Ca River basin by the MIKE NAM model are reliable during both calibration and verification with Nash–Sutcliffe criteria ranging from 0.72 to 0.82. Thus, the MIKE NAM model parameters after being calibrated and validated can be used to calculate runoff for different scenarios.

Table 3. Calibration and Verification results of MIKE–NAM model parameters.

No.	Hydrological stations	Calibration		Verification	
		Period	Nash	Period	Nash
1	Dua	1986–1995	0.80	1996–2005	0.76
2	Nghia Khanh	1986–1995	0.77	1996–2005	0.82
3	Hoa Duyet	1997–2001	0.82	2002–2005	0.72
4	Son Diem	1997–2001	0.76	2002–2005	0.79

3.2. Runoff calculation results under Climate change scenarios

The MIKE–NAM model parameters after calibration and verification are used to calculate the runoff to the Dua, Nghia Khanh, Hoa Duyet, and Son Diem sub–basins for the baseline period 1986–2005 and future periods 2016–2035, 2046–2065, 2080–2099 under RCP4.5 and RCP8.5 scenarios. The results of the calculation of average monthly water discharge in the baseline period 1986–2005 and the periods 2016–2035, 2046–2065, 2080–2099 under the scenarios RCP4.5 and RCP8.5 are summarized in Table 4.

In Table 4, discharges in the baseline period are measured data at the hydrological stations; discharges in the period 2016–2035, 2046–2065, 2080–2099 under the scenarios RCP4.5 and RCP8.5 are simulated from the MIKE–NAM model. The bold runoff values are values greater than the annual mean runoff values and these are considered flood season runoff.

Table 4. Results of the calculation of average water discharge over time by climate change scenarios.

Station	Scenarios	Period	I	II	III	IV	V	VI	VII	VIII	IX	X	XI	XII	Annual Average
Nghia Khanh	Baseline	1986–2005	57.6	51.3	48.1	49.6	96.1	120.8	123.1	208.5	305.9	251.1	117.3	69.0	124.9
	RCP4.5	2016–2035	110.4	95.2	130.7	167.3	267.7	241.2	233.8	291.9	477.6	375.3	212.8	121.3	227.1
		2046–2065	129.6	113.7	126.6	181.5	230.3	309.6	163.1	263.0	430.3	473.0	286.8	148.5	238.0

Station	Scenarios	Period	I	II	III	IV	V	VI	VII	VIII	IX	X	XI	XII	Annual Average
		2080–2099	123.6	112.5	129.8	178.9	319.0	237.0	207.0	334.4	540.9	518.3	260.7	138.5	258.4
		2016–2035	103.4	94.1	122.9	181.5	261.4	238.7	282.3	333.5	422.0	296.3	235.9	132.2	225.3
	RCP8.5	2046–2065	132.6	108.2	118.9	183.7	263.9	218.0	210.2	280.5	439.5	460.8	239.1	147.8	233.6
		2080–2099	138.5	121.7	142.3	139.9	280.0	437.6	225.0	337.8	485.7	547.0	294.5	154.3	275.4
Dua	KBN	1986–2005	152.5	127.2	115.7	111.3	224.3	365.9	521.5	844.3	1023.4	708.9	339.1	196.6	394.2
		2016–2035	222.4	182.4	164.2	140.5	435.2	503.0	743.6	1273.0	1353.6	956.1	571.9	288.0	569.5
	RCP4.5	2046–2065	238.2	193.3	190.4	185.9	419.7	467.7	551.6	913.6	1358.0	1229.7	545.3	315.5	550.7
		2080–2099	237.9	204.5	175.4	180.7	514.8	509.3	847.2	1199.3	1568.1	1001.3	661.1	310.2	617.5
		2016–2035	205.7	170.2	152.0	135.3	402.9	515.3	814.9	1360.1	1238.8	831.5	572.6	297.4	558.0
	RCP8.5	2046–2065	258.2	206.8	202.7	181.3	466.2	557.5	701.3	1052.9	1408.0	1285.1	531.7	335.3	598.9
		2080–2099	238.2	192.8	165.3	153.4	459.8	593.2	793.0	1079.8	1250.9	1120.0	664.9	321.8	586.1
Yen Thuong	KBN	1986–2005	212.5	176.0	158.6	150.6	349.0	459.9	589.5	1002.3	1371.5	1073.4	519.2	297.9	530.0
		2016–2035	299.8	239.2	215.8	188.4	526.6	622.7	831.5	1490.7	1732.5	1303.5	794.4	422.9	722.3
	RCP4.5	2046–2065	331.4	258.5	260.4	263.2	517.5	555.5	627.1	1114.5	1670.5	1577.0	855.0	495.2	710.5
		2080–2099	319.6	268.8	228.7	240.0	650.1	618.3	920.0	1454.4	1880.1	1398.3	972.6	463.7	784.6
		2016–2035	269.8	216.0	198.7	187.8	564.8	641.9	938.2	1640.1	1570.9	1188.7	804.8	435.9	721.5
	RCP8.5	2046–2065	356.8	268.7	264.6	245.6	638.0	680.5	849.1	1255.8	1774.4	1779.6	797.7	510.5	785.1
		2080–2099	320.7	261.6	232.7	220.9	559.9	722.4	891.0	1299.7	1550.0	1557.3	956.2	478.8	754.3
Hoa Duyet	KBN	1986–2005	42.6	34.7	28.5	27.3	54.9	46.7	36.1	77.4	190.8	260.7	128.8	69.8	83.2
		2016–2035	56.7	46.0	41.9	39.6	95.9	99.6	44.6	118.8	251.5	264.1	190.6	85.6	111.3
	RCP4.5	2046–2065	60.7	50.2	46.3	42.8	102.7	78.1	60.1	85.8	162.0	275.0	238.2	111.5	109.4
		2080–2099	56.9	49.6	42.1	40.1	105.3	72.9	76.3	105.5	194.5	256.5	233.4	91.0	110.3
		2016–2035	51.5	41.5	38.6	38.0	97.4	83.7	62.7	117.1	219.1	237.3	210.9	92.2	107.5
	RCP8.5	2046–2065	60.1	50.3	47.5	45.5	109.3	67.4	74.2	81.7	214.5	294.7	201.8	106.9	112.8
		2080–2099	55.4	46.7	40.5	42.3	114.6	82.8	66.4	89.2	225.7	280.0	207.3	88.9	111.6
Son Diem	KBN	1986–2005	18.1	15.6	15.1	13.4	35.2	26.1	29.2	44.9	97.5	111.4	52.1	26.6	40.4
		2016–2035	24.8	21.4	33.1	34.0	47.9	40.2	18.9	57.7	128.2	144.5	70.9	34.4	54.7
	RCP4.5	2046–2065	28.5	23.2	36.1	39.1	64.0	45.1	24.3	49.4	89.4	162.0	99.1	43.2	58.6
		2080–2099	22.0	18.9	34.4	35.0	79.6	39.8	31.3	52.4	118.7	128.3	100.9	39.3	58.4
		2016–2035	21.1	16.6	29.2	38.2	45.5	42.8	29.8	56.6	99.0	119.7	79.6	36.3	51.2
	RCP8.5	2046–2065	28.9	21.5	41.5	26.4	59.7	40.4	26.2	46.8	113.6	150.1	77.3	40.2	56.0
		2080–2099	21.6	17.0	31.4	23.5	79.1	34.7	38.5	53.0	118.5	166.6	80.0	34.6	58.2

3.3. Assessment of the climate change impact on the distribution of flood season in the year

Among the 3 areas in the Ca River basin assessed, the distribution of flood season months in the year in the Hieu river basin (Nghia Khanh station) is most affected by climate change. In the base period, this area has a flood season lasting for 3 months from August to October, however, in future periods according to climate change scenarios, the flood season appears earlier, even earlier than 3 months, and most periods end more than 1 month later (Table 4, Figure 11). Specifically:

– During the period 2016–2035, the flood season appears 3 months earlier in both scenarios RCP4.5 (extended by 3 months, starting from May) and RCP8.5 (extended by 4 months, starting from May to November). Particularly for the RCP8.5 scenario, the flood season ends 1 month later than the baseline period.

– In the period 2046–2065, the flood season ends 1 month later (ending November) compared with the baseline period in both RCP4.5 and RCP8.5 scenarios. Particularly for the RCP4.5 scenario, the flood season appears 2 months earlier than the baseline period.

– In the period 2080–2099 under both RCP4.5 and RCP8.5 scenarios, the start time of the flood season remains unchanged but the flood season ends 1 month later than the baseline period. Thus, the flood season lasts for 1 month more.

In the upstream area of the Ca River basin (Dua station), in the base period, the flood season lasts for 4 months from July to October, however, in most future periods CC scenarios, flood season appears in the same month and ends in the same month or 1 month later, only the period 2080–2099 (RCP8.5) it appears 1 month earlier (Table 3, Figure 10). Specifically:

– In the period 2016–2035, the flood season occurs in the same month and ends 1 month later than the baseline period in both RCP4.5 and RCP8.5 scenarios (extended 1 month more).

– In the period 2046–2065, the flood season appears and ends in the same month as the base period in the RCP8.5 scenario; appears in the same month and ended 1 month later than the baseline period in the RCP4.5 scenario (the flood season was extended 1 month).

– In the period 2080–2099, the flood season occurs in the same month and ends 1 month later than the baseline period in the RCP4.5 scenario (extended 1 month); appears 1 month earlier and ended 1 month later than the baseline period in RCP4.5 scenario (extended 2 months).

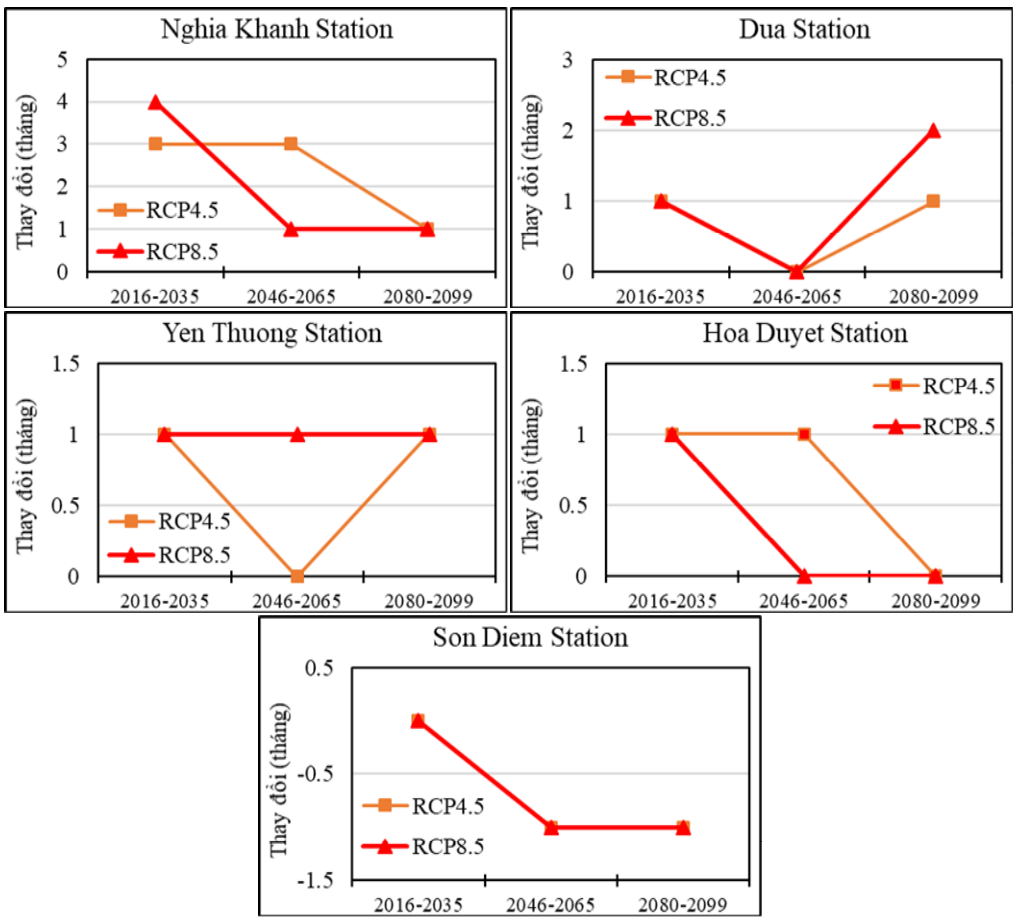

Figure 11. Changes in the number of months in the flood season in the basin of some hydrological stations in the Ca River basin in periods under the scenarios RCP4.5 and RCP8.5 compared to the baseline period.

In the southern part of the Ca River basin, on Ngan Sau River basin (Hoa Duyet station) and Ngan Pho River basin (Son Diem station), the flood seasons are also different in the base period. Flood season lasts for 3 months from September to November on the Ngan Sau river basin and 4 months from August to November on the Ngan Pho River basin. On both these river basins, in the future periods under both RCP4.5 and RCP8.5 scenarios, the flood season ends in the same month compared to the baseline period, ending only 1 month later in the period 2046–2065 according to the RCP4.5 scenario on the Ngan Sau river basin (Table 3, Figure 10). On the Ngan Sau river basin, the flood season in periods of CC scenarios is largely unchanged compared to the baseline period, lasting only more than 1 month in the period 2016–2035 under two scenarios RCP4.5 and RCP8. 5 (appearing 1 month earlier) and the period 2046–2065 under the RCP4.5 scenario (ending 1 month later). On the Ngan Pho river basin, according to both RCP4.5 and RCP8.5 scenarios, the flood season changes compared to the baseline period in the period 2016–2035 and occurs 1 month later in the two periods 2046–2065 and 2080–2099 (1 month less).

Up to Yen Thuong station, in the base period, the flood season lasts for 4 months from July to October, in most future periods under CC scenarios, the flood season occurs in the same month and ends 1 month later compared to the baseline period (extending 1 month more), in the period 2046–2065 (RCP4.5) it appears and ends 1 month later than the baseline period (the number of months in the flood season does not change) (Table 4, Figure 11).

4. Conclusion

Climate change affects the distribution of flows in flood season in all areas in the Ca River basin. Of which, the variation of the flood season is strongest on the Hieu river basin in the north of the Ca River basin and the impact decreases gradually from the north to the south. The cause of changes of flows in the flood–season distribution is attributed to changes in the rainfall patterns derived from the CC scenarios.

Climate change can shift the flood season earlier and end later in some periods under the RCP4.5 and RCP8.5 scenarios compared to the baseline. The flood season occurs up to 3 months earlier in the period 2016–2035 according to both RCP4.5 and RCP8.5 scenarios on the Hieu river basin, the rest appear and end 1 month earlier or later compared to the baseline period. However, this study is solely based on one hydrological model and one climate scenario that may cause uncertainties. Further studies using ensemble of hydrological models and climate models to validate this finding in other basins having similar conditions are necessary.

Author Contributions: Conceptualization: H.T.L.H.; Methodology: H.T.L.H.; Software: H.T.L.H.; Validation: H.T.L.H.; Formal analysis: H.T.L.H.; Investigation: H.T.L.H.; Data curation: H.T.L.H.; Writing–original draft preparation: H.T.L.H.; Writing–review and editing: H.T.L.H.; Visualization: H.T.L.H.; Supervision: H.T.L.H.

Funding: This research was funded by the Target program on climate change response and green growth, grant number 2491/QĐ-BTNMT.

Acknowledgments: The author thanks colleagues at IMHEN for technical support and provision of data required for this research.

Conflicts of Interest: The author declare no conflict of interest.

References

1. Selby, D.; Kagawa, F. Climate Change and Coronavirus: A Confluence of Two Emergencies as Learning and Teaching Challenge. *Policy Pract. Dev. Educ. Rev.* **2020**, 104–114.
2. IPCC Working Group II. Climate Change and Water. In Eos, Transactions American Geophysical Union, 2008.
3. Doll, P.; Schmied, H.M. How is the impact of climate change on river flow regimes related to the impact on mean annual runoff? A global-scale analysis. *Environ. Res. Lett.* **2012**, *7,* 014037.
4. Kundzewicz, Z.W.; Mata, L.J.; Arnell, N.W.; Doll, P.; Kabat, P.; Jimenez, B.; Miller, K.A.; Oki, T.; Sen, Z.; Shiklomanov, I.A. Freshwater resources and their management Climate Change 2007: Impacts, Adaptation and Vulnerability. Contribution of Working Group II to the Fourth Assessment Report of the Intergovernmental Panel on Climate Change. (Eds) Parry, M.L.; Canziani, O.F.; Palutikof, J.P.; van der Linden, P.J.; Hanson, C.E. (Cambridge: Cambridge University Press), 2007, pp. 173–210.
5. Hirabayashi, Y.; Kanae, S.; Emori, S.; Oki, T.; Kimoto, M. Global rojections of changing risks of floods and droughts in a changing climate. *Hydrol. Sci. J.* **2008**, *53*, 754–773.
6. Cloke, H.L.; Wetterhall, F.; He, Y.; Freer, J.E.; Pappenberger, F. Modelling climate impact on floods with ensemble climate projections. *Q. J. R. Meteorolog. Soc.* **2013**, *139*, 282–297.
7. Gain, A.K.; Immerzeel, W.W.; Weiland, F.C.S.; Bierkens, M.F.P. Impact of climate change on the streamflow of the lower Brahmaputra: trends in high and low flows based on discharge-weighted ensemble modelling. *Hydrol. Earth Syst. Sci.* **2011**, *15*, 1537–1545.
8. Arnell, N.W.; Reynard, N.S. The effects of climate change due to global warming on river flows in Great Britain. *J. Hydrol.* **1996**, *183*, 397–424.
9. Kaini, S.; Nepal, S.; Pradhananga, S.; Gardner, T.; Sharma, A.K. Impacts of climate change on the flow of the transboundary Koshi River, with implications for local irrigation. *Int. J. Water Resour. Dev.* **2020**, 1–26. https://doi.org/10.1080/07900627.2020.1826292.
10. Dang, T.; Laux, P.; Kunstmann, H. Future high- and low-flow estimations for Central Vietnam: a hydro-meteorological modelling chain approach. *Hydrol. Sci. J.* **2017**, *62*, 1867-1889.

11. Ministry of Natural Resources and Environment. Climate change and sea–level rise scenarios for Vietnam. Vietnam Publishing House of Natural Resources, Environment, and Cartography, 2016.
12. DHI. MIKE 11: Rainfall–runoff modeling reference manual. DHI, Denmark, 2003.
13. Monteith, J.L. Evaporation and environment. Symposium of the Society for Experimental Biology, The State and Movement of Water in Living Organisms, G. E. Fogg (Ed.) New York: Academic Press. **1965**, *19*, 205–234.
14. Nash, J.E.; Sutcliffe, J.V. River flow forecasting through conceptual models. A Discussion on Principals. *J. Hydrol*. **1970**, *1*, 282–290.

Table of content